The Clinical Value of Intensive Monitoring in Term Asphyxiated Newborns

Renate M.C. Swarte

The Clinical Value of Intensive Monitoring in Term Asphyxiated Newborns

Renate M.C. Swarte

"Education is learning something that you didn't even know that you didn't know"

(A. Einstein)

ISBN
Cover image: Eleonore
Pictures: David Rozemeyer
Design: Wim Dijkers Grafisch Ontwerp
Printed by: Drukkerij Verloop

Copyright © 2010 by R.M.C. Swarte, Rotterdam, The Netherlands

The Clinical Value of Intensive Monitoring in Term Asphyxiated Newborns

De klinische waarde van intensieve monitoring van à terme neonaten met asfyxia

Proefschrift

ter verkrijging van de graad van doctor aan de Erasmus Universiteit Rotterdam op gezag van de rector magnificus Prof.dr. H.G. Schmidt en volgens besluit van het College voor Promoties

De openbare verdediging zal plaats vinden op donderdag 22 april 2010 om 15.30 uur

door

Renate Maria Cornelia Swarte

geboren te Goor

ERASMUS UNIVERSITEIT ROTTERDAM

Promotiecommissie

Promotor	**Prof.dr. J.B. van Goudoever**
Co-promotoren	**Dr. P. Govaert**
	Dr. M.H. Lequin
	Dr. G.H. Visser
Overige leden	**Prof.dr. W.F.M. Arts**
	Prof.dr. F. van Bel
	Prof.dr. A.J. van der Heijden

Table of contents

Chapter 1 | General introduction

1 HYPOXIC-ISCHAEMIC ENCEPHALOPATHY IN TERM NEWBORNS

Perinatal asphyxia is an important cause of brain injury. It may lead to hypoxic-ischaemic encephalopathy (HIE) which occurs in one to six of every 1000 full term births. The risk of death or severe handicap is 0.5-2.0 out of 1000 (1). Following intrapartum asphyxia cerebral hypoperfusion in combination with hypoxia produces characteristic neuropathological changes and related clinical signs (2, 3). After the primary insult there is a thirty minutes period of reperfusion characterized by the partial recovery of cell and metabolic processes. This is followed by a latent phase which may last up to six hours. In this phase oxidative metabolism (near) normalizes (shown by MRspectroscopy) but EEG activity is depressed and the blood flow is likely to be reduced. Secondary energy failure and secondary hyperperfusion ('luxury perfusion') may occur in the neonatal brain within 6-15 hours after an acute ischaemic insult, marked by the acute onset of seizures (peaking at about 12 hours post insult). Excitotoxins accumulate in the cell and cell death may take 72 hours to completion (4, 5). The infant's gestational age and thus the maturational stage of the brain, as well as type, severity and duration of the insult are determinants of the brain injury. During the insult there is redistribution of blood flow to the brain, heart and adrenals. Our current understanding of perinatal asphyxia is based on animal experiments (6). Different and mixed etiologies lead to a range of post asphyxial patterns, usually subdivided into different patterns; acute, chronic or a combination of these two. With chronic, possibly repetitive insults, lesions are predominantly seen in (sub)cortical structures. This has been named watershed injury for its classical distribution along the borderzones between the major pial arteries, sparing thalamus and basal ganglia. From the literature it appears that watershed injury is observed most frequently in context of term birth asphyxia. In acute and (near) total asphyxia the damage is mostly to the thalami, basal ganglia, hippocampus, cerebellum, brain stem and specific areas of the neocortex like the rolandic, calcarine and insular cortex (1, 5, 7-10).

2 EEG

2.1 EEG AND PHYSIOLOGY

The electroencephalogram (EEG) is a signal recorded from the scalp and derived from the activity of cortical neurons and synapses. Postsynaptic activity is the most significant source of the extra cellular current flow that produces EEG potentials. The dendrites and soma (cell body) of a pyramidal neuron form a tree consisting of an electrically conducting interior surrounded by a relatively insulating membrane with tens of thousands of synapses on it (Figure 1). The flow of ions is determined by the excitatory state of the postsynaptic membrane: when it is depolarized it generates excitatory postsynaptic potentials (EPSPs): when hyperpolarized it generates inhibitory post synaptic potentials (IPSPs). Excitatory currents (involving Na^+/Ca^{2+} ions) are associated with a flow of positive ions into the cell thereby creating an extracellular negative field. At the same time there is a passive flow of positive ions out of another part of the cell (IPSPs). Pyramidal cells can be seen as vertically orientated dipoles. The currents pass through the extra cellular and intracellular spaces and generate a very small potential field around the cell. Because the pyramidal cells are arranged in parallel, with the apical dendrites oriented to the surface of the cortex and the axonal poles to the (sub) cortical white matter, their grouped activity can be recorded at the scalp. This is known as the dipole hypothesis. A relative large area of cortex must produce synchronized activity for detection at the scalp (11). These dipole layers of pyramidal neurons in the cortical grey matter are the EEG generators. The following factors influence size, shape and duration of the EEG waves; distance of recording electrode from the current generator, duration of the postsynaptic potentials (PSPs), number of synchronously activated PSPs and the anatomical orientation of the layer of pyramidal cells generating the current. PSPs in the thalamus and brainstem are not large enough to be detected by scalp electrodes because the cells are not aligned as dipoles (12, 13).

FIG 1 | Pyramidal neuron

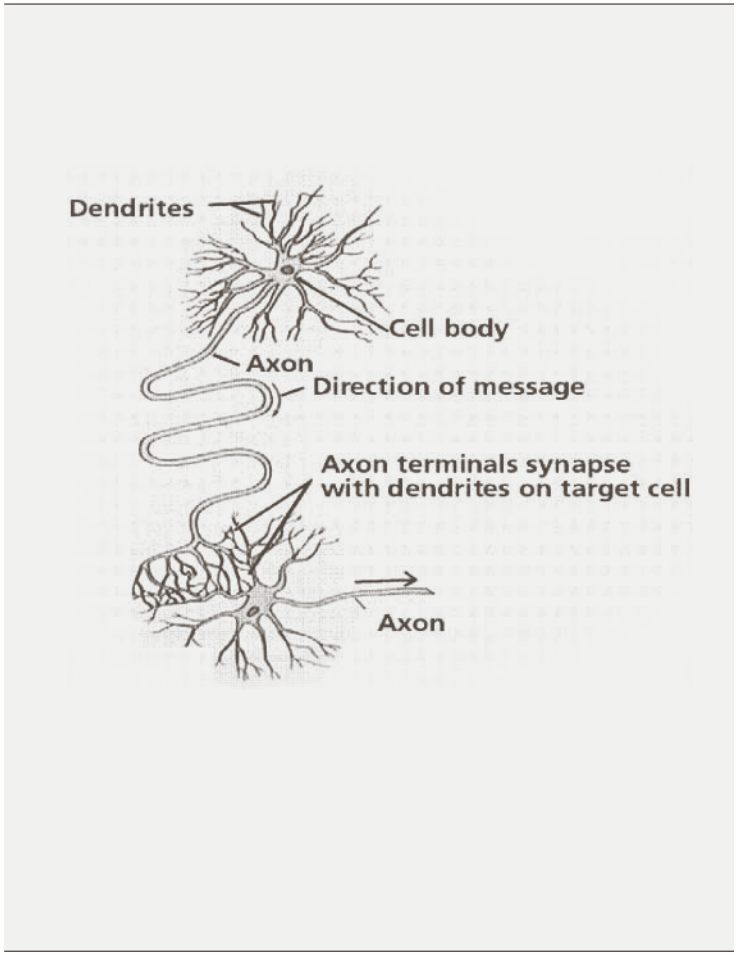

2.2 EEG ACTIVITY

EEG maturation during intrauterine and extra uterine life is thought to proceed almost at the same rate (11). EEG activity in the premature infant (‹35 weeks gestational age) is a severely discontinuous pattern, appearing as brief periods of electrical activity (bursts) interrupted by periods of quiescence (interburst intervals; IBIs) called 'tracé discontinu'. In order to validly interpret the neonatal EEG one must know the gestational age because with maturation the duration of the bursts increases whereas the duration of the IBIs decreases (11). The area of maximal electrical activity in the normal newborn term infant is the rolandic or central region (14). In full term neonates EEG activity is continuous during wakefulness, REM sleep and slow wave quiet sleep. REM sleep is characterized by closed eyes, rapid irregular eye movements and irregular respiration. It is best identified by doing polygraphic registrations along with EEG. In non-REM sleep, the eyes are closed but there are no rapid eye movements and the respiration is regular (15). An alternating pattern, observed in quiet sleep/non-REM sleep (a mature variation of the trace discontinu') is called 'trace alternant'. The normal EEG shows five patterns alternating with each other (Table 1).

The EEG is symmetrical although some interhemispheric asynchrony can be seen mostly in temporal regions and particularly at the onset of non-REM sleep. All the electrical activity is smooth contoured or is relatively sinusoidal in form. Sporadic sharp transients are common in rolandic and temporal areas. During non-REM sleep, reactivity after auditory and tactile stimuli characterized by transient attenuation of EEG voltage, lasting for 3 to 7 seconds, is best seen in term neonates. The closest integration between the cortex and other parts of the brain is during non-REM sleep (5). Figure 2 shows the EEG pattern in wakefulness and non-REM sleep in a term infant.

TABLE 1 | Changes of EEG and behavioural states depending on gestational age (see reference 5)

Gestational age	Basic EEG pattern	Behavioural states	Specific maturational features and EEG patterns
35-37 weeks	Continuous in AS and W. Discontinuous in QS	Well established QS and AS periods, definite W	Continuous mixed activity (M): medium high voltage theta-delta activities with superimposed delta brushes. Continuous low voltage theta activities with superimposed very low amplitude 8-22 Hz rhythms (LVI). FST are better defined in morphology and increase in frequency; they are often associated with ASD that appears at the beginning of this period. Increased number of delta brushes during burst periods
38-42 weeks	Mildly discontinuous during the TA phase of QS	QS periods increase, AS periods reduce. Fully developed sleep cycles	Five basic patterns are present 1. Activité Moyenne; 0,1-10Hz, 25-50 µV seen during W and AS following QS 2. Low voltage intermittent (LVI); low voltage irregular in AS 3. Mixed: activity moyenne with superimposed delta-theta activity in AS 4. High voltage slow wave (HVS); continuous medium voltage delta waves activity in QS 5. Tracé alternant (TA); discontinuous 1-3 Hz, 50-100 µVolt, activity mixed with lower amplitude beta and theta activity in 3-5 s burst occurring at 3-10 s intervals in QS. Prominent FST and ASD.

AS; active sleep (REM sleep), QS; quiet sleep (non-REM sleep), W; wakefulness, FST; frontal sharp transients (or encoche frontale), ASD; anterior slow dysrhytmia

2.3 EEG IN PRACTICE

The average brain of a full term infant weighs about 335 grams. All lobes are clearly distinguishable (11). The neonatal head size makes it difficult to use a full 10/20 EEG electrode placement system. This is why usually fewer electrodes (8-10) are placed (Fp1, Fp2, C3, C4, O1, O2, T3, and T4 if possible also Fz and Cz) (5). The range of clinically interesting neurophysiologic activity in the scalp is between 0 to 50 Hz. Wider frequency bands increase the amount of outside interference and unwanted noise. Therefore filters are used. Recently unfiltered 'full band' EEG recording in neonates has been introduced (16). The EEG technologist must be aware of the sleep waking state and reactivity (17). A minimally 60 minutes recording is recommended including a sleep wake cycle (11). It is important that recording may be disturbed by artifacts (physiological artefacts such as (eye) movement, sucking, respiration, hiccoughs and electrocardiogram and external/non physiological artifacts such as ventilator, warm mattress, infusion pumps etcetera) (11, 18).

The EEG has been recognized as an important investigation in the neurologically sick newborn infant, both in the diagnosis and treatment of neonatal seizures and for prognostication (19). Because reviewing full channel EEG is very time consuming, and the expert clinical interpretation is not available around the clock, the use of simple EEG trends like amplitude integrated EEG (aEEG) has become practice. This monitor was originally designed by Maynard in the late 1960s to perform continuous cortical monitoring in adults (20). In the last 20 years, the aEEG has been applied in newborns with HIE. A single or a two channel EEG is used. The signal is amplified and compressed, using an asymmetric filter (below 2 and above 15 Hz), to minimize artefacts such as sweating, muscle activity and electric interference. The scale is semilogarithmic and the time base is 6 cm/h, displaying about 5 hours of data on a page. Due to this scale characteristics background activity of 0 to 10 µV is enhanced and activity above 10 µV is attenuated. However, there are limitations to a single or a two channel EEG; focal low amplitude and short seizures are not detected and voltage may be influenced by scalp edema and interelectrode distance (21). Furthermore, electrocardiogram (ECG) or high frequency ventilator interference can lead to falsely elevated lower margin of the aEEG band. This is called 'drift of baseline' and can result in misinterpretation of the actual background voltage (22, 23). False negatives (missed seizures) would result in missing the chance to offer a required treatment while false positive detections would result in administration of unnecessary treatment which could have potential adverse effects. The simultaneous raw EEG channels, that are implemented in the newer monitors may help to better identify these artefacts (24).

2.4 EEG AND NEUROPATHOLOGY

Both the duration of the hypoxic insult and the neonate's gestational age influence the neuropathology. A comparison of EEG and neuropathological findings in neonates revealed that normal EEGs were associated with absence of neuropathology (25). Furthermore a correlation between abnormal EEG background activity and the number of damaged structures seen on neuropathological examination has been reported. The cerebral cortex, striatum, thalamus, midbrain and pons were extensively affected in all infants who had an abnormal, isoelectric EEG. In the burst suppression patterns, a wide variety of lesions were seen (25, 26). Focal neuropathological abnormalities were associated with an asymmetrical EEG in 40% of the patients in the study of Aso and colleagues; others have reported higher percentages. No consistent association was found between abnormal asynchrony on EEG and a particular type of neuropathology (25).

3 NEONATAL BRAIN IMAGING, TECHNIQUES AND TIMING

Three different imaging techniques are available to investigate brain injury in newborns with HIE; that is cranial ultrasound (US), computerized tomography (CT) and magnetic resonance imaging (MRI), including diffusion weighted imaging (DWI) and magnetic resonance spectroscopy (MRS).

US is mobile and easy to use on the NICU and allows timing of

FIG 2 | The EEG pattern in wakefulness (left) and non-REM sleep (right) in a term infant

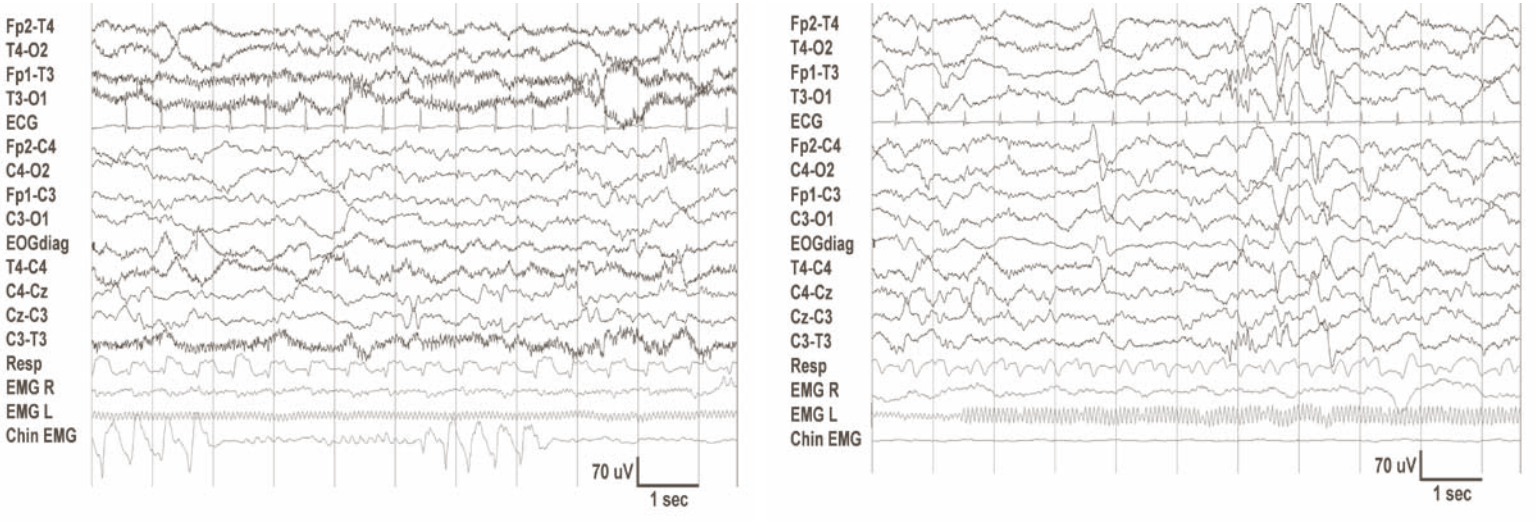

the hypoxic event, monitoring of the evolution of lesions, detecting of lesions by chance findings, or monitoring of for instance treatment of hydrocephalus. However, it is not as accurate as MRI to describe location and extent of the lesions, mainly when situated in areas distant from sonographic windows like the hindbrain and the parieto-occipital cortex (27). The combination of US and MRI is powerful in clinical practice. CT has lost strength for prognostic evaluation in neonates because it's low sensitivity for detecting ischaemic lesions, leukomalacia and disturbance of myelination; this is due to the high water content in the newborn brain, resulting in poor contrast. Furthermore, the high radiation dose is a disadvantage (7, 28).

MRI is the best imaging technique to detect ischaemic brain areas and to assess the extent of the damage areas. It correlates well with abnormalities on histopathology. A positive predictive value of 100% has been attributed to MRI for detecting histological brain injury (29). But this technique has also its drawbacks. First, to get a proper MR scan the neonate should be comfortable during scanning. This may reduce scan time and motion artefacts. Also continuous monitoring of vital parameters is essential, for this one can use a MR compatible incubator. But dealing with all these practical issues, is not a guarantee for an optimal MR scan of an asphyxiated neonate. The moment to plan the MR scan is also essential, because timing of the MR scan is crucial. Conventional

MR sequences depict abnormalities as early as day 3 to 4 following an insult. In basal ganglia and thalami, T1-shortening (high intensity signal) becomes evident from day four after birth. T2-shortening (low signal intensity) develops slightly later. Both normalize in time (months) and atrophy occurs (30). The reason for the shortening in the subacute phase is not clear (5). The T1-shortening due to ischaemia should not be mistaken by areas of normal myelination, because during the first month of life myelination (in deep grey nuclei and in the posterior limb of the internal capsule (PLIC) is also hyperintense on T1-weighted images (31). Cortical edema causes T1- and T2-prolongation resulting in a discontinuous cortex or blurring of the cortex/subcortical white matter boundary, best interpreted on T2-weighted images, whereas thalamus and basal ganglia damage is better assessed on T1-weighted images (27).

DWI with mapping of the apparent diffusion coefficient (ADC) are more sensitive than conventional MRI to delineate damaged brain areas. Abnormalities are visible within hours when the standard T1- and T2-weighted images are still normal. DWI measures the random motion of water within a tissue. If performed on the first day after an insult it may underestimate the extent of the damage because delayed injury with secondary cell swelling has not taken place yet, which makes DWI most sensitive during days 2-4 post insult (27, 32). Visual interpretation of the trace map of DWI is hampered by T2-shinethrough, therefore additional visual assessment of the ADC map is important because of their objectivity in quantifying water motion. If visual assessment is still difficult, one can measure the ADC values and compare them with published normal values. In case of a hypoxic-ischaemic insult ADC values will decrease immediately due to restriction of water motion as a result of cytotoxic edema. After the first hours of the insult ADC values transiently normalize (latent phase; pseudonormalization), and decrease again during the period of secondary energy failure (12-48 hours). Normal ADC values at 24 hours after birth may signify that secondary energy failure has not yet developed. After a week ADC values pseudonormalize again because of a combination of cytotoxic edema (ADC low), vasogenic edema and cell lysis (ADC high). After several days vasogenic edema and tissue dissolution may lead to higher ADC values (4, 32, 33). Therefore, timing of the primary insult is important for the interpretation of DWIs (34).Visual assessment of the ADC maps should be compared with the trace map of the DWI and with the conventional T1- and T2-weighted images.

Proton MR spectroscopy (^{1}H-MRS) is also a useful tool for evaluating the severity and prognosis of HIE noninvasively. It measures the concentrations of intracerebral metabolites in vivo, which can offer information about cellular energy metabolism, disintegration of cellular membrane, the function of neurons, and the activation of selective neurotransmitters. Intracerebral metabolites mainly include glutamate (Glx), N-acetyl-aspertate (NAA), lactate (Lac), choline (Cho), creatine (Cr), and myo-inositol (MI). Several studies suggests that a higher Glx-α/Cr in basal ganglia and thalamus may predict poor neurologic outcome in asphyxiated neonates (35, 36). The increased Glx in the extracellular spaces of the brain plays an important role in neuronal injury and death, as well as in the epileptogenesis and seizure expression induced by ischaemia and hypoxemia. Other studies suggest that increased lactate may be a good predictor for poor outcome. The lactate level of the injured brain increases within the first 24 hours and remains elevated after 24 hours, presumably because of energy failure and the necessity to metabolize glucose anaerobically. But Lac/Cr ratio has lesser power than Glx/Cr ratio to predict poor outcome (35). Also the NAA level may diminish significantly in neonate with HIE but only after 48 hours post insult. The precise time at which NAA begins to diminish in asphyxiated neonates is not precisely known. Therefore, like in all MR technique used for imaging neonates with HIE timing is essential for adequate interpretation of the images and ratios of the intracerebral metabolites in HIE.

Phosphorus MR spectroscopy (P-MRS) can also demonstrate the secondary energy failure. The optimal time to perform is after the end of the secondary energy failure (48 hours after reperfusion). The severity of energy failure correlates closely with neurodevelopmental outcome (37, 38). The combination of conventional MRI, DWI and ADC measurements,

1H MRS and P- MRS can reliable estimate brain injury between 48-72 hours after the event.

4 TOOLS TO PREDICT OUTCOME (SEE TABLE 2)

Reliable prediction of outcome in the first days after birth is of crucial importance in term asphyxiated infants in whom withdrawal of care is considered. The predictive values of different parameters for poor outcome, described in literature, are summarized in this paragraph and listed in Table 2.

4.1 NEUROLOGICAL EXAMINATION

Scoring the severity of encephalopathy following asphyxia has been shown a better predictor for poor outcome than the Apgar scores (39). Several scores were designed. The most widely used classification systems of HIE are the Sarnat (grades I, II, II) and Thompson scores. These proved to have high positive predictive values and sensitivity for poor outcome. Evaluation at the end of the first week is useful in practice; a normal neurological condition after six days carries a good prognosis in contrast to those infants who remain abnormal (40, 41). Finer and colleagues came to the same conclusion. Furthermore, complex scoring systems are described, requiring a trainings course, which makes it less suitable for clinical use (11, 42).

4.2 BIOCHEMICAL VARIABLES

The relation between established clinical parameters (i.e., Apgar score and umbilical artery pH) and outcome has been assessed by various authors. Levene and co-workers found that an Apgar score of 5 or less at 10 minutes is the most sensitive predictor for poor outcome (39). Finer et colleagues found that Apgar scores of 0 to 3 at 5 min after birth were significantly related to severe handicap (43). A review described that the outcome of infants with an Apgar score of zero at 10 minutes is poor in most cases. This is in contrast to the findings of others. (44-46). In individual cases Apgar scores do not reflect the duration of intrapartum asphyxia, and therefore correlates poorly with outcome (39).

Most found that an umbilical artery pH ‹ 7.00 is related to neonatal complications (47). However, many such neonates are normal at discharge (48-50). The metabolic component of fetal acidemia (base deficit) is the most important variable related to outcome because it reflects the severity and duration of the insult (51). CO2 is highly diffusible and rapid changes can occur as a consequence of hypoxia. Base deficits measured in the umbilical artery below 12 mmol/L rarely result in handicap, in contrast to deficits of more than 16 mmol/L (52). Again many neonates beyond this threshold have no complications and survive intact, which is due to fetal compensation mechanisms. In conclusion there is a poor relation between umbilical artery pH, base deficit and outcome (5).

4.3 NEUROPHYSIOLOGICAL PARAMETERS

4.3.1 EEG

Meta analyses have shown that background abnormalities at the EEG performed in the first week of life (burst suppression (BS), persistent slow activity, low voltage and isoelectric EEGs) were associated with poor outcome (53, 54). Most studies were based on thirty minutes EEG registration. The role of EEG in prognostication in neonates with birth asphyxia has been well studied (53, 55 59). EEGs done during the first week were found to be more prognostic than those done later, since inactive EEGs, paroxysmal EEGs and low voltage EEGs may disappear during the second week (57). The mildest disturbance in the EEG activity after hypoxic injury is characterized by an abnormal sleep wake pattern (even before discontinuity becomes obvious) (5, 53). The return of sleep wake cycles detected by EEG or aEEG is a prognostically good sign, especially if this occurs within 36 hours after birth (53, 60). In discontinuous EEGs, a relationship has been found between the longest interburst interval, longest burst duration and amplitude of interburst interval and outcome (61). A persistent discontinuous pattern after the first week post partum was strongly related to poor outcome (19, 26, 56). Animal experiments have shown that when asphyxia was clearly related to the partus, seizures did not start before 6 hours after birth; earlier occurring seizures

TABLE 2 | Predictive values of different parameters for poor outcome (major handicap or death)

Parameter (reference)	Sensitiviteit	Specificiteit	PPV (%)	NPV (%)
Sarnat score II (5)			25	
Sarnat score III (5)			100	
modified Sarnat score I, II, III (3)	100	50	44	100
modified Sarnat score (II, III)	78	78	58	90
Thompson score (score › 15) (41)	71	96	92	82
Apgar Score ≤ 5 at 10 min (39)	43	95		
umbilical artery pH ‹ 7.00 (50)	32	82	70	48
umbilical artery base deficit › 12 mmol/L (52)	9	98	71	68
umbilical artery base deficit › 16 mmol/L (52)	41	96	77	83
moderately/severely abnormal EEG (55)	88	94		
abnormal aEEG (3)	79	89	73	91
discontinuous EEG and IBI › 30s (56)	32	100	100	
abnormal aEEG with early abnormal neurological examination (3)	78	94	85	92
aEEG 3 hours after birth, FT/BS/CLV together (74)	85	77	78	84
aEEG 6 hours after birth, FT/BS/CLV together (60)	93	85	88	91
abnormal VEP within 6 hours of birth (81)	89	67	77	83
abnormal SEP ‹ 6 hours of birth (81)	95	73	82	92
severely abnormal ultrasound ‹ 24 h after birth (82)	47	100	100	50
abnormal ultrasound within 6 hours of age (81)	42	60	57	45
MRI severely abnormal (82)	74	100	100	67
MRI severely abnormal (86)	92	89	71	97
absence of normal PLIC on MRI (83)	90	100	100	87
EEG and MRI severely abnormal (82)	67	100	100	50

suggest an antenatal ischemic event (62). Abnormality of the background activity is a stronger predictor of outcome than the occurrence of seizures (40, 53). However, some authors report that asphyxiated infants with seizures develop worse than those without seizures (63, 64). There is evidence that repetitive seizures disturb brain growth and increase the risk for childhood epilepsy (65, 66). It is known that background abnormalities strongly predicted the occurrence of electrographic seizures. However, no human studies studying post asphyxial neonatal seizures have controlled for abnormalities in the EEG background activity, thus confounding the interpretation of the effect of seizures on development (63, 67). Despite this the medication policy remains controversial, as antiepileptic drugs (AED) such as barbiturates and benzodiazepines can have a deleterious effect on brain development (68).When the initial EEG was normal or only mildly abnormal it was found that there was 96% chance that the neonate would not have seizures on continuous EEG monitoring (67). Therefore, long term monitoring may be indicated to detect the seizure activity in encephalopatic neonates with an abnormal background pattern. Electroclinical dissociation of seizures has been described in neonates with more severe abnormalities of the background activity and is associated with a poor outcome (69). Treatment with AED can also lead to electroclinical dissociation in which case EEG is the only method to detect ongoing seizure activity (70). Poor outcome was seen when abnormal EEG background occurred in combination with seizures and also in status epilepticus (64, 70). The evolution of the EEG in the first few days after birth is important and hence serial EEGs increase the prognostic predictive value after perinatal encephalopathy (71). Finally, the significance of paroxysmal abnormalities, such as positive spikes and sharp waves, in an EEG related to outcome is more controversial (57, 72).

4.3.2 aEEG

In term asphyxiated newborns aEEG has been shown to be a predictor of neurologic outcome 3 to 6 hours after birth (73, 74). Two approaches to scoring aEEG background have been described: pattern recognition and measuring the absolute values of upper and lower margin of the aEEG band (73). Initially, four patterns were described: continuous normal voltage (CNV), continuous low voltage (CLV), flat trace (FT) and burst suppression (BS). Later the pattern of discontinuous normal voltage (DNV) was added (20). Several studies have reported that aEEG and standard EEG correlate well with each other; the positive predictive value of CNV and DNV on aEEG with a standard EEG is 90%, while CLV, FT and BS correlates 100% with the standard EEG. The CNV and DNV patterns are correlated with good outcome, whereas CLV, FT and BS are associated with poor outcome. Different predictive values were reported about the relationship between aEEG and outcome (Table 2). Relationship of aEEG to outcome at 6 hours is slightly better than at 3 hours after birth (74). The BS and the CLV or FT patterns were less predictive in the first 6 hours; these patterns normalized within the first 24 hours in some of the neonates (in 48% of neonates with BS and in 9% with CLV or FT). However, if these patterns persisted during 24 hours the prognosis was poor. The predictive values of BS together with FT and CLV for poor outcome are shown in Table 2. Recovery of an initially poor aEEG pattern within 24 hours need not always predict a normal outcome and hence, complementary investigations like MRI and SEPs are needed for accurate prognostication (60). Furthermore, the return of sleep wake cycles on aEEG is related to the severity of the ischaemic insult and to outcome (60). All in all aEEG does not replace the standard EEG but should only be used as a complementary tool to standard EEG (75). Early aEEG combined with neurological examination enhances the predictive value for outcome (76). Antiepileptic drugs and other sedative medications (such as morphine) can lead to a transient decrease in aEEG amplitude but therapeutic doses generally do not influence the prognostication (21, 77, 78).

4.3.3 Evoked potentials (somatosensory and visual; SEPs and VEPs)

Somatosensory evoked potentials (SEPs) from the upper limb tests the functional pathway consisting of peripheral nerve, brachial

plexus, dorsal spinal root, dorsal columns in the spinal cord, cuneate nucleus and after decussation, medial lemniscus, thalamus and parietal cortex. SEP components are named according to their polarity and latency, although the nomenclature of the component waves differs among laboratories. SEPs can be easily performed in term asphyxiated newborns. Median nerve SEPs are generally well tolerated in neonates, whereas posterior tibial nerve SEPs are more noxious. SEPs proved particularly helpful in identifying risk of adverse outcome in neonates who presented clinically with moderate encephalopathy (79). SEPs are not widely performed in asphyxiated term infants. However, they can distinguish between good and poor outcome. The predictive value of SEPs vary in the literature (sensitivity (89-95%) and specificity (86-92%) (80, 81). Visual evoked potentials (VEPs) are less prognostic than SEPs (80).

4.4 IMAGING

4.4.1 CRANIAL ULTRASOUND

Severely abnormal findings have been shown to have a high positive predictive value of poor outcome but with a low sensitivity. US on admission and serially after that have a role in timing the insult, because hyperechoic changes follow an orderly sequence after an acute intrapartum insult. Deviations of this order of events, e.g. the finding of bright thalami within 24 hours or the absence of slit ventricles on admission, point to a less recent character of the insult (80, 82).

4.4.2 MRI

The relation between MRI and outcome is well documented. Abnormal signal intensity in the posterior limb of the internal capsule (PLIC) on T1-MRI is associated with a poor neurodevelopmental outcome. It is the best predictor of poor outcome in the first 10 days of life (82, 83). Abnormalities within the basal ganglia and thalamus are frequently seen after asphyxia such as injuries to white matter or cortex, depending on the type and severity of the insult. Lesions to deep grey matter may cause cerebral palsy (CP) with even a 'dosage-dependent' effect (extensive injury correlates with more severe motor deficit). Basal ganglia/thalamus injury is associated in about half of the patients with white matter abnormalities, and they further add to cognitive problems. However, severe deep grey matter lesions cause cognitive deficit by themselves (27). ADC values of normal appearing basal ganglia, thalamus and brainstem correlated with outcome at 5 years of age (84). Published MRI scoring systems group link severity of brain injury to outcome (85, 86). The Hammersmith group recognized 8 patterns. Of newborns no injury or with minimal white matter injury, 83% developed normal at school age. Minor neurological dysfunction and/or perceptual-motor difficulties were seen in 80 % of subjects with mild or moderate basal ganglia lesions or more marked white matter lesions (50). After sentinel events (with a recognizable mechanisms like uterine rupture, cord prolapse or abruptio placentae), mainly deep grey matter lesions were observed. Acute total asphyxia with bradycardia is associated with lesions in the PLIC, brainstem, hippocampus, and cortex. Cortical injury is particularly seen in the central fissure and insula (87). In spite of the reliability of MRI alone in predicting outcome, it should never be used in isolation of the other prognostic variables referred to above and below.

4.5 MRI PATTERNS IN RELATION TO EEG ABNORMALITIES

Few studies with small numbers of patients have correlated multichannel EEG with MRI while one study related MRI to aEEG (21, 59, 61, 82). Different definitions were used in classifying the EEG. Severe lesions to thalamaus and basal ganglia correlated with an extremely discontinuous EEG background (interburst interval IBI › 40 s). Abnormal background EEG, in combination with either diffuse white matter damage or with deep grey matter injury with or without cortical involvement, was associated with poor outcome. The combination of EEG and MRI increased the predictive value (82). Furthermore, severe white matter injury was associated with severe discontinuous pattern (IBI 20-40 s) and severe basal ganglia/thalamus injury with extreme discontinuous (IBI › 40 s) or low voltage pattern (‹ 20µV).

5 AIMS OF THIS THESIS AND OUTLINE OF THE THESIS CHAPTERS

Considering the individual neonate we feel the existing MRI scores fall short of their promise: some brain changes are ignored, equivocal findings are common, and the paradigms of injury need further description. For example, caudate injury was not part of any score, isolated leukomalacia is categorized but not detailed with US and isolated cortical injury is not described as an isolated lesion. This is why we developed a new empirical scoring system for brain injury, seen on MRI/US, which is described in chapter 2 of this thesis: "Imaging patterns of brain injury in term birth-asphyxia". This scoring system is based on grading of injury to deep grey matter and to (sub)cortical/white matter. The aims of this thesis therefore were the following:

- To compare our newly developed MRI scoring system with the existing scoring systems in term asphyxiated neonates: "Is there need for a new MRI scoring system in term birth asphyxia?" (chapter 3).
- To determine the prognostic value of somatosensory evoked potentials (SEPs) in addition to 24-hours EEG monitoring and cerebral imaging in term infants with HIE: "Somatosensory Evoked Potentials are of additional prognostic value in certain patterns of brain injury in term birth asphyxia" (chapter 4).
- To describe the relationship between EEG scores based on evolution of discontinuity and sleep wake cycling over 24 hours and cerebral injury patterns seen on MRI: "The evolution of EEG background abnormalities is related to injury patterns on MRI in asphyxiated term infants" (chapter 5).

Clinically related findings such as changes in heart rate and ictal nystagmus (in one patient) related to seizures are described in chapter 6 and 7.

Studies have suggested that early treatment of subclinical seizures lowers the incidence of epilepsy in childhood (65). Visual assessment of a two channel EEG in combination with the raw EEG signal was reported to detect 78% of the electrographic seizures (88). Because the presently available automatic seizure detection algorithms have modest sensitivity and relatively high false positive rates, we have developed an automated seizure detection algorithm. This is described in chapter 8 "Automated neonatal seizure detection mimicking a human observer reading EEG".

REFERENCES

1. Miller SP, Ramaswamy V, Michelson D, Barkovich AJ, Holshouser B, Wycliffe N, et al. Patterns of brain injury in term neonatal encephalopathy. J Pediatr 2005; 146(4):453-60.
2. Perlman JM. Brain injury in the term infant. Semin Perinatol 2004;28(6):415-24.
3. Shalak LF, Laptook AR, Velaphi SC, Perlman JM. Amplitude-integrated electroencephalography coupled with an early neurologic examination enhances prediction of term infants at risk for persistent encephalopathy. Pediatrics 2003;111(2):351-7.
4. L'Abee C, de Vries LS, van der Grond J, Groenendaal F. Early diffusion-weighted MRI and 1H-Magnetic Resonance Spectroscopy in asphyxiated full-term neonates. Biol Neonate 2005;88(4):306-12.
5. Levene MI CF, Whittle M. Fetal and Neonatal Neurology and Neurosurgery. Philadelphia: Churchill Livingstone 2001.
6. Painter MJ. Animal models of perinatal asphyxia: contributions, contradictions, clinical relevance. Semin Pediatr Neurol 1995;2(1):37-56.
7. Volpe J. Neurology of the newborn. Fourth ed. ed. Philadelphia: Saunders; 2001.
8. Leech RW, Alvord EC, Jr. Anoxic-ischemic encephalopathy in the human neonatal period. The significance of brain stem involvement. Arch Neurol 1977;34(2):109-13.
9. Cowan F, Rutherford M, Groenendaal F, Eken P, Mercuri E, Bydder GM, et al. Origin and timing of brain lesions in term infants with neonatal encephalopathy. Lancet 2003; 361(9359):736-42.
10. Pasternak JF, Gorey MT. The syndrome of acute near-total intrauterine asphyxia in the term infant. Pediatr Neurol 1998;18(5):391-8.
11. Pressler RM BC, Cooper R, Robinson R. Neonatal and Paediatric Clinical Neurophysiology. 2nd ed. London: Churchill Livingstone; 2007.
12. Gloor P. Neuronal generators and the problem of localization in electroencephalography: application of volume conductor theory to electroencephalography. J Clin Neurophysiol 1985;2(4):327-54.
13. Schaul N. The fundamental neural mechanisms of electroencephalography. Electroencephalogr Clin Neurophysiol 1998;106(2):101-7.
14. Ellingson RJ. Electroencephalograms of normal, full-term newborns immediately after birth with observations on arousal and visual evoked responses. Electroencephalogr Clin Neurophysiol 1958;10(1):31-50.
15. Lamblin MD, Andre M, Challamel MJ, Curzi-Dascalova L, d'Allest AM, De Giovanni E, et al. [Electroencephalography of the premature and term newborn. Maturational aspects and glossary] Electroencephalographie du nouveau-ne premature et a terme. Aspects maturatifs et glossaire. Neurophysiol Clin 1999;29(2):123-219.
16. Vanhatalo S, Voipio J, Kaila K. Full-band EEG (FbEEG): an emerging standard in electroencephalography. Clin Neurophysiol 2005;116(1):1-8.
17. Prechtl HF. The behavioural states of the newborn infant (a review). Brain Res 1974;76(2):185-212.
18. Ebersole JS PT. Current practice of clinical electroencephalography. 3th ed. Philadelphia: Lippincott Williams & Wilkens; 2003.
19. Biagioni E, Bartalena L, Boldrini A, Pieri R, Cioni G. Constantly discontinuous EEG patterns in full-term neonates with hypoxic-ischaemic encephalopathy. Clin Neurophysiol 1999;110(9):1510-5.
20. de Vries LS, Toet MC. Amplitude integrated electroencephalography in the full-term newborn. Clin Perinatol 2006;33(3):619-32, vi.
21. Shah DK, Lavery S, Doyle LW, Wong C, McDougall P, Inder TE. Use of 2-channel bedside electroencephalogram monitoring in term-born encephalopathic infants related to cerebral injury defined by magnetic resonance imaging. Pediatrics 2006; 118(1):47 55.

22. Hagmann CF, Robertson NJ, Azzopardi D. Artifacts on electroencephalograms may influence the amplitude-integrated EEG classification: a qualitative analysis in neonatal encephalopathy. Pediatrics 2006;118(6):2552-4.
23. El-Dib M, Chang T, Tsuchida TN, Clancy RR. Amplitude-integrated electroencephalography in neonates. Pediatr Neurol 2009;41(5):315-26.
24. de Vries NK, Ter Horst HJ, Bos AF. The added value of simultaneous EEG and amplitude-integrated EEG recordings in three newborn infants. Neonatology 2007;91(3):212-6.
25. Aso K, Scher MS, Barmada MA. Neonatal electroencephalography and neuropathology. J Clin Neurophysiol 1989;6(2):103-23.
26. Pezzani C, Radvanyi-Bouvet MF, Relier JP, Monod N. Neonatal electroencephalography during the first twenty-four hours of life in full-term newborn infants. Neuropediatrics 1986;17(1):11-8.
27. Rutherford M. MRI of the Neonatal Brain. 1st ed. Philadelphia: WB Saunders; 2002.
28. Chao CP, Zaleski CG, Patton AC. Neonatal hypoxic-ischemic encephalopathy: multimodality imaging findings. Radiographics 2006;26 Suppl 1:S159-72.
29. Jouvet P, Cowan FM, Cox P, Lazda E, Rutherford MA, Wigglesworth J, et al. Reproducibility and accuracy of MR imaging of the brain after severe birth asphyxia. AJNR Am J Neuroradiol 1999;20(7):1343-8.
30. Barkovich AJ, Westmark K, Partridge C, Sola A, Ferriero DM. Perinatal asphyxia: MR findings in the first 10 days. AJNR Am J Neuroradiol 1995;16(3):427-38.
31. Liauw L, van der Grond J, van den Berg-Huysmans AA, Palm-Meinders IH, van Buchem MA, van Wezel-Meijler G. Hypoxic-ischemic encephalopathy: diagnostic value of conventional MR imaging pulse sequences in term-born neonates. Radiology 2008;247(1):204-12.
32. Cowan FM, Pennock JM, Hanrahan JD, Manji KP, Edwards AD. Early detection of cerebral infarction and hypoxic ischemic encephalopathy in neonates using diffusion-weighted magnetic resonance imaging. Neuropediatrics 1994;25(4):172-5.
33. Roelants-van Rijn AM, Nikkels PG, Groenendaal F, van Der Grond J, Barth PG, Snoeck I, et al. Neonatal diffusion-weighted MR imaging: relation with histopathology or follow-up MR examination. Neuropediatrics 2001;32(6):286-94.
34. Rutherford M, Counsell S, Allsop J, Boardman J, Kapellou O, Larkman D, et al. Diffusion-weighted magnetic resonance imaging in term perinatal brain injury: a comparison with site of lesion and time from birth. Pediatrics 2004;114(4):1004-14.
35. Zhu W, Zhong W, Qi J, Yin P, Wang C, Chang L. Proton magnetic resonance spectroscopy in neonates with hypoxic-ischemic injury and its prognostic value. Transl Res 2008;152(5):225-32.
36. Groenendaal F, Roelants-Van Rijn AM, van Der Grond J, Toet MC, de Vries LS. Glutamate in cerebral tissue of asphyxiated neonates during the first week of life demonstrated in vivo using proton magnetic resonance spectroscopy. Biol Neonate 2001;79(3-4):254-7.
37. Martin E, Buchli R, Ritter S, Schmid R, Largo RH, Boltshauser E, et al. Diagnostic and prognostic value of cerebral 31P magnetic resonance spectroscopy in neonates with perinatal asphyxia. Pediatr Res 1996;40(5):749-58.
38. Lorek A, Takei Y, Cady EB, Wyatt JS, Penrice J, Edwards AD, et al. Delayed ("secondary") cerebral energy failure after acute hypoxia-ischemia in the newborn piglet: continuous 48-hour studies by phosphorus magnetic resonance spectroscopy. Pediatr Res 1994;36(6):699-706.
39. Levene MI, Sands C, Grindulis H, Moore JR. Comparison of two methods of predicting outcome in perinatal asphyxia. Lancet 1986;1(8472):67-9.

40. Sarnat HB, Sarnat MS. Neonatal encephalopathy following fetal distress. A clinical and electroencephalographic study. Arch Neurol 1976;33(10):696-705.
41. Thompson CM, Puterman AS, Linley LL, Hann FM, van der Elst CW, Molteno CD, et al. The value of a scoring system for hypoxic ischaemic encephalopathy in predicting neurodevelopmental outcome. Acta Paediatr 1997;86(7):757-61.
42. Lipper EG, Voorhies TM, Ross G, Vannucci RC, Auld PA. Early predictors of one-year outcome for infants asphyxiated at birth. Dev Med Child Neurol 1986; 28(3):303 9.
43. Finer NN, Robertson CM, Richards RT, Pinnell LE, Peters KL. Hypoxic-ischemic encephalopathy in term neonates: perinatal factors and outcome. J Pediatr 1981;98(1):112-7.
44. Harrington DJ, Redman CW, Moulden M, Greenwood CE. The long-term outcome in surviving infants with Apgar zero at 10 minutes: a systematic review of the literature and hospital-based cohort. Am J Obstet Gynecol 2007;196(5):463 e1-5.
45. Jain L, Ferre C, Vidyasagar D, Nath S, Sheftel D. Cardiopulmonary resuscitation of apparently stillborn infants: survival and long-term outcome. J Pediatr 1991;118(5):778-82.
46. Nelson KB, Ellenberg JH. Apgar scores as predictors of chronic neurologic disability. Pediatrics 1981;68(1):36-44.
47. Sehdev HM, Stamilio DM, Macones GA, Graham E, Morgan MA. Predictive factors for neonatal morbidity in neonates with an umbilical arterial cord pH less than 7.00. Am J Obstet Gynecol 1997;177(5):1030-4.
48. King TA, Jackson GL, Josey AS, Vedro DA, Hawkins H, Burton KM, et al. The effect of profound umbilical artery acidemia in term neonates admitted to a newborn nursery. J Pediatr 1998;132(4):624-9.
49. Graham EM, Ruis KA, Hartman AL, Northington FJ, Fox HE. A systematic review of the role of intrapartum hypoxia-ischemia in the causation of neonatal encephalopathy. Am J Obstet Gynecol 2008;199(6):587-95.
50. Barnett A, Mercuri E, Rutherford M, Haataja L, Frisone MF, Henderson S, et al. Neurological and perceptual-motor outcome at 5 - 6 years of age in children with neonatal encephalopathy: relationship with neonatal brain MRI. Neuropediatrics 2002;33(5):242-8.
51. van den Berg PP, Nelen WL, Jongsma HW, Nijland R, Kollee LA, Nijhuis JG, et al. Neonatal complications in newborns with an umbilical artery pH ‹ 7.00. Am J Obstet Gynecol 1996;175(5):1152-7.
52. Low JA, Lindsay BG, Derrick EJ. Threshold of metabolic acidosis associated with newborn complications. Am J Obstet Gynecol 1997;177(6):1391-4.
53. Watanabe K, Miyazaki S, Hara K, Hakamada S. Behavioral state cycles, background EEGs and prognosis of newborns with perinatal hypoxia. Electroencephalogr Clin Neurophysiol 1980;49(5-6):618-25.
54. Sinclair DB, Campbell M, Byrne P, Prasertsom W, Robertson CM. EEG and long-term outcome of term infants with neonatal hypoxic-ischemic encephalopathy. Clin Neurophysiol 1999;110(4):655-9.
55. Holmes G, Rowe J, Hafford J, Schmidt R, Testa M, Zimmerman A. Prognostic value of the electroencephalogram in neonatal asphyxia. Electroencephalogr Clin Neurophysiol 1982;53(1):60-72.
56. Menache CC, Bourgeois BF, Volpe JJ. Prognostic value of neonatal discontinuous EEG. Pediatr Neurol 2002;27(2):93-101.
57. Monod N, Pajot N, Guidasci S. The neonatal EEG: statistical studies and prognostic value in full-term and pre-term babies. Electroencephalogr Clin Neurophysiol 1972;32(5):529-44.
58. Rose AL, Lombroso CT. A study of clinical, pathological, and electroencephalographic features in 137 full-term babies with a long-term follow-up. Pediatrics 1970;45(3):404-25.
59. El-Ayouty M, Abdel-Hady H, El-Mogy S, Zaghlol H, El-Beltagy M, Aly H. Relationship between electroencephalography and magnetic resonance imaging findings after hypoxic-ischemic encephalopathy at term. Am J Perinatol 2007;24(8):467-73.

60. van Rooij LG, Toet MC, Osredkar D, van Huffelen AC, Groenendaal F, de Vries LS. Recovery of amplitude integrated electroencephalographic background patterns within 24 hours of perinatal asphyxia. Arch Dis Child Fetal Neonatal Ed 2005;90(3):F245-51.
61. Biagioni E, Mercuri E, Rutherford M, Cowan F, Azzopardi D, Frisone MF, et al. Combined use of electroencephalogram and magnetic resonance imaging in full-term neonates with acute encephalopathy. Pediatrics 2001;107(3):461-8.
62. Filan P, Boylan GB, Chorley G, Davies A, Fox GF, Pressler R, et al. The relationship between the onset of electrographic seizure activity after birth and the time of cerebral injury in utero. Bjog 2005;112(4):504-7.
63. McBride MC, Laroia N, Guillet R. Electrographic seizures in neonates correlate with poor neurodevelopmental outcome. Neurology 2000;55(4):506-13.
64. Wertheim D, Mercuri E, Faundez JC, Rutherford M, Acolet D, Dubowitz L. Prognostic value of continuous electroencephalographic recording in full term infants with hypoxic ischaemic encephalopathy. Arch Dis Child 1994;71(2):F97-102.
65. Toet MC, Groenendaal F, Osredkar D, van Huffelen AC, de Vries LS. Postneonatal epilepsy following amplitude-integrated EEG-detected neonatal seizures. Pediatr Neurol 2005;32(4):241-7.
66. Holmes GL, Gairsa JL, Chevassus-Au-Louis N, Ben-Ari Y. Consequences of neonatal seizures in the rat: morphological and behavioral effects. Ann Neurol 1998; 44(6):845 57.
67. Laroia N, Guillet R, Burchfiel J, McBride MC. EEG background as predictor of electrographic seizures in high-risk neonates. Epilepsia 1998;39(5):545-51.
68. Mizrahi EM. Consensus and controversy in the clinical management of neonatal seizures. Clin Perinatol 1989;16(2):485-500.
69. Monod N, Ducas P. The prognostic value of the EEG during the first two years of life. Electroencephalogr Clin Neurophysiol 1969;27(1):107.
70. Boylan GB, Pressler RM, Rennie JM, Morton M, Leow PL, Hughes R, et al. Outcome of electroclinical, electrographic, and clinical seizures in the newborn infant. Dev Med Child Neurol 1999;41(12):819-25.
71. Zeinstra E, Fock JM, Begeer JH, van Weerden TW, Maurits NM, Zweens MJ. The prognostic value of serial EEG recordings following acute neonatal asphyxia in full-term infants. Eur J Paediatr Neurol 2001;5(4):155-60.
72. Biagioni E, Boldrini A, Bottone U, Pieri R, Cioni G. Prognostic value of abnormal EEG transients in preterm and full-term neonates. Electroencephalogr Clin Neurophysiol 1996;99(1):1-9.
73. al Naqeeb N, Edwards AD, Cowan FM, Azzopardi D. Assessment of neonatal encephalopathy by amplitude-integrated electroencephalography. Pediatrics 1999;103(6 Pt 1):1263-71.
74. Toet MC, Hellstrom-Westas L, Groenendaal F, Eken P, de Vries LS. Amplitude integrated EEG 3 and 6 hours after birth in full term neonates with hypoxic-ischaemic encephalopathy. Arch Dis Child Fetal Neonatal Ed 1999;81(1):F19-23.
75. Hellstrom-Westas L, Rosen I. Continuous brain-function monitoring: state of the art in clinical practice. Semin Fetal Neonatal Med 2006;11(6):503-11.
76. Shalak L, Perlman JM. Hypoxic-ischemic brain injury in the term infant-current concepts. Early Hum Dev 2004;80(2):125-41.
77. Osredkar D, Toet MC, van Rooij LG, van Huffelen AC, Groenendaal F, de Vries LS. Sleep-wake cycling on amplitude-integrated electroencephalography in term newborns with hypoxic-ischemic encephalopathy. Pediatrics 2005;115(2):327-32.
78. Niemarkt HJ, Halbertsma FJ, Andriessen P, Bambang Oetomo S. Amplitude-integrated electroencephalographic changes in a newborn induced by overdose of morphine and corrected with naloxone. Acta Paediatr 2008;97(1):132-4.
79. De Vries LS, Pierrat V, Eken P, Minami T, Daniels H, Casaer P. Prognostic value of early somatosensory evoked potentials for

adverse outcome in full-term infants with birth asphyxia. Brain Dev 1991;13(5):320-5.
80. de Vries LS. Somatosensory-evoked potentials in term neonates with postasphyxial encephalopathy. Clin Perinatol 1993;20(2):463-82.
81. Eken P, Toet MC, Groenendaal F, de Vries LS. Predictive value of early neuroimaging, pulsed Doppler and neurophysiology in full term infants with hypoxic-ischaemic encephalopathy. Arch Dis Child Fetal Neonatal Ed 1995;73(2):F75-80.
82. Leijser LM, Vein AA, Liauw L, Strauss T, Veen S, Wezel-Meijler G. Prediction of short-term neurological outcome in full-term neonates with hypoxic-ischaemic encephalopathy based on combined use of electroencephalogram and neuro-imaging. Neuropediatrics 2007;38(5):219-27.
83. Rutherford MA, Pennock JM, Counsell SJ, Mercuri E, Cowan FM, Dubowitz LM, et al. Abnormal magnetic resonance signal in the internal capsule predicts poor neurodevelopmental outcome in infants with hypoxic-ischemic encephalopathy. Pediatrics 1998;102(2 Pt 1):323-8.
84. Liauw L, van Wezel-Meijler G, Veen S, van Buchem MA, van der Grond J. Do apparent diffusion coefficient measurements predict outcome in children with neonatal hypoxic-ischemic encephalopathy? AJNR Am J Neuroradiol 2009;30(2):264-70.
85. Barkovich AJ, Hajnal BL, Vigneron D, Sola A, Partridge JC, Allen F, et al. Prediction of neuromotor outcome in perinatal asphyxia: evaluation of MR scoring systems. AJNR Am J Neuroradiol 1998;19(1):143-9.
86. Haataja L, Mercuri E, Guzzetta A, Rutherford M, Counsell S, Flavia Frisone M, et al. Neurologic examination in infants with hypoxic-ischemic encephalopathy at age 9 to 14 months: use of optimality scores and correlation with magnetic resonance imaging findings. J Pediatr 2001;138(3):332-7.
87. Okereafor A, Allsop J, Counsell SJ, Fitzpatrick J, Azzopardi D, Rutherford MA, et al. Patterns of brain injury in neonates exposed to perinatal sentinel events. Pediatrics 2008;121(5):906-14.
88. Shah DK, Mackay MT, Lavery S, Watson S, Harvey AS, Zempel J, et al. Accuracy of bedside electroencephalographic monitoring in comparison with simultaneous continuous conventional electroencephalography for seizure detection in term infants. Pediatrics 2008;121(6):1146-54.

Chapter 2 | Imaging patterns of brain injury in term birth-asphyxia

Renate Swarte

Maarten Lequin

Perumpillichira Cherian

Alexandra Zecic

Johannes van Goudoever

Paul Govaert

Acta Paediatrica 2009;98:586-592

ABSTRACT

Aim: To develop an extended asphyxia score based on cerebral ultrasound and MRI in order to gain further insight into the pathophysiology of asphyxia.

Patients and Methods: First week cerebral US and MRI of 80 asphyxiated term infants were scored according to a new scoring system based on separate grading of injury to deep grey matter and to (sub) cortical/white matter. Our findings were compared with published scoring systems.

Results: Six paradigms were derived: deep grey matter injury with either limited or extensive cortical involvement, damage to deep grey matter with watershed injury, isolated watershed injury, isolated white matter injury (leukomalacia) and isolated cortical necrosis. The mortality rate was considerable in patterns with extensive cortical injury.

Conclusion: Six patterns of brain injury, following term birth asphyxia were found using a new imaging score.

INTRODUCTION AND METHODOLOGY

Postasphyxial encephalopathy affects 1 to 3 per 1000 term newborns (1,2). Many efforts have been directed on prediction of outcome. Miller et al. in 2005 found that patterns of brain injury are associated with different neurodevelopmental outcomes at 30 months, but that measured perinatal risk factors did not predict the pattern of brain injury (3). Also biochemical and clinical perinatal variables such as umbilical artery pH, Apgar score or interval to onset of spontaneous breathing are typically of limited predictive value (1). Various neonatal encephalopathy scores have been developed, using different parameters to predict outcome. Kaufman et al. used a 6 item clinical score and found that this score combined with first day clinical seizures can predict acute imaging findings and outcome (4). Encephalopathy scores are least powerful for moderate encephalopathy, which is the category of interest during acute management (5). Detailed description of neurophysiological findings is outside the scope of this report. Brain imaging was introduced as an important tool in the acute stage and different MRI scores for use in the late first or second week were developed (6,7). These scores, however, just seem to discriminate between good and poor outcome failing to predict with certainty the degree of dysfunction. For this reason we applied an empirical scoring system to a cohort of 80 term newborns admitted from 1999-2007 with perinatal asphyxia and found 26 combinations of injury in six patterns (Table 1). Inclusion criteria were either an Apgar score at 5 minutes lower than six or umbilical artery pH less than or equal to 7.10 (1). Newborns with congenital brain or heart malformation were excluded. These criteria were this wide so as not to miss injury patterns. We used a hierarchical (six degrees) evaluation - as detected with MRI and ultrasound (US) together - of increasing injury to deep grey matter (thalamus/basal ganglia; TBG) and to (sub)cortical/white matter (CWM). MRI scans were performed at a mean of 4 days (range 1-22) after birth. A diffusion-weighted sequence (DWI) was available in 38 % of the infants. Radiological details will be reported in another article.

Six injury patterns were derived from findings in 62 infants (Table

TABLE 1 | Scoring system

Deep grey matter (thalamus/basal ganglia, TBG) injury

grade	description
0	normal
1	perforator stroke
2	isolated bilateral thalamic injury
3	abnormal signal intensity in ventrolateral thalamus and putamen on US or MR without signal inversion of PLIC
4	abnormal signal intensity in ventrolateral thalamus and putamen on US and MR with signal inversion of PLIC; caudate not involved
5	= 4 + caudate involvement
6	= 5 + injury to entire thalamus

(Sub)cortical/white matter injury (CWM)*

grade	description
0	normal
1	bilateral, non-confluent punctate periventricular white matter haemorrhage (high signal on T1, low signal on T2)
2	high T2 signal intensity in subcortical white matter in watershed area(s) with intact cortical ribbon; diffuse hyperechoic change with predominance in the periventricular and parasagittal area
3	2 + focal disappearance of the cortical ribbon in either one rostral or caudal watershed area, or in one hemisphere in both watershed areas
4	2 + focal disappearance of the cortical ribbon in rostral and caudal watershed areas of both cerebral hemispheres
5	diffuse periventricular and subcortical hyperechoic change in white matter, together with abnormal signal intensity on MR (high on T2 and low on T1, indicative of ischaemia and not haemorrhage)
6	extensive cortical injury extending beyond perirolandic and peri-insular cortex; laminar hyperechoic pattern on US and disappearance of the cortical ribbon on T2

* Perirolandic, peri-insular and/or hippocampal cortical highlighting (high signal T1 and low signal on T2, especially in the depths of the sulci) was variably associated with TBG scores 3 to 6 and is not included separately in the CWM score

TABLE 2 | Scoring results

CWM TBG	0	1	2	3	4	5	6	total
0	8	4	4	2	3	2	2	25
1	1	1	1	0	0	3	3	9
2	3	1	0	0	2	0	0	6
3	3	0	0	1	0	0	2	6
4	6	0	0	0	0	0	5	11
5	3	0	2	1	0	0	6	12
6	0	0	0	0	1	0	10	11
total	24	6	7	4	6	5	28	80

1. Deep grey matter injury with limited cortical involvement (rolandic, hippocampal, insular) (12/80, 15%)(TBG 3-6, CWM 0-1)(Figure 1)
2. Deep grey matter injury with extensive cortical involvement (23/80, 29 %) (TBG 3-6, CWM 6)(Figure 2)
3. Deep grey matter injury with watershed injury (7/80, 9 %) (TBG 2-6, CWM 2-4)(Figure 3)
4. Isolated watershed injury (10/80, 13 %) (TBG 0-1, CWM 2-4)(Figure 4)
5. Isolated white matter injury (5/80, 6 %) (TBG 0-1, CWM 5)(Figure 5)
6. Isolated extensive cortical injury (5/80, 6 %) (TBG 0-1, CWM 6)(Figure 6)

The remainder had normal imaging results (n=8), isolated punctate periventricular white matter haemorrhage (n=5, one with perforator stroke), isolated thalamic injury (n=4, 1 with punctate white matter haemorrhage) or isolated perforator stroke (n=1).

CWM: (Sub)cortical/white matter injury score on x-axis
TBG: Deep grey matter (thalamus/basal ganglia) injury score on y-axis

2, Figures 1-6). The three deep grey matter patterns were seen most frequently: a subgroup of the patients involved had clinical brainstem damage. Although sentinel events very often precede injury to deep grey matter (8), they may also relate to watershed injury (3). We review all patterns, focusing on neuropathology and imaging, adding some obstetric and clinical findings. In Figure 7 the patterns we observed are linked with the presence or absence of a sentinel event. Figure 8 presents relations between patterns of injury and outcome.

DEEP GREY MATTER INJURY (PATTERNS 1, 2 AND 3)

In human autopsies of children with birth asphyxia, marbling (status marmoratus) is conspicuous in putamen, thalamus (dorsal, ventrolateral as well as dorsomedial nuclei), caudate, claustrum and subthalamic nucleus (9). Pallidum is affected in about 60 % of cases. A complex mixture is reported of additional lesions in cortex (often in hippocampus, but also in the central gyri and paracentral lobule, calcarine and insular cortex), white matter, brainstem and cerebellum (dentate nuclei and Purkinje cells) (10). Selective vulnerability of the thalamo-cortico-striatal motor loop is linked to glutamate-induced excitotoxic damage; concurrent hypoglycaemia or hyperbilirubinemia might enhance the risk of cell death in pallidum (11). Clinical findings often correlate with regional cell death; these literature findings are presented in Table 3 (2). Pathologists further delineated the neonatal cardiac arrest type of diencephalic and brainstem/cerebellum injury, often with prolonged fetal bradycardia as a common antecedent. The hallmark of brainstem injury is symmetrical inferior collicular necrosis, but other vulnerable nuclei are tegmental reticular formation, cranial nerve nuclei, superior collicles, red nucleus, substantia nigra, locus ceruleus, cuneate and gracile nuclei, inferior olive and spinal cord anterior horn cells (12,13). A protective effect of cooling on deep grey matter injury is therefore likely and this was found for infants with moderately abnormal early amplitude-integrated EEG findings (14).

On any imaging sequence, the lesions are by definition bilateral and symmetrical (Figure 1). Thalamus is almost constantly affected (15,16). Hypersignal in thalamus and putamen can be seen on DWI within 24-48 hours (17). The MR appearance varies with severity and duration of injury and time between injury and imaging: affected nuclei develop T1-hyperintensity and T2-hypointensity mixed with punctiform hypersignal together with a variable decrease in T1-signal of the posterior limb of the internal capsule (PLIC) referred to as signal inversion (15,16).

In the present study deep grey matter injury presented on US from the second day on with a relatively hypoechoic internal capsule, standing out against a hyperechoic thalamus. The echo-bright thalamus was present for months, due to gliosis and ferrugination. After three days putamen became hyperechoic: this presented as 'four columns' of hyperechoic change in coronal sections (Figure 1). Changes in putamen subsided after two weeks. Cavitation may occur in putamen, not in thalamus.

Deep grey matter injury was associated with either mild (pattern 1) or extensive (pattern 2) cortical lesion, Sentinel events seemed to predispose to extensive cortical injury (Figure 2). Injury to globus pallidus correlated with extensive cortical injury. Watershed injury, leukomalacia and cortical injury occurred in isolation of or in combination with deep grey matter injury. The association of severe deep grey matter with watershed injury is unusual but it was seen in seven newborns (pattern 3, Figure 3). Most children with extensive deep grey matter injury died a few days after birth, others developed spastic quadriplegic or dyskinetic quadriplegic (athetosis and/or dystonia) cerebral palsy (CP). These conditions likely are related to the extent of cortical injury (18).

ISOLATED WATERSHED INJURY (PATTERN 4)

During a brief episode of cerebral hypoperfusion, not severe enough to cause frank infarction or widespread necrosis, arterial border zones are especially vulnerable. Watershed injury culminates in the posterior parietal areas (19). It is one of the acute changes preceding ulegyria (focal gyral atrophy). Watershed injury was identified in the living newborn using technetium and PET scan (20). The acute MRI finding is parasagittal hyperintensity on T2-weighted MRI mainly of the centrum

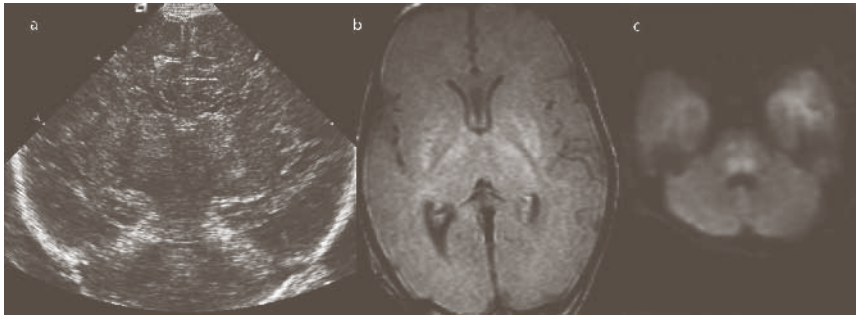

FIG 1 | Pattern (1 a) coronal US; 2 columns of hyperechoic change in thalamus, (b) proton density MR; hypersignal in lateral thalamus and putamen, (c) DWI; hypersignal in ventral (corticospinal tracts) and dorsal (tegmentum and cranial nuclei) pons

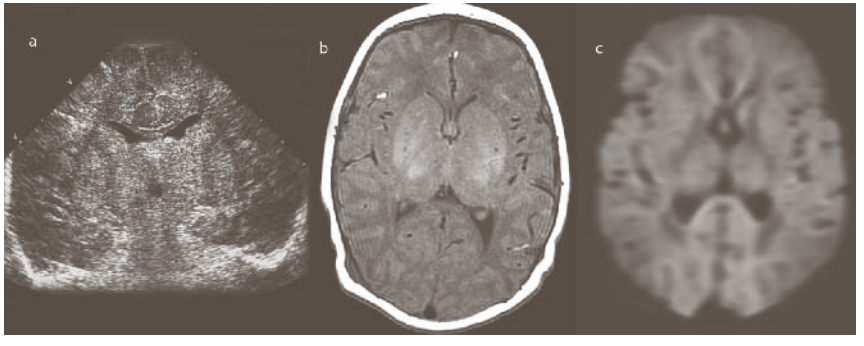

FIG 2 | Pattern (2 a) coronal US; 4 columns of hyperechoic change in thalamus and striatum, also hyperechoic change in caudate head, (b) T1-weighted MRI; hypersignal in lateral thalamus and putamen with signal inversion of PLIC, (c) DWI; hypersignal in thalamus, putamen, caudate and entire cerebral (sub)cortex ('white cerebrum')

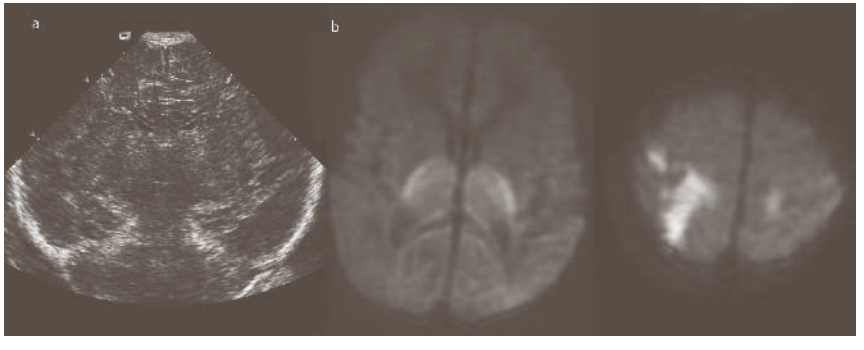

FIG 3 | Pattern (3 a) coronal US; mild hyperechoic damage in thalami on coronal US, (b) DWI; hypersignal in thalamus and PLIC on both sides (left), hypersignal in right posterior parieto-occipital watershed area (right)

semiovale but extending into the subcortex in arterial border zones (21). In the present study MRI is superior to US to describe such - often relatively subtle - subcortical lesions (Figure 4). We did not always observe clinical neonatal seizures unlike other researchers (22). Ulegyria may be associated with childhood epilepsy for which drug refractoriness is not uncommon (23). None of the patients in our study developed epilepsy within the first year. CP may be a consequence of extensive watershed injury (3) as in three of our patients. On the other hand, one patient developed attention deficit disorder without motor dysfunction at 5 years of age, in line with reports of cognitive/behavioral dysfunction following isolated perinatal watershed injury (3).

PRIMARY LEUKOMALACIA (PATTERN 5)

White matter injury is often described with the watershed injury pattern (6,15). A recent report acknowledges the existence of primary white matter injury due to term perinatal asphyxia (24). The Hammersmith group also recognized mild, moderate and severe white matter changes (7,14). White matter injury was visualized in the first week of life by virtue of high signal on proton density images and of decreased cortex/white matter differentiation on T1- and T2-weighted MRI; in the second week cortex/white matter differentiation returned or even increased. At 2 years follow-up, development of these infants was characterized by developmental quotients (DQs) below 85, and by seizures and microcephaly rather than by CP. On the other hand, some infants with multicystic leukomalacia developed spastic quadri- or diplegia. US correlation was absent.

In our experience high resolution US is essential for detecting postasphyxial leukomalacia. A striking observation in the present study was gradual increase in echo contrast between relatively dark cortex and extremely bright subcortical white matter in areas extending beyond the border zones and perirolandic cortex, for instance in cingulate gyrus (Figure 5). It may be difficult to distinguish extreme watershed injury from leukomalacia. We saw this pattern on day 2 but it intensified over the next few days, contrary to what was observed for congestion or punctate haemorrhage. This suggests an ongoing process, maturing over days, in all likelihood a primary axonal pattern of damage. Extreme hyperechogenicity may precede cyst formation or early ventriculomegaly without cavitating intermediary. In three of the five newborns with primary leukomalacia in the present study, caudate nucleus was gradually (probably secondarily) affected. Outcome varied: one infant died, one developed spastic quadriplegia, two showed normal development at the age of two years, and one was lost to follow-up. The EEG's in the child who developed CP, and in the one who died were severely abnormal, suggesting EEG predicts outcome in this heterogeneous group.

ISOLATED CORTICAL NECROSIS (PATTERN 6)

Regional grey matter injury in cerebral cortex, including hippocampus (subiculum and H1), and internal cerebellar granular layer, was the salient postmortem finding in term newborns with postasphyxial status epilepticus (25). All lobes can be affected, at the convexity of the gyri and in the depths of the sulci. Total necrosis is seen next to patchy necrosis, inhibitory neurons may survive the insult (26). Neocortical cell death is often reported in association with the deep grey matter-brainstem injury. From the present study it appears that it can also be a pattern of its own. On first week MRI scans a shortening of T1-weighted signal in pre- and postcentral gyral cortex caused 'cortical highlighting' (Figure 6). Extensive (sub)cortical injury presented as 'white cerebrum' in acute DWI as is reported in the literature (27). Using sonography cortical necrosis was only recognizable in the latter part of the first week when a variable border of subcortical white matter tended to merge into one hyperechoic zone with cortex and sulcus, in a variegate pattern, well seen in sulcus cinguli and parasagittal and insular sulci. Hyperechoic change may turn into subcortical cysts at the end of the second week. Ventriculomegaly is often associated. All five patients with isolated cortical necrosis developed early clinical seizures. Four died, and the fifth showed delayed development without CP at 2 years.

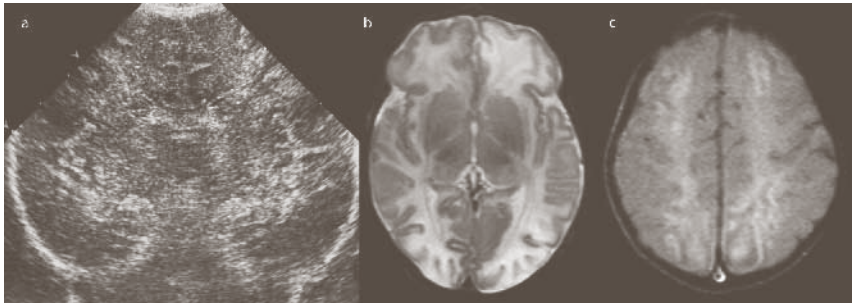

FIG 4 | Pattern (4 a) coronal US: hyperechoic change in both parasagittal watershed areas between anterior and middle cerebral arteries, (b) T2-weighted MRI: hyperintensity of white matter and blurring of adjacent cortex in left anterior and posterior and in right posterior watershed areas, (c) proton density MR; findings as in b

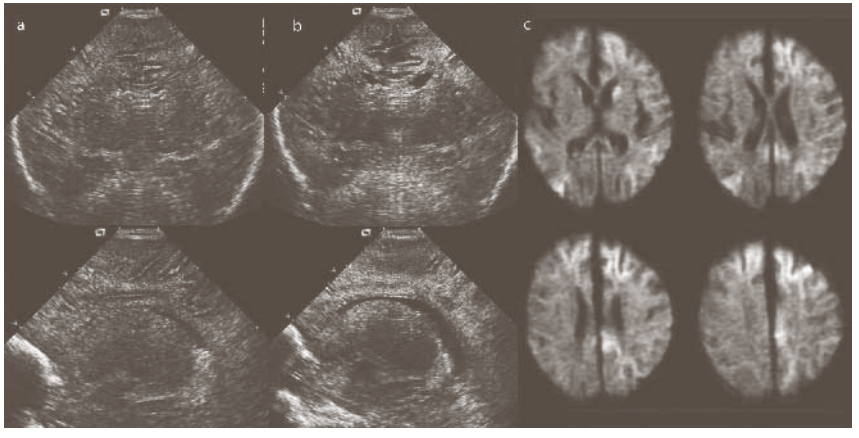

FIG 5 | Pattern (5 a,b) sequential coronal (a,b) and parasagittal (a,b) US scans: the evolution of white matter hyperechoic change from day 2 to day 6, with increase of subcortical brightness (contrasting with dark cortex) in the first week; observe hyperechoic change of caudate in parasagittal section on day 6, (c) DWI: hypersignal in frontal and parietal white matter and in caudate head on day 5

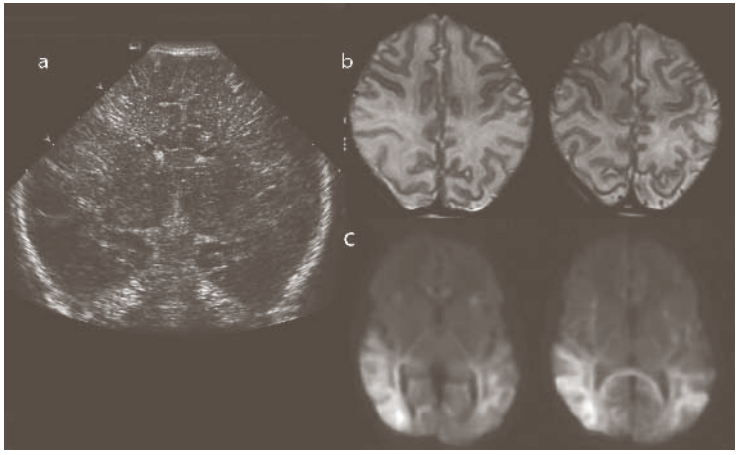

FIG 6 | Pattern (6 a) coronal US: blurring of insular and posterior frontal cortex by hyperechoic change around sulci (day 5), (b) T2-weighted MRI: hypersignal in parietal and temporo-occipital (sub)cortex with disappearance of the cortical ribbon (day 5), (c) DWI; as in b plus hypersignal in splenium; normal deep grey matter (day 5)

MILD WHITE MATTER INJURY

Often punctate echodensities in white matter did not reflect injury but rather congestion, mild increase in cellularity or punctate bleeding of limited consequence. They were rated 1 in the (sub)cortical/white matter injury score. Reversal of these findings within a few days is a good prognostic sign. Corresponding punctate or conglomerate areas of T1 and T2 shortening are seen in the periventricular zone (28).

TRANSAXONAL NETWORK CHANGES

Our group found that following the above primary injuries, connected thalamic and brainstem nuclei undergo excitotoxic injury due to cortical hyperactivity or delayed neurodegeneration due to loss of trophic support from their cortical targets (29). Others recently reported an association between thalamic injury and atrophy of cerebellar vermis in term asphyxia (30). Caudate involvement in our cohort possibly followed extensive (sub)cortical or white matter injury as a secondary pattern. Such associations need to be studied further in the light of existing network injury.

CONCLUSION

In an empirical scoring system based on two arms of injury (to deep grey matter and (sub)cortical/white matter) and applied to a cohort of 80 newborns with perinatal asphyxia we found 26 combinations of injury in six patterns. We do not claim superiority of the score to predict outcome, but it is a fine tool to demonstrate the patterns of injury. Sentinel events not always precede deep grey matter damage. Brainstem damage needs further study (e.g. on the correlation between clinical signs and regional ADC-values). We add isolated cortical necrosis and primary leukomalacia to the existing injury patterns. US correlation is important for the latter. Pallidal injury is probably a primary lesion in severe asphyxia only. Caudate cell death may follow extensive (sub)cortical injury. Prospective use of this score will permit refined prediction of cognitive and behavioural outcome.

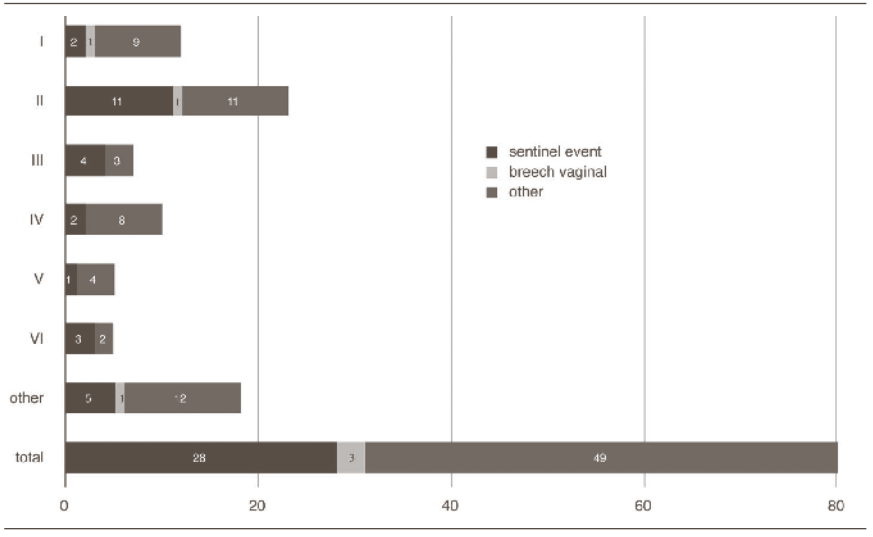

FIG 7 | relation in 80 patients between injury pattern on y-axis and presence (n=28)/absence (n=49) of a sentinel event on the x-axis; sentinel event defined as: abruptio, uterine rupture, cord prolapse, maternal collapse, severe antepartum haemorrhage or terminal fetal bradycardia; three infants were asphyxiated during vaginal breech delivery

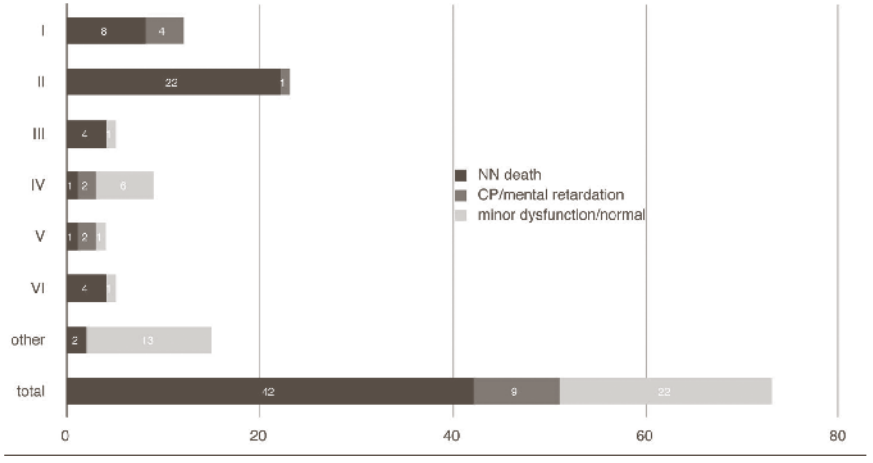

FIG 8 | relation in 73 patients between injury pattern on y-axis and crude outcome data on the x-axis; 7 other infants were lost to follow-up (NN early neonatal)

TABLE 3 | Relation between injury side and clinical findings

Region	Neonatal findings	Outcome
cerebral cortex	lowered level of consciousness, seizures, pseudobulbar paresis	mental dysfunction, spastic CP, pseudobulbar palsy, cerebral visual impairment
thalamus	abnormal arousal, abnormal SSEPs, seizures, tremor	impaired intellect
striatum	early changes in muscle tone, tremor	dyskinetic CP (can be of delayed onset; dystonia correlates with pallidal injury; signs less conspicuous with concomitant pyramidal tract injury), contribution to visual deficits
hypothalamus	diabetes insipidus, inappropriate ADH secretion, hyper- and hypotension	early sexual maturation
dorsal brainstem	oculomotor disturbances (including ptosis, ictal nystagmus), abnormal ABR, abnormal arousal (reticular formation)	hearing deficit, oculomotor dyspraxia, bulbar palsy necessitating tube feeding
spinal cord	hypotonia, weakness, hypo- or areflexia, disturbed swallowing and sucking, facial weakness, tongue fasciculations	atonic CP

REFERENCES

1. Levene MI. The asphyxiated newborn infant. In: Levene MI, Chervenak FA, Whittle M. Fetal and Neonatal Neurology and Neurosurgery. 3th ed. Toronto: Churchill Livingstone, 2001.
2. Volpe JJ. Hypoxic-ischemic encephalopathy. In: Volpe JJ. Neurology of the newborn. 4th ed. Boston: WB Saunders, 2001.
3. Miller SP, Ramaswamy V, Michelson D, Barkovich AJ, Holshouser B, Wycliffe N, et al. Patterns of brain injury in term neonatal encephalopathy. J Pediatr 2005;146:453-460.
4. Kaufman SA, Miller SP, Ferriero DM, Glidden DH, Barkovich AJ, Partridge JC. Encephalopathy as a predictor of magnetic resonance imaging abnormalities in asphyxiated newborns. Pediatr Neurol 2003;28:342-346.
5. Lindstrom K, Hallberg B, Blennow M, Wolff K, Fernell E, Westgren M. Moderate neonatal encephalopathy: pre- and perinatal risk factors and long-term outcome. Acta Obstet Gynecol Scand 2008;87:503-509.
6. Barkovich AJ, Hajnal BL, Vigneron D, Sola A, Partridge JC, Allen F, et al. Prediction of neuromotor outcome in perinatal asphyxia: evaluation of MR scoring systems. AJNR Am J Neuroradiol 1998;19:143-149.
7. Haataja L, Mercuri E, Guzzetta A, Rutherford M, Counsell S, Flavia Frisone M, et al. Neurologic examination in infants with hypoxic-ischemic encephalopathy at age 9 to 14 months: use of optimality scores and correlation with magnetic resonance imaging findings. J Pediatr 2001;138:332-337.
8. Okereafor A, Allsop J, Counsell SJ, Fitzpatrick J, Azzopardi D, Rutherford MA, et al. Patterns of brain injury in neonates exposed to perinatal sentinel events. Pediatrics 2008;121:906-914.
9. Malamud N. Status marmoratus; a form of cerebral palsy following either birth injury or inflammation of the central nervous system. J Pediatr 1950;37:610-619.
10. Leech RW, Alvord EC, Jr. Anoxic-ischemic encephalopathy in the human neonatal period. The significance of brain stem involvement. Arch Neurol 1977;34:109-113.
11. Johnston MV, Hoon AH, Jr. Possible mechanisms in infants for selective basal ganglia damage from asphyxia, kernicterus, or mitochondrial encephalopathies. J Child Neurol 2000;15:588-591.
12. Schneider H, Ballowitz L, Schachinger H, Hanefeld F, Droszus JU. Anoxic encephalopathy with predominant involvement of basal ganglia, brain stem and spinal cord in the perinatal period. Report on seven newborns. Acta Neuropathol (Berl) 1975;32:287-298.
13. Clancy RR, Sladky JT, Rorke LB. Hypoxic-ischemic spinal cord injury following perinatal asphyxia. Ann Neurol 1989;25:185-189.
14. Rutherford M, Ward P, Allsop J, Malamatentiou C, Counsell S. Magnetic resonance imaging in neonatal encephalopathy. Early Hum Dev 2005;81:13-25.
15. Barkovich AJ, Westmark K, Partridge C, Sola A, Ferriero DM. Perinatal asphyxia: MR findings in the first 10 days. AJNR Am J Neuroradiol 1995;16:427-438.
16. Rutherford MA, Pennock JM, Schwieso JE, Cowan FM, Dubowitz LM. Hypoxic ischaemic encephalopathy: early magnetic resonance imaging findings and their evolution. Neuropediatrics 1995;26:183-191.
17. Barkovich AJ, Miller SP, Bartha A, Newton N, Hamrick SE, Mukherjee P, et al. MR imaging, MR spectroscopy, and diffusion tensor imaging of sequential studies in neonates with encephalopathy. AJNR Am J Neuroradiol 2006;27:533-547.
18. Krageloh-Mann I, Helber A, Mader I, Staudt M, Wolff M, Groenendaal F, et al. Bilateral lesions of thalamus and basal ganglia: origin and outcome. Dev Med Child Neurol 2002;44:477-484.
19. Brann AW, Myers RE. Central nervous system findings in the newborn monkey following severe in utero partial asphyxia. Neurology 1975;25:327-338.

20. Volpe JJ, Herscovitch P, Perlman JM, Kreusser KL, Raichle ME. Positron emission tomography in the asphyxiated term newborn: parasagittal impairment of cerebral blood flow. Ann Neurol 1985;17:287-296.
21. Kuenzle C, Baenziger O, Martin E, Thun-Hohenstein L, Steinlin M, Good M, et al. Prognostic value of early MR imaging in term infants with severe perinatal asphyxia. Neuropediatrics 1994;25:191-200.
22. Sato Y, Okumura A, Kato T, Hayakawa F, Kuno K, Watanabe K. Hypoxic ischemic encephalopathy associated with neonatal seizures without other neurological abnormalities. Brain Dev 2003;25:215-219.
23. Villani F, D'Incerti L, Granata T, Battaglia G, Vitali P, Chiapparini L, et al. Epileptic and imaging findings in perinatal hypoxic-ischemic encephalopathy with ulegyria. Epilepsy Res 2003;55:235-243.
24. Li AM, Chau V, Poskitt KJ, Sargent MA, Lupton BA, Hill A, et al. White Matter Injury in Term Newborns with Neonatal Encephalopathy. Pediatr Res 2008.
25. Larroche JC. [Massive cerebral necrosis in newborn infants. Its relation to maturation, its clinical and bioelectric symptoms]. Biol Neonat 1968;13:340-360.
26. Marin-Padilla M. Perinatal brain damage, cortical reorganization (acquired cortical dysplasias), and epilepsy. Adv Neurol 2000;84:153-172.
27. Vermeulen RJ, Fetter WP, Hendrikx L, Van Schie PE, van der Knaap MS, Barkhof F. Diffusion-weighted MRI in severe neonatal hypoxic ischaemia: the white cerebrum. Neuropediatrics 2003;34:72-76.
28. Cornette LG, Tanner SF, Ramenghi LA, Miall LS, Childs AM, Arthur RJ, et al. Magnetic resonance imaging of the infant brain: anatomical characteristics and clinical significance of punctate lesions. Arch Dis Child Fetal Neonatal Ed 2002;86:F171-177.
29. Govaert P, Zingman A, Jung YH, Dudink J, Swarte R, Zecic A, et al. Network injury to pulvinar with neonatal arterial ischemic stroke. Neuroimage 2008;39:1850-1857.
30. Sargent MA, Poskitt KJ, Roland EH, Hill A, Hendson G. Cerebellar vermian atrophy after neonatal hypoxic-ischemic encephalopathy. AJNR Am J Neuroradiol 2004;25:1008-1015.

Chapter 3 | Is there need for a new MRI scoring system in term birth asphyxia?

Renate M.Swarte

Paul Govaert

Alexandra Zecic

Maarten Lequin

Submitted

ABSTRACT

Background: Several patterns of brain injury follow perinatal asphyxia at term. Prognostication from published MRI scores and patterns remains difficult.

Objective: To evaluate existing scoring systems for brain damage after asphyxia, based on MRI.

Materials and Methods: We developed a new Sophia scoring system in a cohort of 84 term babies, based on a two-armed grading of injury i.e. to thalamus and basal ganglia, and to (sub)cortex and white matter. Retrospectively 84 MRIs were scored and compared with the existing scoring systems. Follow-up examination was performed at a minimum age of 2 years.

Results: A significant correlation was found for the Sophia MRI sum score with the Hammersmith score (r =0.87) as well as the Barkovich score (BG/W score; r =0.81). Deep grey matter injury was common and associated with a mortality rate of 89 %. Our Sophia MRI sum score depicts post asphyxial leukomalacia and isolated extensive cortical injury as new paradigms.

Conclusion: We found that the Hammersmith score is most useful in clinical practice; the Sophia score is preferred for studying additional injury patterns.

INTRODUCTION

Selective neuronal cell death, which follows asphyxia around term birth, occurs in two regional distributions: (i) one in the brainstem, striatum and thalamus and (ii) the other in the cerebral cortex with a rostral to caudal decrease of vulnerability, the brain stem least sensitive (1). Subsequent studies added parasagittal cerebral injury ("border zone infarction") (2) and focal infarction (arterial or venous occlusion). It is still unclear how selective neuronal cell death is related to hypoperfusion in each brain area. Patterns may be mixed, however, because asphyxia during delivery of the human infant may start as prolonged hypoxia, but is superimposed in the end by cardiovascular collapse of variable duration. Neonatal MRI scores relating extent of injury to outcome have previously been developed (3-7). The two most used are revealed by the Hammersmith and Barkovich group (Appendix). These scores discriminate between good and poor outcome at a minimum age of 12 months. The one developed by Hammersmith is based on signal intensity change in and around the posterior limb of the internal capsule (PLIC) and in the cortical ribbon (3,7). It distinguishes seven subgroups of increasing degree of injury [6, see Appendix for details]. Cerebral palsy (CP) at 4 years and suboptimal neurological status at 1 year, were seen in various proportions of all subgroups except in those with moderate white matter

or minimal basal ganglia injury. Barkovich and coworkers assess basal ganglia injury (BG), watershed lesions (W) and a combination thereof (BG/W). The BG/W score appeared most useful for predicting short term outcome and predictive accuracy was stronger for MRI performed in the late neonatal period [4,8]. These scores are limited, however, in several aspects: impossibility to score isolated cortical injury; no interpretation of discrete injury to different deep grey nuclei; lumping of injury to (sub) cortex and deep grey matter.

In this article we describe a new scoring system (referred to as the Sophia score) and compare it with the existing ones. We scored 84 instances of term birth asphyxia. The Sophia score assumes the existence of separate injury paradigms for deep and cortical grey matter as well as for white matter, and uses hierarchical arms to score thalamus and basal ganglia (Sophia TBG-score) versus (sub)cortex and white matter (Sophia CWM-score). The main goal was not to propose the ideal score, which will need robust long term outcome data in many survivors, but to describe, as completely as possible, separate imaging paradigms of injury in term birth asphyxia, as currently depicted with MR in our daily clinical practice. These findings add to recent efforts to delineate post asphyxial injury patterns (9-13). The clinical relevance of understanding these patterns was discussed in a related paper (14).

MATERIALS AND METHODS

Patients. We retrospectively analyzed the clinical records and imaging studies of 84 encephalopathic term newborns (gestational age › 37 weeks), born January 2001 to May 2006, and admitted to the Sophia Children's Hospital. Asphyxia was defined by a combination of fetal distress, depression at birth, and early (within 24 hours) neonatal encephalopathy (15). Depression at birth was defined as either an Apgar score at 5 minutes lower than 6 or umbilical cord pH less than or equal to 7.10, if available. Newborns with congenital brain anomaly were excluded. Imaging had been part of routine management.

Magnetic Resonance Imaging. Over the study period three different MR imaging systems had been used: a Philips 1.0 Tesla system (Eindhoven, the Netherlands), a Philips 1.5 Tesla system (Eindhoven, the Netherlands) and a GE 1.5 Tesla scanner (Milwaukee, WI). All studies adhered to the same protocol, i.e. axial dual T2 spin echo, axial T1 spin echo or axial T13D spoiled gradient echo, sagittal T1 spin echo and coronal fluid attenuated inversion recovery. On the two Philips systems, DW images were obtained in 6 gradient directions with sensitivity of b = 1000 s/mm (1.5 Tesla system) or b = 783 s/mm² (1.0 Tesla system), TR/TE = 8000/111.8-91.8 ms, one average, field of view of 18-24 cm, slice thickness 4 mm and a spacing of 0.4 mm. On the GE scanner, diffusion tensor images were acquired using multi repetition, single shot echo-planar sequence with a slice thickness of 3 mm with no gap. The images were gathered in 25 gradient directions with sensitivity of b = 1000 s/mm², TR/TE = 9150/98-91 ms, field of view 18-24 cm. A standard quadrature head coil was used on the Philips systems and a dedicated neonatal coil on the GE system. Scoring was performed building on information of all of these sequences.

Scoring. MR scoring was independently performed by a paediatric neuroradiologist and two neonatologists; all three were unaware of the outcome. Final classification was by consensus. A brain part was considered injured when all three observers agreed on definite signal intensity alteration in any MR sequence. This visual based scoring system is described in Table 1 and Figures 1a and 1b, respectively for the TBG-arm (Sophia TBG-score) and for the CWM-arm (Sophia CWM-score). Concerning the scoring system we limited to MRI and left out US findings in order to compare to the existing MRI scoring systems. It comprises a six-step grading for each of the arms, based on our clinical experience with severity estimation. Lumping both scores is the Sophia MRI sum score. The most severe of the clearly abnormal changes in any sequence decided the score. CWM-score 5 was assigned only when MRI findings were limited to subcortical white matter and did not involve the cortical ribbon. After consensus had been reached on Sophia score results, one observer (PG) scored the images of all patients by the Barkovich and Hammersmith systems. A pattern was felt to be consistent if at least three patients presented with similar findings.

Outcome. Crude outcome data (poor: neonatal death or CP, good: normal or impairment without CP) were collected. Outpatients underwent a neurological exam and a Denver developmental screening test up to two years of age.

Statistical analysis. Cross tables with Fisher's exact Test were used for the categorical variables. Scores were correlated with outcome using the Spearman correlation coefficient. A p-value ‹ 0.05 was considered significant. Receiver operator curves were drawn for thresholds in several scores in relation to outcome.

The Erasmus MC Medical Ethical Review Board granted permission to use patient data for scientific publication.

TABLE 1 | Sophia MRI imaging scoring system

grade	thalamus/basal ganglia (TBG-score)	(sub)cortex/white matter (CWM-score)
0	normal	normal
1	focal infarction or bleeding	bilateral, non-confluent punctate periventricular white matter haemorrhage (high signal on T1, low signal on T2)
2	isolated bilateral thalamic injury, MRI with normal PLIC	high T2 signal intensity in subcortical white matter in watershed area(s) with intact cortical ribbon
3	abnormal signal intensity in ventrolateral thalamus and putamen with normal PLIC signal intensity on T1	2 + focal disappearance of the cortical ribbon in either one rostral or caudal watershed area, or in one hemisphere in several watershed areas
4	abnormal signal intensity in ventrolateral thalamus and putamen with inverted PLIC signal intensity on T1; caudate not involved	2 + focal disappearance of the cortical ribbon in rostral and caudal watershed areas of both cerebral hemispheres
5	4 + caudate involved	Abnormal signal intensity in diffuse periventricular and subcortical white matter(high on T2 and low on T1)
6	4 or 5 + injury to the entire thalamus	extensive cortical injury extending beyond perirolandic and peri-insular cortex; disappearance of the cortical ribbon on T2 in affected areas

Perirolandic, peri-insular and/or hippocampal cortical highlighting (high signal T1 and low signal on T2, especially in the depths of the sulci) was variably associated with TBG scores 3 to 6 and is not included separately in the CWM score

FIG 1 | Sophia score for TBG in *a*, for CWM in *b*. An image is representative for each grade. Grading is detailed in Table 1

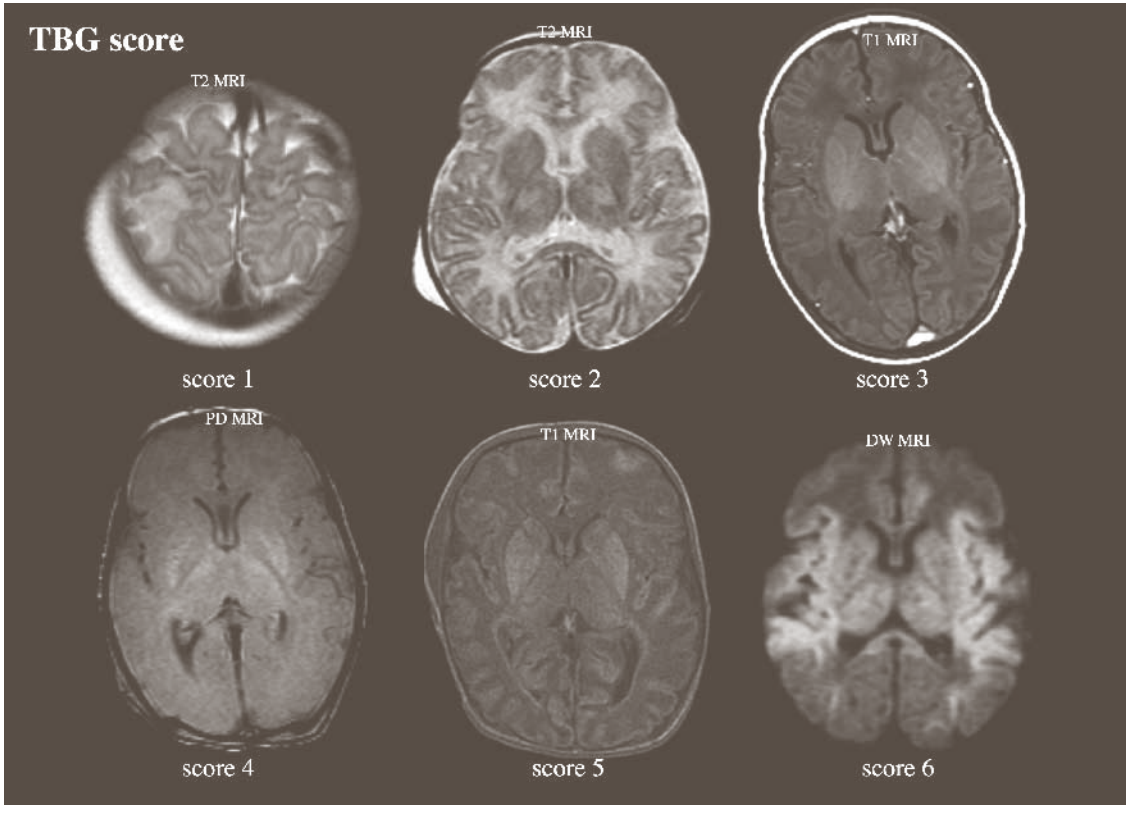

Fig. 1a

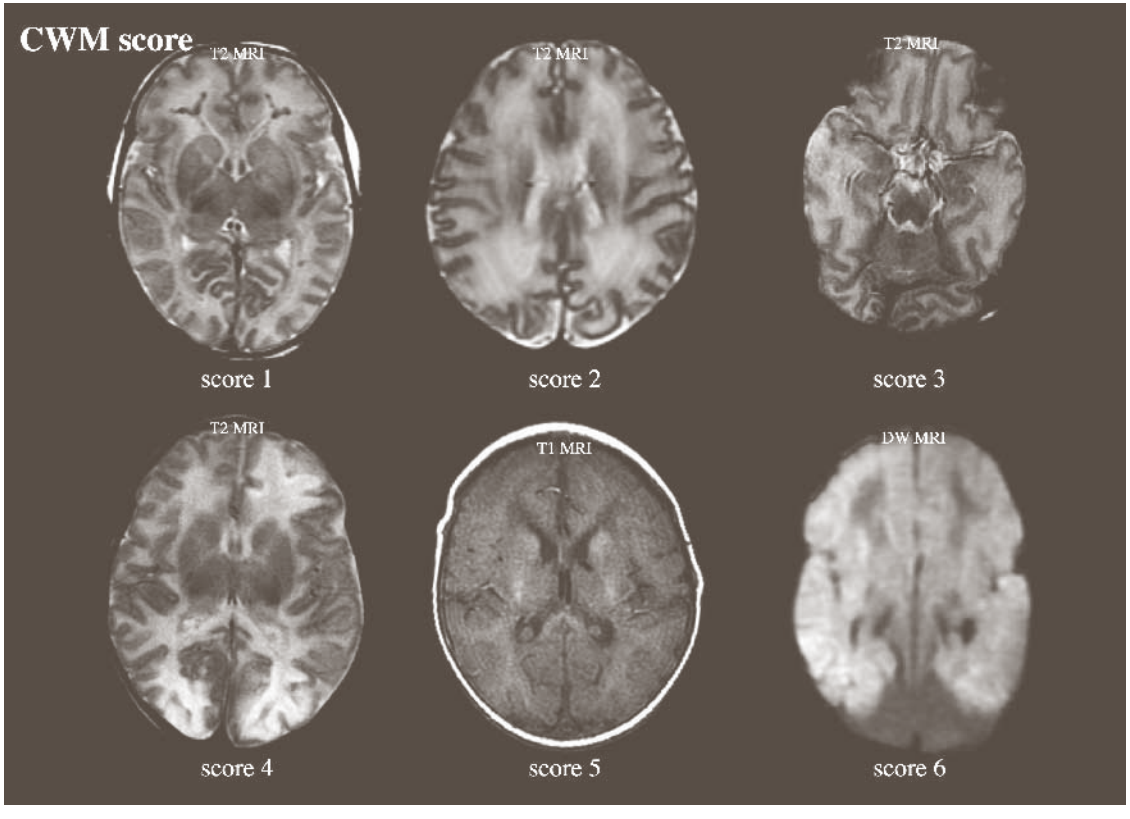
CWM score
T2 MRI
score 1
T2 MRI
score 2
T2 MRI
score 3
T2 MRI
score 4
T1 MRI
score 5
DW MRI
score 6

Fig. 1b

RESULTS

We studied MR sequences of 84 patients, made at a median of 4 days after birth (range 2 to 10 days). In our hospital the extent of brain injury is customarily studied on day four, when infants often are still on a ventilator. T1- and T2- sequences were available in all patients, proton density sequences in 82 (99 %), a coronal FLAIR sequence in 50 (60 %), and a diffusion sequence (recently DTI) in 59 (70 %). Fifty-four of the 84 infants died in the neonatal period. Of the 31survivors 9 developed CP, 2 impairment without CP, 15 developed within normal limits, and 4 were lost to follow-up.

Prediction of poor outcome: the Sophia MRI sum score strongly correlated with both the Hammersmith score (r =0.87) and the Barkovich score (BG/W; r =0.81). Table 2 compares the Sophia MRI score with outcome; deep grey matter injury (TBG-scores 3-6) was common and associated with a mortality rate of 89%. Using ROC curves for the MRI scores described above; the Hammersmith score seems to be the best score for predicting outcome (Figure 2). Table 3 compares different Sophia MRI scoring thresholds with the Hammersmith score. Sensitivity, specificity, positive and negative predictive values and confidence intervals for outcome were counted. Positive predictive values and sensitivity were highest for [Sophia TBG + CWM: 7-12 versus 0-6], [Sophia TBG 3-6 versus 0-2], [Hammersmith 6-7 versus 0 5].

The score permitted recognition of six injury patterns (table 4).

Other findings: several abnormalities did not fit into the Sophia score, some of which - like bilateral extensive multifocal symmetrical white matter haemorrhage with patent sinus and deep veins - may well be patterns of injury of their own (Figure 3).

FIG 2 | ROC curves for imaging scores based on MRI

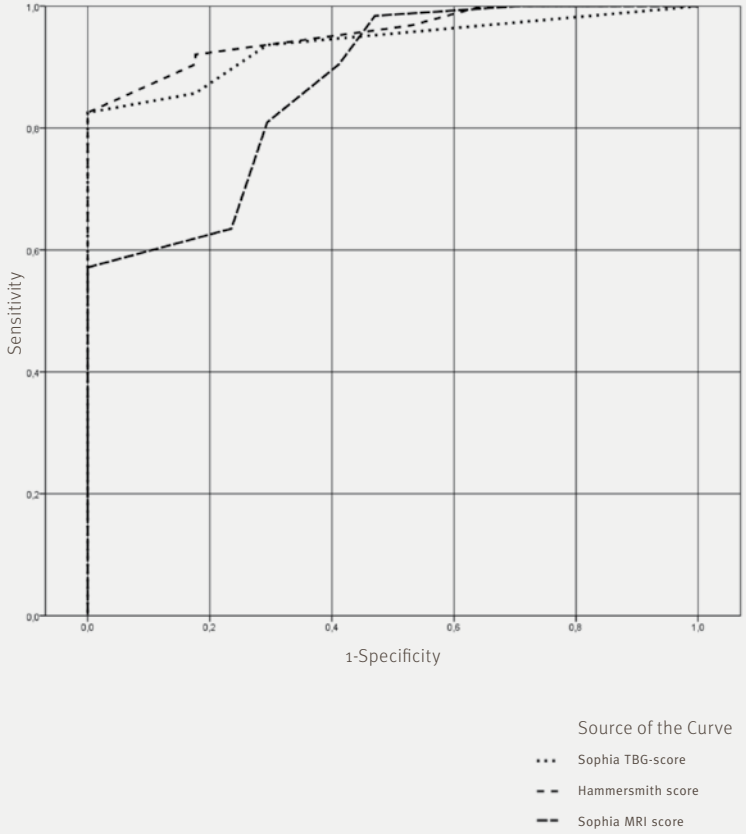

TABLE 2 | Sophia MRI score related to outcome

TBG-score	n	Neonatal death	CP	Impairment	Normal development	Lost to follow-up
0	18	2	2	1	11	2
1	7	2	3	1	1	0
2	5	2	0	0	3	0
3	9	6	2	0	0	1
4	13	12	1	0	0	0
5	18	16	1	0	0	1
6	14	14	0	0	0	0
Subtotal TBG	**84**	**54**	**9**	**2**	**15**	**4**
CWM-score						
0	22	13	3	0	5	1
1	5	2	0	0	3	0
2	7	1	1	0	3	2
3	5	2	2	0	1	0
4	4	0	1	0	3	0
5	7	2	2	1	2	0
6	34	33	0	1	0	0
Subtotal CWM	**84**	**53**	**9**	**2**	**17**	**3**

DISCUSSION

In this study a hierarchical brain imaging score of injury to thalamus plus basal ganglia and to (sub)cortex plus white matter was applied to a cohort of 84 term newborns with perinatal asphyxia. At least six consistent patterns of injury were derived, and some additional lesions may prove to be patterns of their own. The different patterns are depicted in Figure 4. The deep grey matter pattern was most common, and was associated with a mortality rate of 64 %. Our findings are consistent with the existence of a wide spectrum of (sub)cortical injury associated with deep grey matter damage. Isolated leukomalacia and isolated cortical injury were for the first time embedded in a classification system. Below we will describe the patterns of injury observed.

Regional grey matter injury (TBG-scores 3-6, combined with different degrees of (sub)cortical injury into patterns I, II and III, as in Table 4). Deep grey matter injury with watershed injury was defined as TBG-scores 3-6/CWM-scores 2-4 in contrary to the reference article (14). We now think that deep grey matter injury with serious consequences starts from TBG-score 3 instead of TBG-score 2. The end stage of this pattern, myelinated scarring (status marmoratus), is seen in dorsal thalamic nuclei, lateral as well as medial, and also in putamen, caudate, claustrum and subthalamic nucleus (16-18). Leech and Alvord confirmed at postmortem dorsomedial and ventrolateral thalamic injury in the early (neonatal) stage (1). They reported additional lesions in cortex (often in hippocampus, but also in the central gyri and paracentral lobule, calcarine cortex, insular cortex), white matter, brainstem (colliculi and reticular formation) and cerebellum (dentate nuclei and Purkinje cells). A cycle of injury is triggered in the thalamo-cortico-striatal loop, often sparing pallidum due to lower glutamate exposition (19). Within this entity pathologists delineated the neonatal cardiac arrest type of combined diencephalic and brainstem/cerebellum injury (20-22), for which prolonged fetal bradycardia is a common antecedent (23). The hallmark here is symmetrical inferior collicular necrosis, but also vulnerable are thalamus, hypothalamus and hippocampus; tegmental reticular formation, adjacent

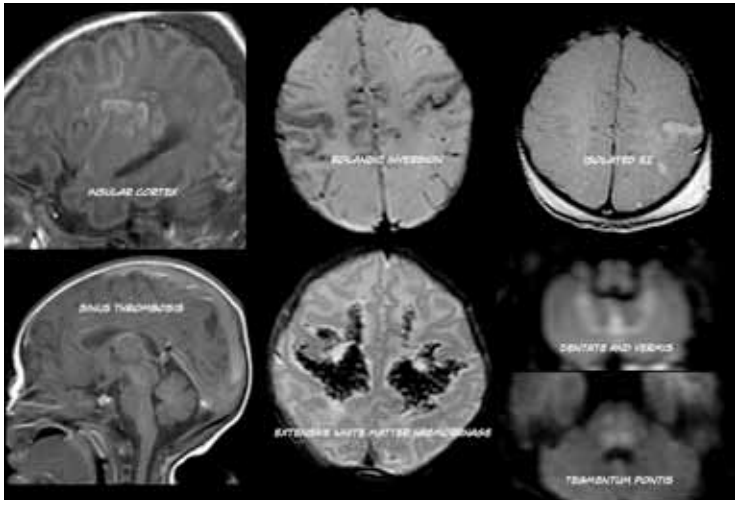

FIG 3 | Unclassified injuries: isolated insular cortex injury without deep grey matter injury and without injury to rolandic cortex; extensive injury throughout cerebral cortex sparing the rolandic area (cortical inversion); isolated unilateral non-haemorrhagic injury in primary sensory cortex; superior sagittal sinus thrombosis; bilateral extensive multifocal symmetrical white matter haemorrhage with patent sinus and deep veins; injury to brainstem tegmentum, injury to dentate nuclei and/or cerebellar cortex

TABLE 3 | Prediction by MRI scores of poor outcome (neonatal death or cerebral palsy)

Score cut-off	Sensitivity(%) CI	Specificity(%) CI	PPV (%) CI	NPV (%) CI
Sophia TBG + CWM: 7-12 versus 0-6	57 0,44-0,70	100 0,80-1,00	100 0,90-1,00	39 0,24-0,55
Sophia TBG + CWM: 6-12 versus 0-5	64 0,50-0,75	77 0,50-0,93	91 0,78-0,97	36 0,21-0,54
Sophia TBG + CWM: 5-12 versus 0-4	81 0,69-0,89	71 0,44-0,90	91 0,80-0,97	50 0,29-0,71
Sophia TBG + CWM: 4-12 versus 0-3	90 0,80-0,96	59 0,33-0,82	89 0,79-0,95	63 0,35-0,84
Sophia TBG + CWM: 3-12 versus 0-2	98 0,91-0,99	53 0,28-0,77	89 0,79-0,95	90 0,55-0,99
Sophia TBG score 6 versus 0-5	22 0,13-0,34	100 0,80-1,00	100 0,77-1,00	26 0,12-0,33
Sophia TBG scores 5-6 versus 0-4	49 0,36-0,62	100 0,80-1,00	100 0,89-1,00	35 0,22-0,50
Sophia TBG scores 4-6 versus 0-3	70 0,56-0,81	100 0,80-1,00	100 0,92-1,00	47 0,30-0,65
Sophia TBG scores 3-6 versus 0-2	83 0,71-0,91	100 0,80-1,00	100 0,93-1,00	61 0,41-0,79
Sophia TBG scores 2-6 versus 0-1	86 0,75-0,93	84 0,57-0,96	95 0,85-0,99	61 0,39-0,80
Hammersmith score 7 versus 0-6	49 0,36-0,62	100 0,80-1,00	100 0,89-1,00	35 0,22-0,50
Hammersmith scores 6-7 versus 0-5	83 0,70-0,91	100 0,80-1,00	100 0,93-1,00	61 0,41-0,78
Hammersmith scores 5-7 versus 0-4	90 0,80-0,96	82 0,56-0,96	95 0,86-0,99	70 0,46-0,88

PPV positive predictive value, NPV negative predictive value, CI confidence interval

cranial nerve nuclei, superior collicles, red nucleus and substantia nigra, locus ceruleus, cuneate and gracile nuclei, inferior olive and spinal cord anterior horn cells (24). On any brain imaging sequence, deep grey matter and hindbrain lesions are by definition bilateral and symmetrical. Thalamus is almost constantly affected (› 90% of cases) (25,26). The MRI appearance varies with severity and duration of injury and time after the insult. T1-hyperintensity of deep nuclei can be observed on day 2, together with T2-hypointensity, mixed with punctiform T2 prolongation, with or without the presence of a normal or decreased T1-signal of the PLIC (3-6). Important early findings are cortical highlighting and inversion of signal in the PLIC (11). Hypersignal in thalamus and putamen can be seen on DWI within 24-48 hours. Aspects of diffusion-weighted imaging changes in term birth asphyxia are discussed elsewhere (26-31). In this study we confirmed the joint occurrence of TBG injury with either extensive or mild cortical lesions: differences in insult severity leading to this duality could not be studied because of the retrospective nature of this work. Pattern III, the combination of deep grey matter and border zone injury, but has not yet been discussed in previous studies. Athetoid and/or spastic tetraplegia as well as cognitive dysfunction follow deep grey matter injury (14).

Border zone injury (TBG-scores 0-1/CWM-scores 2-4, pattern IV). "Watershed" injury culminates at postmortem exam in the posterior parietal areas, apparently within a border zone between the three major cerebral arteries (12,32). It is one of the acute changes preceding ulegyria (focal gyral atrophy). Border zone injury was identified in the living newborn using technetium and PET scan (33). First detailed by Kuenzle and Baenziger, the acute MRI findings are integrated into our CWM-score (7). The differences in pathogenesis between leukomalacia, watershed injury and isolated cortical necrosis are not fully understood and deserve future study. In our patients we did not always observe clinical seizures contrary to what others reported before (13,34). Ulegyria can be associated with childhood epilepsy for which drug refractoriness is not uncommon (35). CP may be a consequence of extensive watershed injury, as may be attention deficit disorders.

Isolated white matter injury (TBG-scores 0-1/CWM-score 5, pattern V). Specific postmortem descriptions of leukomalacia following term birth asphyxia, are absent. The Barkovich MRI score does not cover isolated extensive white matter injury, but recent findings have corrected this absence (10,36). The Hammersmith score grades mild, moderate and severe white matter changes (25,27). White matter injury is observed in the first week of life in the form of high signal on proton density images and decreased cortex/white matter differentiation on T1- and T2-weighted MRI; in the second week white matter becomes brighter on T2, leading to a return or even increase of cortex/white matter differentiation. This pattern is heterogeneous, as it precedes various outcome patterns such as spastic diplegia, cognitive dysfunction with microcephaly and seizures or even spastic quadriplegia with profound developmental delay. In our experience ultrasonography (US) may be helpful; the hallmark is a gradual and characteristic increase in echocontrast between relatively dark cortex and extremely bright subcortical and periventricular white matter in areas extending beyond the parasagittal border zones and perirolandic cortex, for instance in cingulate gyrus. This pattern is seen as early as day 2 and is intensifying over the following days, contrary to the pattern seen in congestion or haemorrhage. This suggests an ongoing process, maturing over days, in all likelihood a primary axonal pattern. In three of the five newborns in the present study who showed pattern V, caudate head was the only affected deep grey matter nucleus. This would suggest that injury to that nucleus may follow damage to nuclei connected by the injured axons. All three developed seizures within the first 3 days of life. The EEGs were strongly abnormal by a very high seizure load in two of the children who developed CP. It would be worthwhile, therefore, to study the potential of EEG to discriminate between good or bad outcome in this heterogeneous group. Furthermore, leukomalacia with deep grey matter injury was depicted in two newborns. These two neonates died. Mild white matter injury may present with punctate bleeding of limited consequence. Corresponding to areas of T1 and T2 shortening seen in the periventricular zone (37).

FIG 4 | Scheme summarizing the main patterns of injury observed in term birth asphyxia.

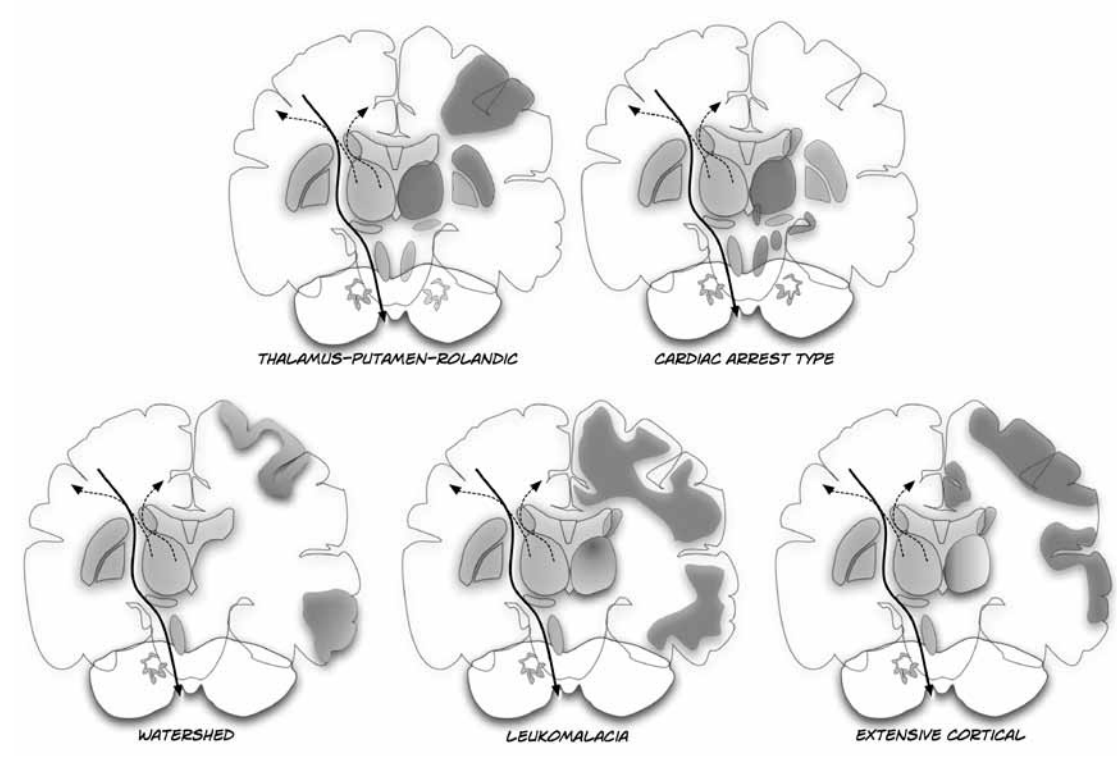

Isolated cortical necrosis (TBG-scores 0-1/CWM-score 6, pattern VI). Cell death in cerebral neocortex, hippocampus (subiculum and H1) and internal cerebellar granular layer, was the salient postmortem finding in some term newborns with postasphyxial status epilepticus (38). All lobes were affected, gyri in their crowns and sulci in their depths. Total necrosis was seen next to laminar and patchy necrosis. Such neocortical cell death is often reported in association with the deep grey matter-brainstem paradigm. Our experience suggests that it can also be a pattern of its own. On MRI T1-weighted hypersignal in pre- and postcentral gyral cortex is the cause of cortical highlighting. This is more prominent in gyral depths. Extensive cortical injury presents as "white cerebrum" in acute DWI (39). One of our survivors with extensive posterior cerebral cortical injury, showed delayed development and CP at 2 years. Ventriculomegaly is often associated. Cortical injury presents with early clinical seizures, compatible with this paradigm in experimental work (40).

In general, network injury starts immediately after birth: connected thalamic and brainstem nuclei undergo excitotoxic injury due to cortical hyperactivity or delayed neurodegeneration due to loss of trophic support from their cortical targets [41]. An association between thalamic injury and atrophy of cerebellar vermis in term asphyxia was reported recently (42,43).

Which imaging score performs best? The Sophia MRI sum score correlated well with both the Hammersmith score and Barkovich score (BG/W). The Hammersmith score and Sophia TBG-score had equally high correlation with poor outcome; respectively r =0.67 and 0.63. Lumping of Sophia TBG- and CWM-scores decreased the correlation (r =0.52), however, because outcomes after (sub)cortical and white matter injury are heterogeneous. It seems, therefore, that the Hammersmith score is best used in clinical practice. On the other hand, the two-arm Sophia score seems more suited for studying injury patterns and further pattern description. Other researchers, for that matter, have pointed out that in addition to scores using conventional MRI, objective measurement of regional apparent diffusion coefficient (ADC) and fractional anisotropy (FA) are useful in the clinical management of term perinatal asphyxia (26-31).

This study is limited in that it is retrospective. Furthermore, the use of different MRI sequences throughout the study period was a source of error we could not avoid. But in our experience, the signal intensity difference visually scored on the T1-weighted and T2-weighted images, FLAIR and diffusion weighted images did not change too much that we had interpretation problems or less consensus. Second, we did not use ADC or FA values for scoring (which is definitely influenced by the field strength and b-value). But we only did visual scoring assessment on the T2 map and ADC map. For lack of long term outcome data the predictive value of our score needs prospective study, mainly in relation to long term (cognitive and behavioural) outcome.

CONCLUSION

The Hammersmith scoring system can be used in daily practice. But using a scoring system, based on an arm for deep grey matter and one for (sub)cortex/white matter injury, will depict additional paradigms of injury. We propose post asphyxial leukomalacia and isolated cortical necrosis as new paradigms. Furthermore, this scoring system will need to be refined by correlation with the timing and mechanism of injury (sentinel event description), by studying the degree of injury (both primary and secondary) in subnuclei of thalamus and in different striatal nuclei, by adding unknown patterns, and by correlation with long term outcome in survivors.

TABLE 4 | Injury patterns

CWM TBG	0	1	2	3	4	5	6	total
0	4	2	4	1	2	3	2	18
1	0	1	1	1	1	2	1	7
2	2	0	0	0	1	0	2	5
3	3	1	0	2	0	1	2	9
4	5	1	0	1	0	1	5	13
5	7	0	2	0	0	0	9	18
6	1	0	0	0	0	0	13	14
total	22	5	7	5	4	7	34	84

I. Deep grey matter injury with limited cortical involvement (rolandic, hippocampal, insular) (18/84, 21%)(TBG 3-6, CWM 0-1)
II. Deep grey matter injury with extensive cortical involvement (23/84, 27 %) (TBG 3-6, CWM 6)
III. Deep grey matter injury with watershed injury (5/84, 6 %) (TBG 3-6, CWM 2-4)
IV. Isolated watershed injury (10/84, 12 %) (TBG 0-1, CWM 2-4)
V. Isolated white matter injury (5/84, 6 %) (TBG 0-1, CWM 5)
VI. Isolated extensive cortical injury (5/84, 6 %) (TBG 0-1, CWM 6)

The remainder had normal imaging results (n=4), isolated punctate periventricular white matter haemorrhage (n=3, one with perforator stroke), isolated thalamic injury (n=2), thalamic plus extensive cortical injury (n=2) or white matter injury combined with deep grey matter injury (n=2)

CWM: (Sub)cortical/white matter injury score on x-axis
TBG: Deep grey matter (thalamus/basal ganglia) injury score on y-axis

APPENDIX

SCORING SYSTEM BARKOVICH GROUP

Basal ganglia (BG)

0. Normal or isolated focal cortical infarct
1. Abnormal signal in thalamus
2. Abnormal signal in thalamus and lentiform nucleus
3. Abnormal signal in thalamus, lentiform nucleus, and perirolandic cortex
4. More extensive involvement

Watershed (W)

0. Normal
1. Single focal infarction
2. Abnormal signal in anterior or posterior watershed white matter
3. Abnormal signal in anterior or posterior watershed cortex and white matter
4. Abnormal signal in both anterior and posterior watershed zones
5. More extensive cortical involvement

Basal ganglia/watershed (BG/W)

0. Normal
1. Abnormal signal in basal ganglia or thalamus
2. Abnormal signal in cortex
3. Abnormal signal in cortex and basal nuclei (basal ganglia or thalami)
4. Abnormal signal in entire cortex and basal nuclei

Summation (S)

Arithmetic sum of BG and W

SCORING SYSTEM HAMMERSMITH GROUP

1. Normal: normal basal ganglia and thalami, white matter, and cortex.
2. Mild basal ganglia and thalami: focal abnormalities in the basal ganglia and thalami, normal PLIC, and normal white matter with or without mild highlighting of rolandic cortex
3. Moderate white matter: focal abnormalities in the white matter with or without cortical involvement but with normal basal ganglia and thalami and PLIC.
4. Moderate basal ganglia and thalami: focal abnormalities in the basal ganglia and thalami and equivocal or abnormal PLIC with or without cortical involvement.
5. Moderate white matter and basal ganglia and thalami: focal abnormalities in the white matter and mild or moderate abnormalities in the basal ganglia and thalami with or without cortical involvement.
6. Severe white matter: multifocal abnormalities with or without white matter haemorrhage with cortical involvement but with normal basal ganglia and thalami and PLIC.
7. Severe basal ganglia and thalami with subcortical white matter: widespread abnormalities in the basal ganglia and thalami always, with abnormal PLIC with focal abnormalities in the subcortical white matter and in the cortex.
8. Severe basal ganglia and thalami with diffuse white matter: widespread abnormalities in the basal ganglia and thalami, with abnormal PLIC with widespread abnormalities in the white matter and cortex.

REFERENCES

1. Leech RW, Alvord EC, Jr (1977) Anoxic-ischemic encephalopathy in the human neonatal period. The significance of brain stem involvement. Arch Neurol 34(2):109-13.
2. Volpe JJ, Pasternak JF (1977) Parasagittal cerebral injury in neonatal hypoxic-ischemic encephalopathy: clinical and neuroradiologic features. J Pediatr 91(3):472-6.
3. Barkovich AJ, Westmark K, Partridge C, Sola A, Ferriero DM (1995) Perinatal asphyxia: MR findings in the first 10 days. AJNR Am J Neuroradiol 16(3):427-38.
4. Barkovich AJ, Hajnal BL, Vigneron D, Sola A, Partridge JC, Allen F, et al (1998) Prediction of neuromotor outcome in perinatal asphyxia: evaluation of MR scoring systems. AJNR Am J Neuroradiol 19(1):143-9.
5. Rutherford MA, Pennock JM, Schwieso JE, Cowan FM, Dubowitz LM (1995) Hypoxic ischaemic encephalopathy: early magnetic resonance imaging findings and their evolution. Neuropediatrics 26(4):183-91.
6. Haataja L, Mercuri E, Guzzetta A, Rutherford M, Counsell S, Flavia Frisone M, et al (2001) Neurologic examination in infants with hypoxic-ischemic encephalopathy at age 9 to 14 months: use of optimality scores and correlation with magnetic resonance imaging findings. J Pediatr 138(3):332-7.
7. Kuenzle C, Baenziger O, Martin E, Thun-Hohenstein L, Steinlin M, Good M, et al (1994) Prognostic value of early MR imaging in term infants with severe perinatal asphyxia. Neuropediatrics 25(4):191-200.
8. Barkovich AJ, Westmark KD, Bedi HS, Partridge JC, Ferriero DM, Vigneron DB (2001) Proton spectroscopy and diffusion imaging on the first day of life after perinatal asphyxia: preliminary report. AJNR Am J Neuroradiol 22(9):1786-94.
9. Okereafor A, Allsop J, Counsell SJ, Fitzpatrick J, Azzopardi D, Rutherford MA, Cowan FM (2008) Patterns of brain injury in neonates exposed to perinatal sentinel events. Pediatrics 121(5):906-14.
10. Li AM, Chau V, Poskitt KJ, Sargent MA, Lupton BA, Hill A, Roland E, Miller SP (2008) White Matter Injury in Term Newborns with Neonatal Encephalopathy. Pediatr Res, epub Aug 6.
11. Liauw L, van der Grond J, van den Berg-Huysmans AA, Laan LA, van Buchem MA, van Wezel-Meijler G (2008) Is there a way to predict outcome in (near) term neonates with hypoxic-ischemic encephalopathy based on MR imaging? AJNR Am J Neuroradiol 29(9):1789-94.
12. Nikas I, Dermentzoglou V, Theofanopoulou M, Theodoropoulos V (2008) Parasagittal lesions and ulegyria in hypoxic-ischemic encephalopathy: neuroimaging findings and review of the pathogenesis. J Child Neurol 23(1):51-8.
13. Sato Y, Hayakawa M, Iwata O, Okumura A, Kato T, Hayakawa F, Kubota T, Maruyama K, Hasegawa M, Sato M, Oshiro M, Kito O, Kojima S (2008) Delayed neurological signs following isolated parasagittal injury in asphyxia at term. Eur J Paediatr Neurol 12(5):359-65.
14. Swarte R, Lequin M, Cherian P, Zezic A, van Goudoever J, Govaert P (2009) Imaging patterns of brain injury in term birth asphyxia. Acta Paediatrica
15. Levene MI (2001) The asphyxiated newborn infant. In: Levene MI, Chervenak FA, Whittle M. Fetal and Neonatal Neurology and Neurosurgery. Churchill Livingstone, Toronto, pp 471-504.
16. Malamud N. (1950) Status marmoratus; a form of cerebral palsy following either birth injury or inflammation of the central nervous system. J Pediatr 37(4):610-9.
17. Sylvester P (1960) Marbling and perinatal anoxia. Acta Paediatr 49:338-44.
18. Friede RL, Schachenmayr W (1977) Early stages of status marmoratus. Acta Neuropathol (Berl) 38(2):123-7.

19. Johnston MV, Hoon AH, Jr (2000) Possible mechanisms in infants for selective basal ganglia damage from asphyxia, kernicterus, or mitochondrial encephalopathies. J Child Neurol 15(9): 588-91.
20. Norman MG (1972) Antenatal neuronal loss and gliosis of the reticular formation, thalamus, and hypothalamus. A report of three cases. Neurology 22(9):910-6.
21. Schneider H, Ballowitz L, Schachinger H, Hanefeld F, Droszus JU (1975) Anoxic encephalopathy with predominant involvement of basal ganglia, brain stem and spinal cord in the perinatal period. Report on seven newborns. Acta Neuropathol (Berl) 32(4):287-98.
22. Dambska M, Dydyk L, Szretter T, Wozniewicz J, Myers RE (1976) Topography of lesions in newborn and infant brains following cardiac arrest and resuscitation. Damage to brain and hemispheres. Biol Neonate 29(3-4):194-206.
23. Okumura A, Hayakawa F, Kato T, Kuno K, Watanabe K (2000) Bilateral basal ganglia-thalamic lesions subsequent to prolonged fetal bradycardia. Early Hum Dev 58(2):111-8.
24. Friede RL (1989) Perinatal lesions of gray matter In: Developmental Neuropathology. Springer-Verlag, Berlin, p.p. 82-114.
25. Rutherford M, Ward P, Allsop J, Malamatentiou C, Counsell S (2005) Magnetic resonance imaging in neonatal encephalopathy. Early Hum Dev 81(1):13-25.
26. Barkovich AJ, Miller SP, Bartha A, Newton N, Hamrick SEG, Mukherjee P, Glenn OA, Xu D, Partridge JC, Ferriero DM, Vigneron DB (2006) MR Imaging, MR Spectroscopy, and Diffusion Tensor Imaging of Sequential Studies in Neonates with Encephalopathy. Am J Neurorad 27: 533-547.
27. Rutherford M, Counsell S, Allsop J, Boardman J, Kapellou O, Larkman D, et al (2004) Diffusion-weighted magnetic resonance imaging in term perinatal brain injury: a comparison with site of lesion and time from birth. Pediatrics 114(4):1004-14.
28. L'Abee C, de Vries LS, van der Grond J, Groenendaal F. (2005) Early diffusion-weighted MRI and 1H-Magnetic Resonance Spectroscopy in asphyxiated full-term neonates. Biol Neonate 88(4):306-12.
29. Boichot C, Walker PM, Durand C, Grimaldi M, Chapuis S, Gouyon JB, et al (2006) Term neonate prognoses after perinatal asphyxia: contributions of MR imaging, MR spectroscopy, relaxation times, and apparent diffusion coefficients. Radiology 239(3):839-48.
30. Ward P, Counsell S, Allsop J, Cowan F, Shen Y, Edwards D, et al (2006) Reduced fractional anisotropy on diffusion tensor magnetic resonance imaging after hypoxic-ischemic encephalopathy. Pediatrics 117(4):e619-30.
31. Liauw L, van Wezel-Meijler G, Veen S, van Buchem MA, van der Grond J (2008) Do Apparent Diffusion Coefficient Measurements Predict Outcome in Children with Neonatal Hypoxic-Ischemic Encephalopathy? AJNR Am J Neuroradiol Oct 8.
32. Brann AW, Jr., Myers RE (1975) Central nervous system findings in the newborn monkey following severe in utero partial asphyxia. Neurology 25(4):327-38.
33. Volpe JJ, Herscovitch P, Perlman JM, Kreusser KL, Raichle ME (1985) Positron emission tomography in the asphyxiated term newborn: parasagittal impairment of cerebral blood flow. Ann Neurol 17(3):287-96.
34. Sato Y, Okumura A, Kato T, Hayakawa F, Kuno K, Watanabe K (2003) Hypoxic ischemic encephalopathy associated with neonatal seizures without other neurological abnormalities. Brain Dev 25(3):215-9.
35. Villani F, D'Incerti L, Granata T, Battaglia G, Vitali P, Chiapparini L, et al (2003) Epileptic and imaging findings in perinatal hypoxic-ischemic encephalopathy with ulegyria. Epilepsy Res 55(3):235-43.
36. Miller SP, Ramaswamy V, Michelson D, Barkovich AJ, Holshouser B, Wycliffe N, et al (2005) Patterns of brain injury in term neonatal encephalopathy. J Pediatr 146(4):453-60.

37. Cornette LG, Tanner SF, Ramenghi LA, Miall LS, Childs AM, Arthur RJ, et al (2002) Magnetic resonance imaging of the infant brain: anatomical characteristics and clinical significance of punctate lesions. Arch Dis Child Fetal Neonatal Ed 86(3):F171-7.
38. Larroche JC (1968) [Massive cerebral necrosis in newborn infants. Its relation to maturation, its clinical and bioelectric symptoms]. Biol Neonat 13(5):340-60.
39. Vermeulen RJ, Fetter WP, Hendrikx L, Van Schie PE, van der Knaap MS, Barkhof F (2003) Diffusion-weighted MRI in severe neonatal hypoxic ischaemia: the white cerebrum. Neuropediatrics 34(2):72-6.
40. Williams CE, Gunn AJ, Mallard C, Gluckman PD (1992) Outcome after ischemia in the developing sheep brain: an electroencephalographic and histological study. Ann Neurol 31(1):14-21.
41. Govaert P, Zingman A, Jung YH, Dudink J, Swarte R, Zecic A, et al (2008) Network injury to pulvinar with neonatal arterial ischemic stroke. Neuroimage 39(4):1850-1857.
42. Sargent MA, Poskitt KJ, Roland EH, Hill A, Hedson G (2004) Cerebellar vermian atrophy after neonatal hypoxic-ischemic encephalopathy. AJNR Am J Neuroradiol 25(6):1008-1015.
43. Connolly DJ, Widjaja E, Griffiths PD (2007) Involvement of the anterior lobe of the cerebellar vermis in perinatal profound hypoxia. AJNR Am J Neuroradiol 28(1):16-9.

Chapter 4 | Somatosensory Evoked Potentials are of additional prognostic value in certain patterns of brain injury in term birth asphyxia

Renate M. Swarte

Joseph Cherian

Maarten Lequin

Gerhard Visser

Paul Govaert

Submitted

ABSTRACT

Aim: a: to determine the prognostic value of somatosensory evoked potentials (SEPs) in addition to 24-hours EEG monitoring and cerebral imaging in term infants with birth asphyxia, and b: to relate MRI patterns of brain injury to SEPs.

Methods: Between 2003 and 2006, 51 consecutive neonates were studied. Survivors were followed for at least two years. Poor outcome was defined as neonatal death or moderate/severe cerebral palsy or mental retardation. Polygraphic full EEG monitoring was performed for at least 24 hours and scored according to an eight grade system. SEPs and MRIs were performed in the first week. Brain injury patterns were classified according to a scoring system.

Results: Binary logistic regression analysis revealed a significant relation to outcome separately for 24-hours EEG, deep grey matter injury and SEPs. SEPs provided additional value when added to EEG and MRI in the model (p=0.03). Normal/unilaterally abnormal SEPs result showed a sensitivity of 85% (17/20) and specificity of 90% (27/30) in predicting good outcome. SEPs were of particular value in isolated watershed, white matter and extensive cortical injury.

Conclusion: SEPs are of additional prognostic value after term birth asphyxia, especially in some of the defined patterns of brain injury.

INTRODUCTION

Post asphyxial hypoxic-ischaemic encephalopathy (HIE) affects 1 to 3 per 1000 live term births. Many survivors sustain motor and cognitive deficits (1). The outcome is often difficult to ascertain early in life. A variety of neuroradiological (MRI), neurophysiological [a-EEG, multichannel EEG and evoked potentials (EPs)] and neurobehavioural tests have been assessed for their prognostic value in the first few days after birth (2-12). Although SEPs may increase important prognostic value they are not routinely done in asphyxiated term infants (9,13). SEPs could be particularly helpful in identifying adverse outcome in neonates with moderate encephalopathy (7). Sensitivity (89-95%) and specificity (86-92%) of SEPs reported in the literature vary, likely due to differences in patient populations and day of recording (8,14). SEPs evaluate the integrity of the ascending sensory pathways. The first cortical negative response is referred to as *N*1 (in adults and older children, it is termed *N*20 as it occurs after 20 msec). The mean (SD) latency of *N*1 in newborns varies (15, 16). In this study we evaluated the prognostic value of SEPs in addition to MRI and multichannel 24-hours EEG in asphyxiated term infants. To our knowledge, a detailed correlation between MRI and SEPs in perinatal asphyxia in term neonates has not been reported in the literature.

METHODS

Between January 2003 and May 2006, all term neonates admitted to the neonatal intensive care unit (NICU) for asphyxia were studied with MRI (except for three studied with ultrasound (US) only), 24-hours EEG monitoring and SEPs. Inclusion criteria for asphyxia were either an Apgar score at 5 minutes of less than 6 or an umbilical artery pH ≤ 7.10. Newborns with congenital brain or heart malformation were excluded. All test data were available digitally for review.

SEP studies. SEPs were recorded using a Nicolet Viking ™ IV EMG system (Nicolet Biomedical, Madison, WI). We used filter settings of 5-1500 Hz and a stimulus rate of 0.6 to 1 Hz. If no consistent cortical response was obtained at 1Hz, a second series with stimulation at a rate of 0.6 Hz was recorded after at least 5 minutes. The median nerve was stimulated at the wrist through two strips of self-adhesive 3M™ Red Dot ™ ECG surface electrodes (3M Health Care, St. Paul, MN), placed one centimeter apart, and connected to the stimulator, with the cathode proximally. A stimulus intensity of 14-20 mA with duration of 0.2 ms was used to produce a minimal twitch of the thumb. Recording electrodes were silver-silver chloride cups of 1cm diameter, fixed with conductive paste and further secured with tape. They were placed at Erb's point, spinous process of seventh cervical vertebra and over the left and right parietal regions. The scalp recording locations were 2 cm behind the C3 and C4 positions of the 10-20 International System of electrode placement. The reference electrode was placed at Fz and the ground electrode on the forearm. Impedance values were kept ‹5 kΩ. Responses to 100-250 stimuli were averaged. A sweep of 200 milliseconds was used. Two runs on each median nerve were recorded and these were superimposed to verify reproducibility. Latency to N1 was measured. Cortical SEPs were scored as absent only when the peripheral response over Erb's point and the cervical response were normally present. Published normative data were used (17). SEPs were reviewed by a clinical neurophysiologist and a neonatologist, unaware of the other results, together and were classified into two groups:

1 Normal/unilaterally abnormal: the *N* 1 peaks of cortical SEPs were bilaterally normal, or unilaterally abnormal;
2 Bilaterally abnormal: increased latency bilaterally (› 36 msec), bilaterally absent or unilaterally absent with increased latency contralaterally.

Neuroimaging methodology. MRIs were scored by a paediatric neuroradiologist who was unaware of the results of the SEPs, EEG and clinical outcome of survivors. Scoring was according to brain injury patterns (18); deep grey matter injury with limited cortical involvement (pattern 1), deep grey matter injury with extensive cortical involvement (pattern 2), deep grey matter injury with watershed injury (pattern 3), isolated watershed injury (pattern 4), isolated white matter injury (leukomalacia, pattern 5) and isolated extensive cortical injury (pattern 6). These were further grouped into two grades depending on whether there was deep grey matter injury (patterns 1, 2 and 3) or not (patterns 4, 5 and 6). Pattern 7 consists lesions not fitting in the six patterns. In these subgroups we also assessed whether the lesions were symmetrical or not.

EEG monitoring. Continuous amplitude integrated (aEEG) plus full EEG monitoring with polygraphy was done from admission, starting usually on the first post partum day, for at least 24 hours. The electrodes were applied according to the 10-20 international system of electrode placement and a Nervus™ monitor was used (Taugagreining hf, Reykjavik, Iceland). EEGs were blindly scored by a clinical neurophysiologist and reviewed again by the clinical neurophysiologist together with a neonatologist. Consensus was reached in all cases.

An eight grade scoring system was used:

0=normal EEG: normal voltage, adequate for conceptional age with clear differentiation of sleep wake cycling (SWC); **1**= mild discontinuity (mean interval amplitude10-25 μV), and mildly abnormal sleep-wake cycling (SWC) along with increased-, abnormal-, paroxysmal activity like sharp waves, short (‹6 sec) runs of theta and delta activ-

ity; **2**= more severe discontinuity (‹10 µV) lasting ‹10 sec, and absent SWC but preserved reactivity to external stimuli with variability in the length of interburst intervals; **3**= severe discontinuity (‹10 µV) of 10-20 sec at the start of the monitoring, with very little variability and reactivity, but improving to grade 2 within 24 h; **4**=longer periods of severe discontinuity (‹10 µV, ›20 sec), but improving to grade 2 within 24 h; **5**= severe discontinuity (‹10 µV) of 10-20 sec at the start of monitoring, remaining unchanged over 24 h; **6**=severe discontinuity (‹10 µV) of ›20 sec at start of monitoring improving to grade 5 (10-20 s) within 24 h; **7**= severe discontinuity (‹10 µV) of 10-20 sec, worsening further within 24 h, with discontinuous periods of ›20 sec; **8**= very long periods of severe discontinuity (‹10 µV, ›20 sec), or persistent low voltage (‹10 µV) remaining unchanged over 24 hours.

Severity of discontinuity is fairly easy to assess and has been shown to predict outcome (19,20). This scoring system was derived from published literature and modified based on our clinical experience. Classification was based predominantly on discontinuity and evolution over 24 hours as well as presence of SWC. For scoring the discontinuity, the most frequently occurring values for the amplitude and duration of the discontinuous periods were used. Discontinuity was defined if voltage attenuation ‹ 25µV for mild discontinuity and ‹10 µV for severe discontinuity was seen in at least 50% of the EEG channels, lasting for a period of 6 seconds or more.

We omitted parameters such as frequency content and duration of the EEG bursts, occurrence of sporadic or rhythmic sharp waves within and outside the bursts, because we wanted the classification to be readily applicable at the bedside.

Outcome. A paediatrician unaware of the results of the SEPs, EEGs and MRI scans performed follow-up examinations until at least two years of age. Bayley Scales of Infant Development (BSID) were used. Those in whom cerebral palsy (CP) was detected were referred to the paediatric neurologist. The patients with a normal development at one year who were not further followed at our clinic were assessed with a telephonic questionnaire administered to the parents and based on the Pediatric Stroke Outcome Measure (PSOM) (21). The Gross Motor Functional Classification System (GMFCS) was used to classify the severity of CP. Outcome was classified into good: normal/mild disability [normal, minimal abnormalities at neurological examination or mild CP (GMFCS 1-2)] and poor: moderate/severe disability [Mental Developmental Index (BSID; MDI) ‹ 70 or severe CP (GMFCS 3-5) or death].

Statistical analysis. As there were not enough patients for a three way grouping (normal/ mild scores 0-1, moderate scores 2-4, and severe scores 5-8), statistical analysis was performed with a dichotomous grouping of patients into normal/moderate (scores 0-4) and severe (scores 5-8) EEG abnormalities. Mean, median and range were used to describe dispersion. Sensitivity, specificity and predictive values of the SEPs were calculated by constructing 2x2 tables. Binary logistic regression analysis served to ascertain separate relationships of the MRI results, EEG monitoring data and SEP results with outcome. All tests were performed using the statistical software package SPSS™ version 16.0. A p value of ‹0.05 was considered significant.

The Erasmus MC Medical Ethical Review Board granted permission to use patient data for scientific publication.

RESULTS

The study population consisted of 57 neonates (Table 1). Six neonates, in whom SEPs were technically unsatisfactory over both hemispheres were excluded from further analysis. Three of these developed normally and three died. The remaining 51 were included in this study and had a mean gestational age of 39 4/7 (range 36 1/7 - 42) weeks. EEG monitoring was started within the first 24 h after birth in 45 neonates; on day 2 in five and on day 3 in one. The MRI scans were performed on a median of day 4 (range 1-14) and SEPs studies were recorded on a median of day 4 post partum (range 1-7). In four neonates, the SEPs on one side

TABLE 1 | MRI patterns, SEPs and outcome

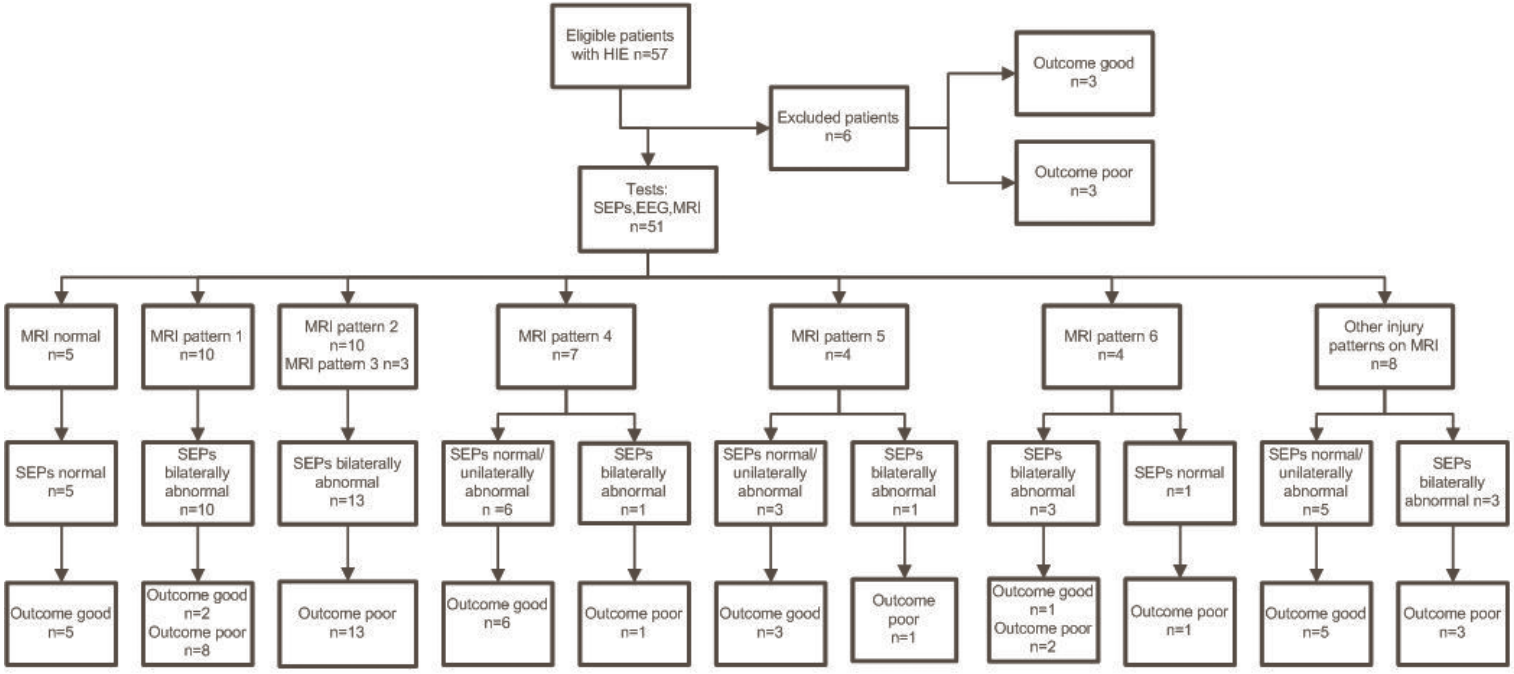

MRI pattern 1: Deep grey matter injury with limited cortical involvement
MRI pattern 2: Deep grey matter injury with extensive cortical involvement
MRI pattern 3: Deep grey matter injury with watershed injury
MRI pattern 4: Isolated watershed injury
MRI pattern 5: Isolated white matter injury (leukomalacia)
MRI pattern 6: Isolated extensive cortical injury

Outcome good CP GMFCS 1-2, or minimal abnormalities at neurological examination
Outcome poor: CP GMFCS 3-5, MDI < 70 or death

SEPs normal or unilaterally abnormal
SEPs bilaterally abnormal

were difficult to interpret; three of them, in whom the SEPs on one side were normal, were included in the group normal/unilaterally abnormal, while the fourth with prolonged SEP latency was included in the group bilaterally abnormal.

All except one in the group bilaterally abnormal SEPs, had bilaterally absent SEPs. Twenty-eight of the 31 had a poor outcome including the child with bilaterally increased latency. Serial cerebral US were used for scoring in three neonates in whom MRI had not been performed; two of these had no abnormalities and one showed hyperechoic thalami. Twenty-six of the 51 died in the neonatal period. The BSID II (MDI, PDI) were administered to 19 of the 25 survivors at the age of two years; they underwent neurological examination as well. The other six survivors were evaluated with the telephonic questionnaire; neurological outcome was normal for five of them. One had neurological symptoms and subsequently underwent a Bayley test (BSID II) and a neurological examination at the age of three years, both revealing normal findings.

Predictive value of SEPs. The binary logistic regression model showed a significant relationship between outcome and each of SEPs, EEG and MRI subgroup. Given the MRI results, the SEPs were still found to influence outcome (p=0.001) when EEG was excluded from the model. Also, given a MRI and EEG result, the SEPs offered additional predictive value (p=0.03).

Five patients with normal MRI scans had a good outcome. Six MRI patterns of post asphyxial brain injury were seen in the others (18, Table 1). Normal or unilaterally abnormal SEPs were associated with a good outcome. Conversely, bilaterally abnormal SEPs were strongly associated with a poor outcome.

The predictive values for the combinations of MRI pattern and SEPs are shown in Table 2. For neonates with MRI patterns 1, 2 or 3 the SEPs had no additional value in predicting outcome. For the remaining patterns (4, 5, or 6) outcome prediction was improved by SEPs findings. Hence these patterns were examined in more detail.

In patterns 4 and 5, (isolated watershed injury and isolated white matter injury) both asymmetrical and symmetrical lesions were seen. Asymmetrical MRI injury of the posterior frontal and parietal cortex correlated with hemiparesis and unilaterally abnormal SEP (Table 3). When the posterior frontal and parietal cortex were normal, SEPs and subsequently the motor outcomes were normal. Symmetrical injury patterns correlated with symmetrical SEPs (bilaterally normal or abnormal). In pattern 4 (symmetrical watershed injury) one neonate had striking bilateral insular lesions and bilaterally absent SEPs and subsequently a poor outcome. In three patients with pattern 5 (symmetrical leukomalacia) SEPs predicted motor outcome. In pattern 6 (isolated extensive cortical injury, 4 patients), only symmetrical lesions were seen and they correlated with symmetrical SEPs. One of these patients with isolated parieto-occipital cortical injury (starting from the central sulcus and leaving primary motor cortex intact) had subsequently bilaterally absent SEPs and a normal development (Table 3, Figure 1). We did not repeat the SEPs studies in this patient. The other three patients with this pattern of brain injury died in the neonatal period. Two of them had bilaterally absent SEPs. However, one of them with injury to mainly bilateral insular and frontal cortex with intact parietal cortex had bilaterally normal SEPs. The EEG findings associated with these three patterns in these 15 patients varied (Table 3).

DISCUSSION

SEPs showed a reasonably high sensitivity and specificity to predict outcome in this cohort, similar to those reported in the literature (8,9,13,22,23).

The mortality rate of 50% is higher than that reported in previous studies of perinatal HIE wich may be due to our selection criteria for long term EEG monitoring, favouring the inclusion of neonates with moderate to severe encephalopathy (10,13). The contribution of subcortical structures is important in SEPs. This may to some extent explain the discrepancy between SEPs and EEG in some of our patients. Comparison of EEG

TABLE 2 | Predictive values for MRI in the 38 neonates with patterns 1 to 6 and SEPs

Ability to predict poor outcome	Sensitivity(%)	Specificity(%)	PPV (%)	NPV (%)
MRI patterns 1,2 or 3	21/28 (75)	8/10 (80)	21/23 (91)	8/15 (53)
MRI patterns 1,2,3 and SEPs bilaterally abnormal	21/21 (100)	0/2 (0)	21/23 (91)	0
MRI patterns 4, 5 or 6	7/28 (25)	2/10 (20)	7/15 (47)	2/23 (9)
MRI patterns 4, 5 or 6 and SEPs bilaterally abnormal	4/7 (57)	7/8 (88)	4/5 (80)	7/10 (70)
EEG scores 5-8	23/30 (77)	19/20 (95)	23/24 (96)	19/26 (73)
SEPs bilaterally abnormal	28/31 (90)	17/20 (85)	28/31 (90)	17/20 (85)
Ability to predict good outcome	**Sensitivity(%)**	**Specificity(%)**	**PPV (%)**	**NPV (%)**
SEPs normal/unilaterally abnormal	17/20 (85)	27/30 (90)	17/20 (85)	27/30 (90)

MRI pattern 1: Deep grey matter injury with limited cortical involvement
MRI pattern 2: Deep grey matter injury with extensive cortical involvement
MRI pattern 3: Deep grey matter injury with watershed lesions
MRI pattern 4: Isolated watershed lesions
MRI pattern 5: Isolated white matter lesions (leukomalacia)
MRI pattern 6: Isolated extensive cortical injury

PPV: positive predictive value, NPV: negative predictive value

abnormalities to imaging findings is the subject of another study and will be discussed in a subsequent paper.

Our cohort reflects the NICU population in a tertiary hospital where multimodal evaluation (neurological, MRI, EEG and evoked potentials) is best suited to ascertain the nature and severity of brain injury and to help make tailored outcome predictions. In such a population, SEPs are of additional prognostic value even when EEG and MRI results are known. Still, this finding is probably of modest clinical relevance as EEG monitoring findings alone already show a high positive predictive value in our cohort (Table 2). The value of SEPs in this context depends on the associated pattern of injury on imaging. Neonates with injury to basal ganglia and thalamus have a poor prognosis24. When severe deep grey matter injury is combined with extensive cortical or watershed injury (patterns 2 and 3) there is no additional value of SEPs. In case of injury to thalamus and basal ganglia with limited cortical involvement (pattern 1), SEPs were bilaterally absent. However, 2 out of the 10 neonates in whom this was observed survived, showing only mild motor abnormalities on follow-up. It is plausible that these had only partial injury to the ascending sensory system, with some function in either thalamus or cortex preserved, albeit not enough to keep SEPs normal. In case of isolated watershed injury or leukomalacia (patterns 4 and 5), SEPs agreed with the MRI findings when the lesions were asymmetrical; parietal cortex affected on one side correlated with unilaterally abnormal SEPs over the same hemisphere. These observations suggest that frontal injury rostral to the primary motor cortex, with intact SEPs, does not lead to severe CP. In symmetrical generalized leukomalacia (pattern 5) the only infant with bilaterally absent SEPs developed severe CP, whereas the other two with normal SEPs had a normal motor outcome, suggesting that also in this group the SEPs accurately predict motor outcome. Remarkably, two patients (one with asymmetrical isolated frontal watershed injury and the other with symmetrical leukomalacia) with normal or mildly abnormal EEG (scores 0-2) and bilaterally normal SEPs, still developed mental retardation. This suggests that in these brain injury paradigms, SEPs are more accurate in predicting motor than cognitive outcome.

Overall it seems reasonable to suggest that in patients with (sub) cortical injury an accurate prediction of motor outcome is possible on the basis of combined MRI and SEPs results, barring few exceptions.

There are several limitations to this study. First, there is a lack of serial SEPs studies. Both improvement (associated with a good outcome) and deterioration of the SEPs (related to poor outcome) by the end of the first week of life and at two months have been reported before (13,22). Second, the sample sizes were small, which makes our study suitable to generate hypotheses but genuine proof will need further prospective work. Third, the use of anticonvulsants and sedative drugs may have confounded the interpretation of the SEPs (25). Many patients had seizures detected by EEG monitoring and based on our policy of treating all subclinical seizures, phenobarbitone, midazolam and lidocaine were administered depending on the response to treatment. Fourth, the normative SEPs data were those from a study that applied similar technical parameters (17). Filter settings, stimulation rate and the number of stimuli used are also known to influence the results of SEPs studies in neonates (13,17,26). We only studied the N1 component, but later components might have yielded additional information (27). However, these responses are even more sensitive to changes in state and the use of medication.

We conclude that in predicting outcome following post asphyxial HIE, first week SEPs add valuable information to that obtained by multichannel 24-hours EEG monitoring and MRI. Particularly in certain MRI patterns (patterns 4, 5 and 6), it is best to use both MRI and SEPs. Bilaterally abnormal SEPs in the first week of life are highly predictive of poor outcome.

ACKNOWLEDGMENT

We thank the parents of the babies included in the study and the NICU staff for their co-operation. The neurotechnologists, especially Els Bröker and Jolanda Geerlings expertly performed the SEPs and EEG registrations.

Injury pattern	EEG score (hours after birth)	SEPs		Outcome			
		R stimulus (left hemisphere)	L stimulus (right hemisphere)	motor	GMFCS	MDI	PDI
Asymmetrical isolated watershed and isolated white matter injury (patterns 4 or 5)							
leukomalacia R > L (Fig1)	1 (43)	normal	difficult to interpret	normal		102	173
bilateral watershed injury R > L in anterior frontal areas (Fig 1)	1 (49)	normal	normal	normal		104	108
bilateral watershed injury in frontal L > R and symmetrical occipital areas (Fig 1)	0 (12)	normal	normal	normal		66	90
bilateral watershed injury in posterior frontal and parietal R > L (Fig 1)	2 (17)	normal	delayed	left hemiparesis	1	85	85
bilateral watershed injury in posterior frontal and parietal R > L (Fig 1)	2 (22)	normal	delayed	left hemiparesis	1	117	94
Symmetrical isolated watershed (pattern 4)							
bilateral frontal watershed injury	2 (15)	normal	normal	normal		102	98
bilateral frontal watershed injury	0 (10)	normal	normal	CP	1		
bilateral insular watershed injury	4 (17)	absent	absent	died			
Symmetrical isolated white matter injury (leukomalacia, pattern 5)							
all white matter areas	5 (12)	absent	absent	CP	3		
all white matter areas	2 (6)	normal	normal	normal		55	86
all white matter areas except parietal lobe	0 (12)	normal	normal	normal		81	92
Symmetrical isolated extensive cortical injury (pattern 6)							
entire cerebral cortex	8 (6)	absent	absent	died			
entire cerebral cortex	7 (4)	absent	absent	died			
parietal and occipital cortex only (Fig 1)	4 (12)	absent	absent	normal		109	89
bilateral insular and frontal cortical injury	4 (26)	normal	normal	died			

TABLE 3 | Selection of MRI patterns, EEG results, SEPs and outcome
SEPs: Somatosensory Evoked Potentials, GMFCS: Gross Motor Functional Classification System, MDI: Mental Developmental Index, PDI: Psychomotor Developmental Index

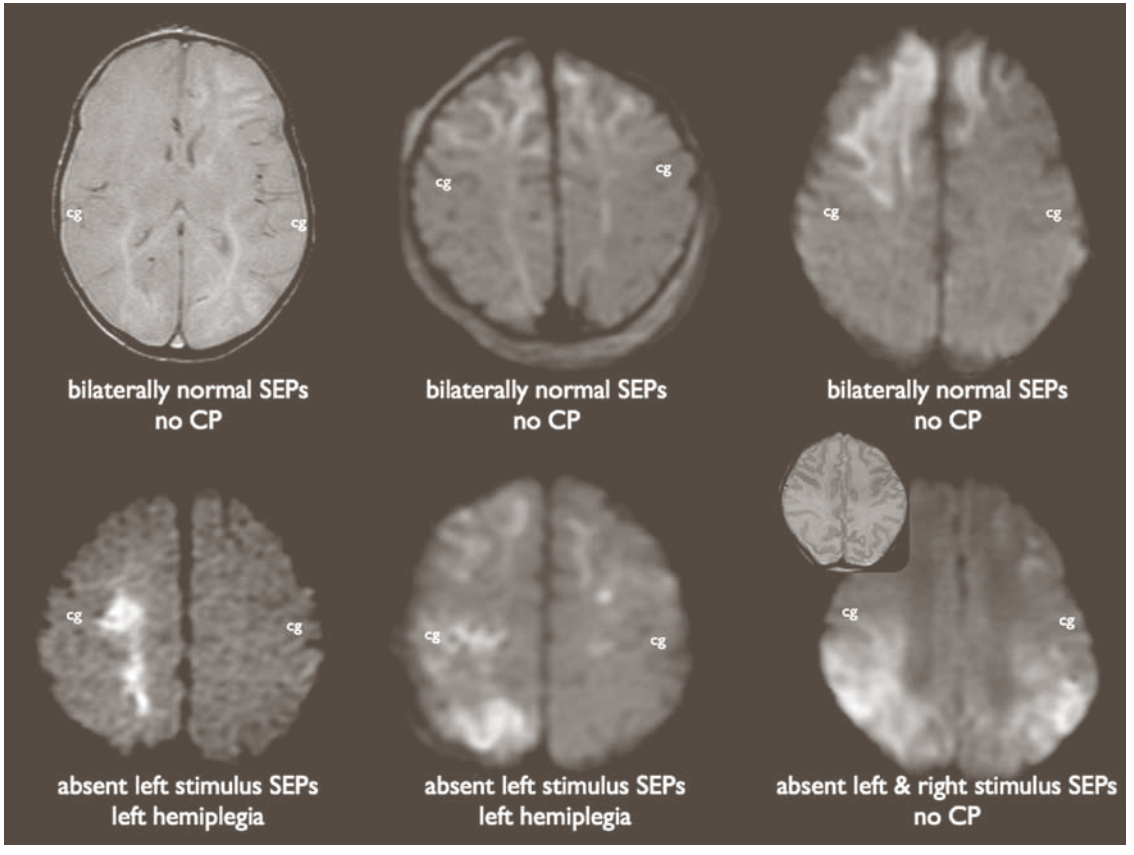

FIG 1 | Selected patients with their MRI patterns (see also Table 3 for patient details) **Top:** (left) Proton density image shows bilateral watershed injury involving frontal regions asymmetrically (L›R) and occipital regions symmetrically, (middle) Diffusion weighted image (DWI) shows leukomalacia (R›L), (right) DWI shows bilateral watershed injury in anterior frontal areas (R›L). **Bottom:** (left) DWI shows bilateral watershed injury in posterior frontal and parietal areas (R›L), (middle) DWI shows bilateral watershed injury involving posterior frontal and parietal areas(R›L), (right) DWI shows isolated extensive cortical injury involving bilateral parietal and occipital areas (inset: T2-weighted image from the same patient shows that the central gyrus (cg) is not affected)

REFERENCES

1. Volpe JJ. Hypoxic-ischemic encephalopathy. 4th ed. Boston: WB Saunders; 2001.
2. Levene M. I. Chervenak FA WM. The asphyxiated newborn infant 3th ed. Toronto: Churchill Livingstone; 2001.
3. Miller SP, Ramaswamy V, Michelson D, et al. Patterns of brain injury in term neonatal encephalopathy. J Pediatr 2005;146(4):453-60.
4. Toet MC, Hellstrom-Westas L, Groenendaal F, Eken P, de Vries LS. Amplitude integrated EEG 3 and 6 hours after birth in full term neonates with hypoxic-ischaemic encephalopathy. Arch Dis Child Fetal Neonatal Ed 1999;81(1):F19-23.
5. Toet MC, van der Meij W, de Vries LS, Uiterwaal CS, van Huffelen KC. Comparison between simultaneously recorded amplitude integrated electroencephalogram (cerebral function monitor) and standard electroencephalogram in neonates. Pediatrics 2002;109(5):772-9.
6. De Vries LS, Pierrat V, Eken P. The use of evoked potentials in the neonatal intensive care unit. J Perinat Med 1994;22(6):547-55.
7. De Vries LS, Pierrat V, Eken P, Minami T, Daniels H, Casaer P. Prognostic value of early somatosensory evoked potentials for adverse outcome in full-term infants with birth asphyxia. Brain Dev 1991;13(5):320-5.
8. Eken P, Toet MC, Groenendaal F, de Vries LS. Predictive value of early neuroimaging, pulsed Doppler and neurophysiology in full term infants with hypoxic-ischaemic encephalopathy. Arch Dis Child Fetal Neonatal Ed 1995;73(2):F75-80.
9. Majnemer A, Rosenblatt B. Evoked potentials as predictors of outcome in neonatal intensive care unit survivors: review of the literature. Pediatr Neurol 1996;14(3):189-95.
10. Sarnat HB, Sarnat MS. Neonatal encephalopathy following fetal distress. A clinical and electroencephalographic study. Arch Neurol 1976;33(10):696-705.
11. Kaufman SA, Miller SP, Ferriero DM, Glidden DH, Barkovich AJ, Partridge JC. Encephalopathy as a predictor of magnetic resonance imaging abnormalities in asphyxiated newborns. Pediatr Neurol 2003;28(5):342-6.
12. Gibson NA, Graham M, Levene MI. Somatosensory evoked potentials and outcome in perinatal asphyxia. Arch Dis Child 1992;67(4 Spec No):393-8.
13. Taylor MJ, Murphy WJ, Whyte HE. Prognostic reliability of somatosensory and visual evoked potentials of asphyxiated term infants. Dev Med Child Neurol 1992;34(6):507- 15.
14. de Vries LS. Somatosensory-evoked potentials in term neonates with postasphyxial encephalopathy. Clin Perinatol 1993;20(2):463-82.
15. Gibson NA, Brezinova V, Levene MI. Somatosensory evoked potentials in the term newborn. Electroencephalogr Clin Neurophysiol 1992;84(1):26-31.
16. Laureau E, Majnemer A, Rosenblatt B, Riley P. A longitudinal study of short latency somatosensory evoked responses in healthy newborns and infants. Electroencephalogr Clin Neurophysiol 1988;71(2):100-8.
17. George SR, Taylor MJ. Somatosensory evoked potentials in neonates and infants: developmental and normative data. Electroencephalogr Clin Neurophysiol 1991;80(2):94-102.
18. Swarte R, Lequin M, Cherian P, Zecic A, van Goudoever J, Govaert P. Imaging patterns of brain injury in term-birth asphyxia. Acta Paediatr 2009;98(3):586-92.
19. Watanabe K, Miyazaki S, Hara K, Hakamada S. Behavioral state cycles, background EEGs and prognosis of newborns with perinatal hypoxia. Electroencephalogr Clin Neurophysiol 1980;49(5-6):618-25.
20. Menache CC, Bourgeois BF, Volpe JJ. Prognostic value of neonatal discontinuous EEG. Pediatr Neurol 2002;27(2):93-101.

21. Lo W, Zamel K, Ponnappa K, et al. The cost of pediatric stroke care and rehabilitation. Stroke 2008;39(1):161-5.
22. Majnemer A, Rosenblatt B, Riley PS. Prognostic significance of multimodality evoked response testing in high-risk newborns. Pediatr Neurol 1990;6(6):367-74.
23. Scalais E, Francois-Adant A, Nuttin C, Bachy A, Guerit JM. Multimodality evoked potentials as a prognostic tool in term asphyxiated newborns. Electroencephalogr Clin Neurophysiol 1998;108(2):199-207.
24. Roland EH, Poskitt K, Rodriguez E, Lupton BA, Hill A. Perinatal hypoxic-ischemic thalamic injury: clinical features and neuroimaging. Ann Neurol 1998;44(2):161-6.
25. Green JB, Walcoff MR, Lucke JF. Comparison of phenytoin and phenobarbital effects on far-field auditory and somatosensory evoked potential interpeak latencies. Epilepsia 1982;23(4):417-21.
26. Bongers-Schokking CJ, Colon EJ, Hoogland RA, Van den Brande JL, De Groot KJ. The somatosensory evoked potentials of normal infants: influence of filter bandpass, arousal state and number of stimuli. Brain Dev 1989;11(1):33-9.
27. Vanhatalo S, Lauronen L. Neonatal SEP - back to bedside with basic science. Semin Fetal Neonatal Med 2006;11(6):464-70.

Chapter 5 | The evolution of EEG background abnormalities is related to injury patterns on MRI in asphyxiated term infants

Renate M. Swarte

Perumpillichira J. Cherian

Maarten Lequin

Gerhard H. Visser

Paul Govaert

Submitted

ABSTRACT

Introduction: Both EEG background activity and extensive injury on MRI are related to outcome in term infants with hypoxic-ischaemic encephalopathy (HIE). Conclusions about the relationship between MRI and EEG are based on small cohorts.

Aim: a) To relate EEG background with brain injury visible on MRI. b) To assess outcome in relation to both 24-hours EEG collected in the acute phase and MRI.

Methods: In 72 consecutive term neonates with HIE, 24-hours EEG was recorded after admission. MRI was scored for severity of (sub)cortical and deep grey matter injury. EEG was scored based on evolution of discontinuity over 24 hours. Outcome was evaluated at two years of age. Poor outcome equaled death or CP with impairment.

Results: A high correlation was found between EEG and MRI (r =0.82). Severely abnormal EEGs were always associated with severe brain damage on MRI: either deep grey matter injury or isolated extensive cortical injury. Normal/moderate EEG abnormalities predicted good outcome (PPV 79%), which could be improved to 88% when MRI findings were added.

Conclusion: MRI offers additional prognostic value only if the EEG is moderately abnormal. 24h-EEG scores were highly predictive of both cerebral lesion pattern on MRI and of outcome.

INTRODUCTION

Background electroencephalography (EEG) is related to outcome in term infants with hypoxic-ischaemic encephalopathy (HIE) when it is recorded sufficiently long and at an appropriate moment after the insult. The prognostic role of EEG in term neonates with asphyxia has been well studied (1-3). The existing EEG classification systems are not based on acute 24-hours monitoring and rely to some extent on late neonatal EEG findings. Studies of background patterns and their evolution even on a single channel compressed EEG trend recording, like amplitude integrated EEG (aEEG), have confirmed its prognostic value (3-8). Normal and maturationally delayed EEGs performed within the first two weeks after birth are associated with normal outcome whereas low voltage, inactive and burst suppression EEGs are highly correlated with poor outcome (1). EEGs recorded during the first week are of higher prognostic value because inactive, paroxysmal and low voltage EEGs tend to improve during the second week (9, 10). Particular value has been attributed to discontinuity of the background activity (11-14). Epileptiform activity on the EEG is not as predictive of outcome as background activity (2, 10).

Brain injury documented on MRI in term infants with HIE is also related to outcome (15-19). Just a few studies, based on small cohorts with varying lesion definition and diverse EEG classification, have described the relationship between MRI and EEG. Normal MRI scans or minimal lesions to the basal ganglia are associated with a normal EEG background (14). Both extreme discontinuity on EEG (interburst interval IBI › 40 seconds) and constantly low voltage background (‹ 20 μV) are found in severe deep grey matter injury associated with either focal or diffuse damage to cortex and white matter (14). Varying degrees of discontinuity were found in association with moderate damage to basal ganglia and/or white matter (20, 21). In only one MRI-EEG study was the full EEGs were recorded for a longer period (about 24 hours) (14). We studied a cohort of 72 infants with full EEG monitoring over 24 hours from admission and observed the evolution of discontinuity. We related the EEGs to MRI documented injury patterns and related both to outcome.

METHODS

Between 2004 and 2007, 72 consecutive term asphyxiated infants were included. MRI, serial ultrasound (US) and 24-hours EEG were performed in all. Inclusion criteria for asphyxia were either a five minute Apgar score below six or an umbilical artery pH ≤ 7.10. Newborns with brain or heart malformation were excluded. When the initial 30 minutes EEG was normal, monitoring was stopped (except for 2 patients). None of the patients had therapeutic hypothermia. When seizures were detected (either electro-clinical or electrographic) treatment was initiated by protocol: starting with two doses of phenobarbital (20 mg/kg) and when seizures persisted followed by midazolam infusion (loading dose of 0.1mg/kg followed by a maintenance dose of 0.1 to 0.5 mg/kg/hour) and lidocaine (loading dose 2 mg/kg followed by a maintenance dose of 6 mg/kg/hour). Lidocaine was weaned over 30 hours (22).

EEG. aEEG plus full EEG monitoring with polygraphy and video was done from admission, starting usually on the first postnatal day, for at least 24 hours. The scalp electrodes were applied according to the 10-20 international system of electrode placement and a Nervus™ monitor was used (Taugagreining hf, Reykjavik, Iceland). Electrodes were attached using conductive paste and fixed using collodion. Fifty of the 72 infants had a full 10-20 system using17 electrodes while 12 had a restricted 10-20 placement with 13 electrodes (FP 1-2, F 7-8, T 3-4, T 5-6, O 1-2, C 3-4 and Cz electrodes). Polygraphic channels consisted of ECG, electro-oculogram, chin EMG, respiration, limb movements and peripheral oxygen saturation. EEGs were reported by a clinical neurophysiologist at the time of recording. All the data were digitally available for review. For the purpose of this study the EEGs were reviewed again by the clinical neurophysiologist together with a neonatologist and scored blindly to outcome and MRI pattern. Consensus was reached in all cases. The scoring system used emphasizes discontinuity (voltage and duration of the discontinuous periods) and its evolution over 24 hours as well as presence of sleep wake cycling (SWC) (Table 1). It was derived from published literature and modified based on our clinical experience (1, 2, 12, 23). Severity of discontinuity is easy to assess and has been shown to predict outcome.

To score discontinuity, the most frequently occurring measure of the amplitude and of the duration of the discontinuous periods was used. Discontinuity was defined as voltage attenuation (‹ 25µV for mild discontinuity and ‹10 µV for severe discontinuity) seen in at least 50 % of the EEG channels, lasting at least 6 seconds. In order to provide a readily applicable classification at the bedside we omitted parameters such as frequency content and duration of the EEG bursts, frequency of sporadic or rhythmic sharp waves within and outside the bursts. For statistical analysis, 24-hours EEGs were further grouped into normal/moderately abnormal (scores 0-4) and severely abnormal (scores 5-8). We further subdivided the normal/moderately group into normal/mildly abnormal EEG (scores 0-1) and moderately abnormal EEG (scores 2-4).

Imaging. Ultrasound scans and MR images were scored by a paediatric neurologist unaware of the 24-hours EEG results and clinical outcome. All MR scan sessions adhered to an “asphyxia” protocol including conventional T1-weighted, T2-weighted images, proton density images, and diffusion weighted images (DWI) with apparent diffusion coefficient (ADC) mapping. A 1,5 Tesla MRI was used. Scoring was performed using information from all sequences. From a published scoring system six injury patterns were extracted (19) (Table 2). Additionally a pattern 7 has been introduced, not fitting one of these six patterns consisting in this cohort focal haemorrhagic lesion at the thalami or at the periventricular white matter. For statistical purposes MRI patterns were classified as normal/moderately abnormal [MRI group I: patterns 0, 4, 5 and 7] and severely abnormal [MRI group II: patterns 1, 2, 3 and 6].

Neurodevelopmental Outcome. All survivors were evaluated at 2 years of age by a developmental paediatrician unaware of the 24-hours EEG and MRI results. The evaluation included administration of the Bayley scales BSDI II (MDI and PDI) and a clinical neurological examination. Children in whom cerebral palsy (CP) was suspected were also evaluated

TABLE 1 | 24-hours EEG score

type	grade/ score	continuity	sleep wake cycling	other
normal	0	continuous	clearly differentiated	normal voltage
mildly abnormal	1	mild discontinuity: mean interval amplitude 10-25 μV	mildly abnormal	increased, abnormal, paroxysmal activity like sharp waves, short (‹6 sec) runs of theta and delta activity
moderately abnormal	2	severe discontinuity: mean interval amplitude ‹ 10 μV lasting ‹ 10 sec	absent	preserved reactivity to external stimuli with variability in the length of interburst intervals
	3	severe discontinuity (‹ 10 μV) of 10-20 sec at the start of the monitoring, but improving to grade 2 within 24 h	absent	with very little variability and reactivity
	4	longer periods of severe discontinuity (‹10 μV, ›20 sec), but improving to grade 2 within 24 h	absent	with very little variability and reactivity
severely abnormal	5	severe discontinuity (‹10 μV) of 10-20 sec at the start of monitoring, remaining unchanged over 24 h	absent	with very little variability and reactivity
	6	severe discontinuity (‹10 μV) of ›20 sec at start of monitoring, but improving to grade 5 within 24 h	absent	no variability and reactivity
	7	severe discontinuity (‹10 μV) of 10-20 sec, worsening further within 24 h, with discontinuous periods of ›20 sec	absent	no variability and reactivity
	8	very long periods of severe discontinuity (‹10 μV, ›20 sec), or persistent low voltage (‹10 μV) remaining unchanged over 24h	absent	no variability and reactivity

TABLE 2 | Scoring system and the patterns of brain injury

grade	thalamus/basal ganglia (TBG-score)	(sub)cortex/white matter (CWM-score)
0	normal	normal
1	focal infarction or bleeding	bilateral, non-confluent punctate periventricular white matter haemorrhage (high signal on T1, low signal on T2)
2	isolated bilateral thalamic injury, MRI with normal PLIC	high T2 signal intensity in subcortical white matter in watershed area(s) with intact cortical ribbon; diffuse hyperechoic change with predominance in the periventricular and parasagittal area
3	abnormal signal intensity in ventrolateral thalamus and putamen on US and MR, with normal PLIC signal intensity on T1	2 + focal disappearance of the cortical ribbon in either one rostral or caudal watershed area, or in one hemisphere in several watershed areas
4	abnormal signal intensity in ventrolateral thalamus and putamen on US and MR with inverted PLIC signal intensity on T1; caudate not involved in both US and MRI	2 + focal disappearance of the cortical ribbon in rostral and caudal watershed areas of both cerebral hemispheres
5	4 + caudate involved	diffuse periventricular and especially subcortical hyperechoic change in white matter, together with heterogeneous abnormal signal intensity on MR (high on T2 and low on T1, indicative of ischaemia and not haemorrhage)
6	4 or 5 + injury to the entire thalamus	extensive cortical injury extending beyond perirolandic and peri-insular cortex; laminar hyperechoic pattern on US and disappearance of the cortical ribbon on T2 in affected areas

Perirolandic, calcarine and peri-insular cortical highlighting (high signal on T1 and low signal on T2, especially in the depths of the sulci) was variably associated with TBG-scores 3 to 6 and is not included separately in the CWM-score
Pattern 0: Normal (MRI group II)
Pattern 1: Deep grey matter injury with limited cortical involvement (TBG 3-6, CWM 0-1) (MRI group I)
Pattern 2: Deep grey matter injury with extensive cortical involvement (TBG 3-6, CWM 6) (MRI group I)
Pattern 3: Deep grey matter injury with watershed injury (TBG 3-6, CWM 2-4) (MRI group I)
Pattern 4: Isolated watershed injury (TBG 0-1, CWM 2-4) (MRI group II)
Pattern 5: Isolated white matter injury (TBG 0-1, CWM 5) (MRI group II)
Pattern 6: Isolated extensive cortical injury (TBG 0-1, CWM 6) (MRI group I)
Pattern 7: Collected patterns not fitting one of the six other patterns
(in this cohort focal thalamic lesions or punctate white matter haemorrhage) (MRI group II)

by a child neurologist. Children with normal short term development were not further followed as outpatients; they were assessed with a telephone questionnaire based on the Paediatric Stroke Outcome Measure (PSOM) (23). The Gross Motor Functional Classification System (GMFCS) was used to classify the severity of CP: mild CP corresponded with GMFCS 1 or 2. Outcome was classified into good [normal or mild disability (minimal abnormalities at neurological examination or mild CP)] and poor [death or Mental Developmental Index (MDI) ‹ 70 or severe CP (GMFCS 3-5)].

Statistics. Data were analysed using SPSS™ version 15.0 statistics software package. The Spearman correlation coefficient, sensitivity and specificity were used to relate 24-hours EEG classification with brain injury on MRI and to relate both to outcome. A p value of ‹0.05 was considered significant.

The Erasmus MC Medical Ethical Review Board granted permission to use patient data for scientific publication.

RESULTS

The median gestational age estimated 39 3/7 (range 36 3/7-42) weeks. EEG recording was started at a median time of 12 hours (range 2-84) after birth. MRI was performed at a median of 4 (range 1-14) days after birth. For six infants ADC maps were not available. In 12 patients in whom 24-hours EEG monitoring was started beyond 24 hours after birth. Four of those had an EEG score of 1 (all developed normally), three had a score of 3 (one died and two developed normally) and five had score of 8 (all died). Seizures were recorded in 42 patients and these were all treated according to protocol. Fourteen of them received Lidocaine for the treatment of persistent seizures in all brain injury patterns except for deep grey matter with watershed injury (pattern 3) and for isolated watershed injury (pattern 4).

Relationship between EEG score and MRI patterns (Tables 3 and 4)

The 24-hours EEG score and MRI pattern of each patient are shown in Table 3. The sensitivity, specificity and predictive values of EEG to predict MRI patterns are listed in Table 4. Normal/moderately abnormal EEGs (scores 0-4) were associated with MRI group I in 79 %, the remaining 21% had lesions in basal ganglia/thalami combined with limited/extensive cortical injury/watershed injury or isolated cortical damage. All patients with severely abnormal EEGs (scores 5-8) fell into MRI group II. A highly significant correlation ($r = 0.82$, $p < 0.001$) was found between the two EEG subgroups (normal/mild/moderate versus severe) and the two MRI subgroups (I versus II).

Normal MRI scans (pattern 0) were associated with EEG scores 1 or 2. Isolated focal thalamic lesions (n=2; score 3) were related to more severe EEG abnormalities than punctate white matter haemorrhage (n=5; score 1 or 2).

EEG score related to outcome (Tables 3, 4 and 5)

A high correlation was found between EEG score (scores 0-4 versus 5-8) and (good versus poor) outcome ($r = 0.79$). Severely abnormal 24-hours EEGS (scores 5-8) had a positive predictive value (PPV) of 100% for poor outcome. In contrast, normal/moderately abnormal EEGS (scores 0-4) predicted good outcome in 79%, but the accuracy increased to 88% when MRI results were added, within MRI group I (pattern 0, 4, 5 and 7). All but one of the 14 patients with normal/mildly abnormal EEGs (scores 0-1) had a normal outcome. This one patient had minimal white matter lesions and died of acute renal failure. Patients with moderately abnormal EEGs (scores 2-4) had mixed outcomes. Combination of EEG scores with MRI patterns improved their PPV from 67 to 82%. Table 5 shows the relation between 24-hours EEG score, poor outcome and MRI pattern.

TABLE 3 | MRI pattern and 24-hours EEG score

MRI pattern **24-hours EEG score**	0	1	2	3	4	5	6	7
8		●●●●●●● ‾‾‾	●●●●●●●●●●●● ‾‾‾‾‾ ●●●●●●●●●●●●	●			●●●● ‾	
7							●	
6		●	● ‾					
5			● ‾				●	
4		○●●		●	○		○	
3		●						○○○ ‾
2	○○ ‾			○	○	●●○ ‾‾		○
1	○○○○○○				○○○	○		●○○
0					○	○		

24-hours EEG score: see Table 1

MRI pattern: see Table 2

○ / ‾○ normal to moderately abnormal outcome without/with lidocaine treatment

● / ‾● severely abnormal outcome without/with lidocaine treatment

TABLE 4 | Relation between 24-hours EEG score, MRI pattern and outcome

	Sensitivity (%)	Specificity (%)	PPV (%)	NPV (%)
EEG to MRI				
24-hours EEG scores 5-8 to MRI group II (patterns 1,2,3,6)	39/46 (85)	26/26 (100)	39/39 (100)	26/33 (79)
24-hours EEG scores 0-4 to MRI group I (patterns 0,4,5,7)	26/26 (100)	39/46 (85)	26/33 (79)	39/39 (100)
EEG to outcome				
24-hours EEG scores 5-8 to poor outcome	39/46 (85)	26/26 (100)	39/39 (100)	26/33 (79)
24-hours EEG scores 0-4 to good outcome	26/26 (100)	39/46 (85)	26/33 **(79)**	39/39 (100)
24-hours EEG scores 0-1 to good outcome	14/26 (54)	6/7 (86)	14/15 (93)	6/18 (33)
24-hours EEG scores 2-4 to good outcome	12/26 (46)	1/7 (14)	12/18 **(67)**	1/15 (7)
MRI to outcome				
MRI group II (patterns 1,2,3,6) to poor outcome	43/46 (93)	23/26 (88)	43/46 (93)	23/26 (88)
MRI group I (patterns 0,4,5,7) to good outcome	23/26 (88)	43/46 (93)	23/26 (88)	43/46 (93)
EEG + MRI to outcome				
24-hours EEG scores 5-8 and MRI group II (patterns 1,2,3,6) to poor outcome	39/43 (91)	23/23 (100)	39/39 (100)	23/26 (88)
24-hours EEG scores 0-4 and MRI group I (patterns 0,4,5,7) to good outcome	23/23 (100)	39/42 (93)	23/26 **(88)**	39/39 (100)
24-hours EEG scores 0-1 and MRI group I (patterns 0,4,5,7) to good outcome	14/25 (56)	2/3 (67)	14/15 (93)	2/11 (18)
24-hours EEG scores 2-4 and MRI group I (patterns 0,4,5,7) to good outcome	9/14 (64)	1/3 (33)	9/11 **(82)**	1/15 (7)

In bold: improvement of prediction of EEG by MRI results

MRI patterns related to outcome (Tables 3, 4 and 5)

A high correlation was found between MRI group (I versus II) and outcome (r =0.76).

In MRI group I (patterns 0, 4, 5 and 7) there was no additional value of the EEG score to predict good outcome. In MRI group II (patterns 1, 2, 3 and 6) the combined use of EEG and MRI improved the PPV from 93 to 100%. A normal MRI predicted a normal outcome in all. Signal inversion in the PLIC on T1 was present in 38/72 neonates. All except 1 (EEG score 4) had a poor outcome.

All patients with leukomalacia (pattern 5) had normal to mild EEG abnormalities (scores 0 to 2) but showed a variable outcome. In the watershed patterns, i.e., either isolated (pattern 4) or with deep grey matter injury (pattern 3), all patients but one [with a normal to moderately abnormal EEG (scores 0-4)] had a normal outcome. All patients except one with isolated extensive cortical injury (pattern 6) had severely abnormal EEGs (scores 5-8) and died. The one newborn with a moderately abnormal EEG (score 4) in this group (injury to parietal and occipital regions only) developed within normal range at 2 years of age but became microcephalic.

DISCUSSION

A 24-hours EEG score (with eight grades), mainly based on the evolution of background discontinuity, was compared with injury patterns on MRI and with short term outcome data. High correlations were found between these variables. Following early EEG monitoring, MRI mainly refines outcome prediction in infants with a moderately disturbed EEG background (scores 2-4). Within the subgroup with severe and or persistent discontinuity (scores 5-8), the prognosis is uniformly poor, although injury patterns vary widely between them.

EEG score in relation to MRI patterns (Tables 3 and 4)

Interestingly, the 39 patients with the most severe abnormalities on EEG (scores 5-8), with a uniformly poor prognosis, showed either of two major injury patterns. Thirty-three had injury to basal ganglia-thalamus (24 had extensive and 8 had limited associated cortical injury, 1 had associated watershed injury), 6 had isolated extensive cortical injury. MRI studies have shown that persistent severe EEG discontinuity is associated with severe basal ganglia/thalamus injury combined with (sub) cortical injury (14). We may add isolated extensive cortical injury (pattern 6) to this group with severe background discontinuity. A previous study correlating EEG with neuropathology has also linked severe encephalomalacia to iso-electric EEGs (24). The 8 patients with normal MRI scan in the present study had mild to moderate EEG abnormalities (scores 1-2). This finding contrasts to that of previous studies in which a normal MRI was associated with normal EEGs only (14, 21). It is safe to assume that the encephalopathy in these patients was almost completely reversible albeit after a period of 24 hours. As the timing of MRI scanning in the present study was almost uniform and several sequences including DWI were evaluated, we believe it is unlikely we have missed brain lesions in these patients.

Within the pattern of isolated white matter injury (leukomalacia pattern 5, n= 5) EEGs ranged from normal to moderately abnormal (scores 0-2). This is a unique pattern of injury. A recent report acknowledges the existence of primary white matter injury due to term perinatal asphyxia that has not been described before (25). In previous studies describing white matter injury, more severe EEG abnormalities were seen, presumably because the cohorts included patients with severe white matter injury combined with diffuse cortical lesions (14, 17, 26). In the group of other brain injuries, not fitting into the well defined six patterns (pattern 7, n=7), infants with mild white matter lesions (punctate periventricular haemorrhages) had mild to moderately abnormal EEGs (EEG scores 1 to 2, n=4) while those with mild focal thalamic lesions had more discontinuous EEGs (score 3, n=3). This group is too small, however, to draw conclusions about the correlation between structure and function.

EEG scores related to outcome separately and in combination with MRI patterns (Tables 3, 4 and 5)

We found that in patients with normal to moderately abnormal EEGs (scores 0-4) the combination with MRI pattern increased the prognostic value. Those with moderately abnormal EEGs (scores 2-4) showed a variety of brain injury patterns and it was difficult to predict the outcome with confidence by using EEG only. MRI improved the prognostication in these patients. However, even when both tools were combined, in some patients the outcome was not accurately predicted. We hypothesize that prolongation of EEG monitoring for another 24 hours to evaluate recovery of background activity and return of SWC may improve prognostication. A normal/mildly abnormal EEG (scores 0-1) as well as a severely abnormal EEG (scores 5-8) were highly predictive for respectively normal and poor outcomes, and this finding is similar to previous studies (8, 14, 21, 27).

MRI patterns related to outcome separately and in combination with EEG scores (Tables 3, 4 and 5)

Almost all our patients without deep grey matter injury on MRI (patterns 0, 4, 5 and 7) had a good outcome. The 24-hours EEG score had no additional value for prognostication in this group. Also, in these patients, MRI predicted outcome better than did EEG alone, in contrast to other studies (20, 21). Severe abnormalities on MRI (MRI patterns 1, 2, 3 and 6) predicted poor outcome. The accuracy was slightly improved by 24-hours EEG score in contrast to a previous study in 23 neonates in which EEG had additional value only in the normal to mildly abnormal MRIs (20).

Signal inversion in the PLIC on T1 was present in 38 of all patients and all of these except one had a severely abnormal outcome. This is similar to what is described in literature (17).

STRENGTHS AND WEAKNESSES OF OUR STUDY

We used an adapted EEG scoring system, that better than existing classifications reflects the dynamics of the acute EEG changes in the first 24 to 48 hours after birth (1, 2). Discontinuity of EEG can easily be assessed at the bedside and is a robust parameter for predicting outcome (2, 11, 12). We purposefully avoided using the term burst suppression because there is no uniform definition of this entity (12). Burst suppression implies absent variability with fairly constant interburst intervals and absent reactivity to external stimuli. Probably our EEG grades of 5 to 7 would qualify for this definition.

Scoring was done blinded to the MRI results and clinical outcome. However, after analysing the MRI and outcome data and seeing the uniformly poor outcome in all patients with grade 5 to 8, we feel that further prognostication tests are not needed for those. In other words, the 8 grade system might be simplified to a 5 grade one, with current grades 5 to 8 lumped into one.

In patients with normal/moderately abnormal EEG (scores 0-4) prediction of outcome purely based on EEG is difficult. Further subdivision of this group into normal/mild (scores 0-1) and moderate (scores 2-4) might be a meaningful option. Scores 0-1 predicted good outcome except for one neonate who died because of acute renal failure and not due to the neurological injury. In patients with EEG scores 2-4, SWC had not returned in the first 24 hours, and this is known to be a predictor of poor outcome; adding MRI results improved prognostic accuracy (2). Another limitation of this scoring system is that it does not account for the onset of monitoring. This is particularly relevant when scores are similar. For example, it is difficult to compare two patients in whom a moderately abnormal EEG with short periods of discontinuity and absent SWC was seen, if the onset of monitoring differed by more than 12 hours. This is important because in the first 24 to 48 hours following asphyxia, the EEG background is dynamic. Hence, for more accurate predictions, the precise time after birth needs to be factored into the score. In addition to the background activity, electrographic seizure burden may be an independent factor of prognostic importance (28, 29). This is the subject of another study.

Antiepileptic drugs (AED) are known to suppress EEG background activity and may have influenced our 24-hours EEG scores. We did not

TABLE 5 | 24-hours EEG score related to poor outcome and MRI pattern

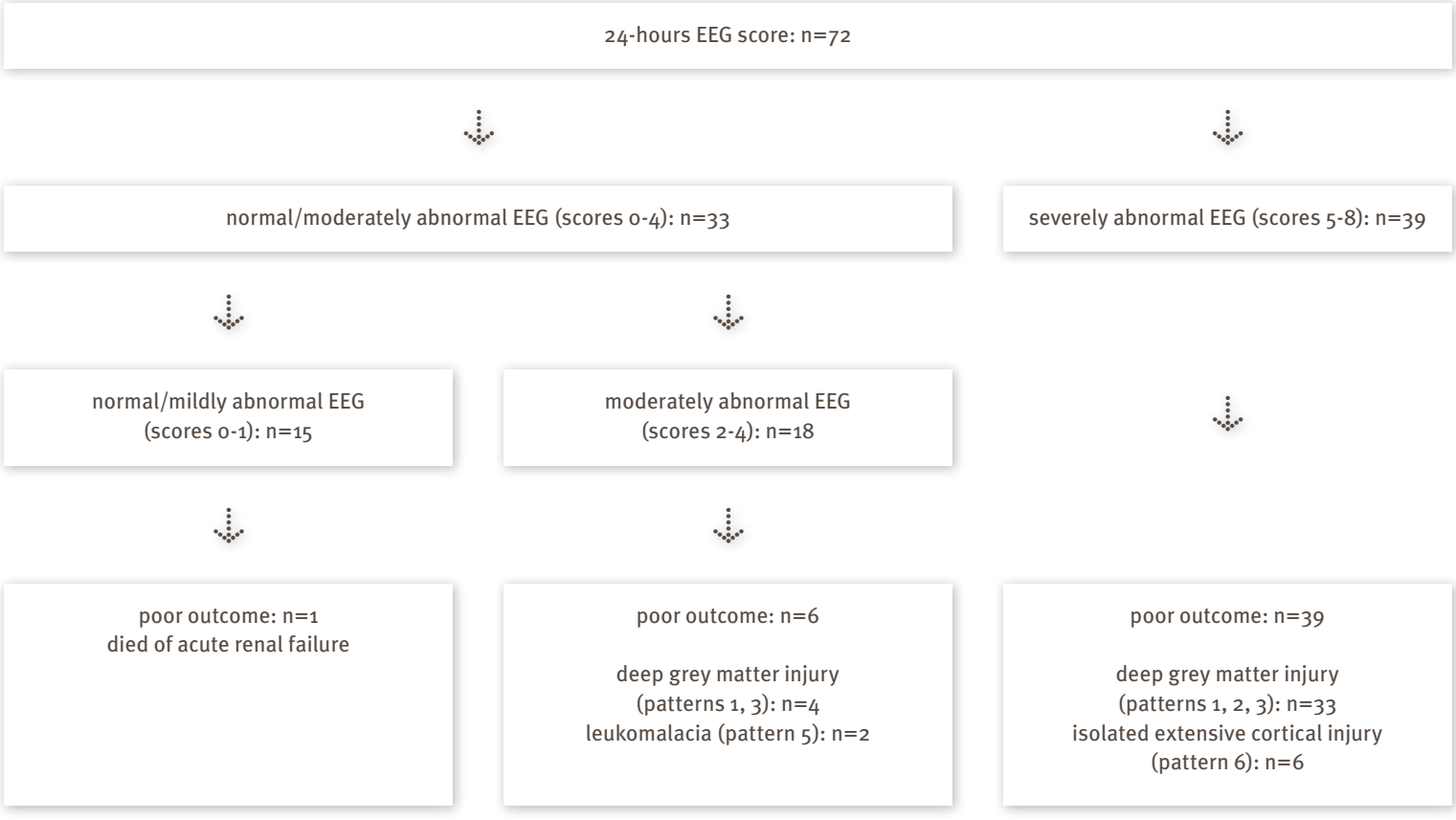

measure the serum levels of these drugs. Nevertheless, we reviewed the entire monitoring period and it was generally possible to recognize transient suppressions caused by infusion of midazolam or lidocaine.

The majority of our patients (46/72) had a poor outcome, because we are a tertiary referral center for severely asphyxiated neonates. Our criteria for selection for EEG monitoring were also biased for the inclusion of more encephalopathic babies. This limits our ability to draw conclusions about the utility of EEG monitoring and MRI in mildly asphyxiated neonates.

In conclusion a high correlation between the 24-hours EEG scores and brain injury patterns was found. Severely abnormal 24-hours EEGs (scores 5-8) always predicted poor outcome. Normal/mildly abnormal EEGs (scores 0-1) highly predicted good outcome, while in patients with moderately abnormal EEGs (scores 2-4) the MRI results refined outcome prediction. In medical ethical decisions MRI must always be considered.

Recently, cooling of asphyxiated term infants has been introduced. Therapeutic hypothermia has to be started before 6 hours after birth. This will shorten the delay to onset of monitoring. However, both EEG and MRI may be influenced by the cooling. Consequently, the prognostic predictive values of EEG and MRI in neonates undergoing therapeutic hypothermia have to be reassessed.

REFERENCES

1. Holmes G, Rowe J, Hafford J, Schmidt R, Testa M, Zimmerman A 1982 Prognostic value of the electroencephalogram in neonatal asphyxia. Electroencephalogr Clin Neurophysiol 53:60-72.
2. Watanabe K, Miyazaki S, Hara K, Hakamada S 1980 Behavioral state cycles, background EEGs and prognosis of newborns with perinatal hypoxia. Electroencephalogr Clin Neurophysiol 49:618-625.
3. Rose AL, Lombroso CT 1970 A study of clinical, pathological, and electroencephalographic features in 137 full-term babies with a long-term follow-up. Pediatrics 45:404-425.
4. Toet MC, Hellstrom-Westas L, Groenendaal F, Eken P, de Vries LS 1999 Amplitude integrated EEG 3 and 6 hours after birth in full term neonates with hypoxic-ischaemic encephalopathy. Arch Dis Child Fetal Neonatal Ed 81:F19-23.
5. van Rooij LG, Toet MC, Osredkar D, van Huffelen AC, Groenendaal F, de Vries LS 2005 Recovery of amplitude integrated electroencephalographic background patterns within 24 hours of perinatal asphyxia. Arch Dis Child Fetal Neonatal Ed 90: F245 251.
6. al Naqeeb N, Edwards AD, Cowan FM, Azzopardi D 1999 Assessment of neonatal encephalopathy by amplitude-integrated electroencephalography. Pediatrics 103:1263-1271.
7. Azzopardi D, Guarino I, Brayshaw C, Cowan F, Price-Williams D, Edwards AD, Acolet D 1999 Prediction of neurological outcome after birth asphyxia from early continuous two-channel electroencephalography. Early Hum Dev 55:113-123.
8. Monod N, Pajot N, Guidasci S 1972 The neonatal EEG: statistical studies and prognostic value in full-term and pre-term babies. Electroencephalogr Clin Neurophysiol 32:529-544.
9. van Lieshout HB, Jacobs JW, Rotteveel JJ, Geven W, v't Hof M 1995 The prognostic value of the EEG in asphyxiated newborns. Acta Neurol Scand 91:203-207.
10. Sarnat HB, Sarnat MS 1976 Neonatal encephalopathy following fetal distress. A clinical and electroencephalographic study. Arch Neurol 33:696-705.
11. Menache CC, Bourgeois BF, Volpe JJ 2002 Prognostic value of neonatal discontinuous EEG. Pediatr Neurol 27:93-101.
12. Biagioni E, Bartalena L, Boldrini A, Pieri R, Cioni G 1999 Constantly discontinuous EEG patterns in full-term neonates with hypoxic-ischaemic encephalopathy. Clin Neurophysiol 110:1510-1515.
13. Pezzani C, Radvanyi-Bouvet MF, Relier JP, Monod N 1986 Neonatal electroencephalography during the first twenty-four hours of life in full-term newborn infants. Neuropediatrics 17:11-18.
14. Biagioni E, Mercuri E, Rutherford M, Cowan F, Azzopardi D, Frisone MF, Cioni G, Dubowitz L 2001 Combined use of electroencephalogram and magnetic resonance imaging in full-term neonates with acute encephalopathy. Pediatrics 107:461-468.
15. Barkovich AJ, Westmark K, Partridge C, Sola A, Ferriero DM 1995 Perinatal asphyxia: MR findings in the first 10 days. AJNR Am J Neuroradiol 16:427-438.
16. Barkovich AJ, Hajnal BL, Vigneron D, Sola A, Partridge JC, Allen F, Ferriero DM 1998 Prediction of neuromotor outcome in perinatal asphyxia: evaluation of MR scoring systems. AJNR Am J Neuroradiol 19:143-149.
17. Rutherford MA, Pennock JM, Counsell SJ, Mercuri E, Cowan FM, Dubowitz LM, Edwards AD 1998 Abnormal magnetic resonance signal in the internal capsule predicts poor neurodevelopmental outcome in infants with hypoxic-ischemic encephalopathy. Pediatrics 102:323-328.
18. Haataja L, Mercuri E, Guzzetta A, Rutherford M, Counsell S, Flavia Frisone M, Cioni G, Cowan F, Dubowitz L 2001 Neurologic examination in infants with hypoxic-ischemic encephalopathy at age 9 to 14 months: use of optimality scores and correlation with magnetic resonance imaging findings. J Pediatr 138:332-337.

19. Swarte R, Lequin M, Cherian P, Zecic A, van Goudoever J, Govaert P 2009 Imaging patterns of brain injury in term-birth asphyxia. Acta Paediatr 98:586-592.
20. Leijser LM, Vein AA, Liauw L, Strauss T, Veen S, Wezel-Meijler G 2007 Prediction of short-term neurological outcome in full-term neonates with hypoxic-ischaemic encephalopathy based on combined use of electroencephalogram and neuro-imaging. Neuropediatrics 38:219-227.
21. El-Ayouty M, Abdel-Hady H, El-Mogy S, Zaghlol H, El-Beltagy M, Aly H 2007 Relationship between electroencephalography and magnetic resonance imaging findings after hypoxic-ischemic encephalopathy at term. Am J Perinatol 24:467-473.
22. Malingre MM, Van Rooij LG, Rademaker CM, Toet MC, Ververs TF, van Kesteren C, de Vries LS 2006 Development of an optimal lidocaine infusion strategy for neonatal seizures. Eur J Pediatr 165:598-604.
23. Biagioni E, Boldrini A, Bottone U, Pieri R, Cioni G 1996 Prognostic value of abnormal EEG transients in preterm and full-term neonates. Electroencephalogr Clin Neurophysiol 99:1-9.
24. Aso K, Scher MS, Barmada MA 1989 Neonatal electroencephalography and neuropathology. J Clin Neurophysiol 6:103-123.
25. Li AM, Chau V, Poskitt KJ, Sargent MA, Lupton BA, Hill A, Roland E, Miller SP 2008 White Matter Injury in Term Newborns with Neonatal Encephalopathy. Pediatr Res.
26. Mercuri E, Ricci D, Cowan FM, Lessing D, Frisone MF, Haataja L, Counsell SJ, Dubowitz LM, Rutherford MA 2000 Head growth in infants with hypoxic-ischemic encephalopathy: correlation with neonatal magnetic resonance imaging. Pediatrics 106:235-243.
27. Wertheim D, Mercuri E, Faundez JC, Rutherford M, Acolet D, Dubowitz L 1994 Prognostic value of continuous electroencephalographic recording in full term infants with hypoxic ischaemic encephalopathy. Arch Dis Child 71:F97-102.
28. Miller SP, Ramaswamy V, Michelson D, Barkovich AJ, Holshouser B, Wycliffe N, Glidden DV, Deming D, Partridge JC, Wu YW, Ashwal S, Ferriero DM 2005 Patterns of brain injury in term neonatal encephalopathy. J Pediatr 146:453-460.
29. McBride MC, Laroia N, Guillet R 2000 Electrographic seizures in neonates correlate with poor neurodevelopmental outcome. Neurology 55:506-513.

Chapter 6 | Heart rate changes are insensitive for detecting postasphyxial seizures in neonates

P.J. Cherian

J.H. Blok

R.M. Swarte

P. Govaert

G.H. Visser

Neurology 2006;67:2221-2223

ABSTRACT

Heart rate (HR) changes during 169 seizures (mean 12 per patient, range 8-18) were studied in 14 neonates with severe birth asphyxia. HR changes were found in 21 seizures (12.4%) of 8 patients (HR increases in 4, decreases in 1 and both patterns in 3 patients), suggesting the existence of neonatal cerebral hemispheric connections with brainstem autonomic regulatory centers. HR monitoring appears to be insensitive for detecting post asphyxial neonatal seizures.

INTRODUCTION

Seizures are a common manifestation of central nervous system dysfunction in newborn babies. They are associated with poor outcome (1). Often, seizures are subclinical, being detectable only by electroencephalography (EEG). Depending on their location, seizures may affect heart function. Heart rate (HR) monitoring has therefore been suggested as method for seizure detection (2). Relative immaturity of the newborn brain may result in cardiac responses to seizures that differ from those seen in older patients, but no study has systematically addressed this issue. We studied HR during seizures in newborn babies that underwent EEG monitoring after birth asphyxia to a) determine whether ictal HR changes occur in these babies, and b) assess the potential of HR monitoring as a tool to support seizure detection.

PATIENTS AND METHODS

We reviewed EEG and ECG data from 40 full-term newborn babies with severe birth asphyxia. Babies with congenital cardiac abnormalities and multiple congenital anomalies were excluded from the study. The 15 babies that showed electrographic seizures had received parenteral loading doses of phenobarbitone (20mg/kg) and subsequently midazolam (0.1mg/kg), followed by maintenance doses of midazolam, varying from 0.1 to 0.5 mg/kg/hour (3). MRI scans of the brain were done between the 3rd to 4th postpartum day in all patients. The study had the approval of the institutional medical ethics committee.

Digital video-EEG with polygraphy was registered continuously for 1-2 days using a Nervus™ monitor (Taugagreining hf, Reykjavik, Iceland). EEG electrodes were placed according to the 10-20 international system. Single channel ECG was recorded from two electrodes placed over the left and right side of the chest. Sample frequency was 256 Hz for both EEG (band-pass filter 0.5-35 Hz) and ECG channels (band-pass filter 1-70Hz).

All EEGs were reviewed in their entirety, and scored for seizure onset and offset, lateralization, localization, spread, and frequency. For ictal HR analysis, we selected only those ictal discharges that lasted at least 20 seconds and showed clear evolution in frequency and amplitude over time. Seizures with clinical manifestations (three in one patient) were excluded to avoid secondary influence of motor activity on HR.

The R tops of the QRS complexes in the ECG were automatically detected and R-R interval plots were generated using MatLab™ software (The MathWorks, Natick, MA). In these plots, each R-R interval was converted to an instantaneous heart rate (beats per minute) and plotted versus time, from 30 seconds before ictal onset to 60 seconds thereafter. R-peak detection by the computer was visually checked to ascertain that artefacts were excluded and that no R peaks were missed. Ictal HR results for each seizure were compared with those obtained from an interictal "baseline" period. These periods were chosen as 60-seconds epochs, not showing any epileptiform abnormalities, ending at least one minute before ictal onset, and within 5 minutes preceding each seizure. This procedure controlled to some extent for other variables that might influence HR like sleep, medications, and metabolic parameters.

We determined the standard deviation (SD) of the HR variability during the baseline epoch and used it to set an upper and lower limit to the "allowed" variability of the ictal HR. For this purpose, we also determined the mean HR from the first 100 instantaneous HR values in the last minute before ictal onset. Next, upper and lower limits were set at this mean HR ± 4 x SD. Any HR change that crossed these limits for at least 10 successive heart beats and occurred between 30 seconds before and 60 seconds after the ictal onset was classified as significant ictal HR increase or decrease. All plots were reviewed by three investigators (PJC, JHB and GHV), and the classification was verified and agreed upon by consensus.

For assessing differences between groups, chi-squared tests were used unless otherwise indicated. All tests were performed using the statistical software package SPSS™ version 10.1. A p value of ≤ 0.05 was considered significant.

RESULTS

Ictal HR analysis could not be performed in one patient due to too many artefacts in the recording. A total of 169 seizures were studied in the remaining 14/40 patients with seizures (mean, 12 per patient; range, 8-18). Clinical data are shown in Table 1. Ictal HR changes were found in 21/169 seizures (12.4%) in 8/14 patients (Tables 1 and 2). Ictal HR increases were seen in four patients, decreases in one and both patterns in three. These changes sometimes preceded ictal onset by 10-30 seconds. Seizures with temporal and extratemporal involvement equally showed HR changes (15/97 vs 6/72, $p = 0.17$), as did right- and left-sided seizures (6/66 right vs 15/103 left, $p = 0.29$). The numbers of right- and left-sided seizures showing an ictal HR increase (5/66 vs 10/103, $p = 0.63$) or decrease (1/66 vs 5/103, $p = 0.25$) were not significantly different, either. In one exceptional patient (no.5, Table 1), ictal HR consistently increased

TABLE 1 | Clinical data and ictal heart rate (HR) variability

Patient no./sex	Location of sz	Abnormalities on MRI brain	Baseline HR variability	Ictal HR variability/ no. of sz	Outcome/duration follow-up (months)
1/F	C, T	Cort, subcort	No	0/11	Died
2/F	C, TO	Subcort	Yes	0/9	Died
3/F	C, O, FT	Cort, subcort	No	↑ 4, ↓1/15	Died
4/F	P, FT, C	Cort, subcort	No	0/18	Died
5/M	T, C, F	Cort, subcort	No	↑ 5/18	Died
6/F	C, T	None	Yes	↑ 1, ↓1/10	Good/7
7/F	C, T	Cort, subcort	Yes	↑ 1/10	Died
8/F	C, T	Cort, subcort	No	↓ 3/11	Severe sequelae/4
9/F	TPO	Subcort	No	↑1, ↓1/10	Died
10/M	C, T	Subcort	Yes	↑ 2/13	Motor delay/12
11/M	T, O	Subcort	No	0/10	Died
12/F	C, T	Cort, subcort	Yes	0/10	Severe sequelae/24
13/M	C, T	Cort, subcort	No	0/13	Died
14/M	FCT, TO	None	No	↑ 1/11	Good/6

Sz: seizure, F: frontal, T: temporal, C: central, P: parietal, O: occipital, ↑: ictal HR increase and ↓: decrease.
MRI abnormalities: Cort: hyperintense signal involving most commonly the rolandic and insular cortex.
Subcort: signal changes involving thalami, basal ganglia or subcortical white matter

when the seizures involved temporal regions and had a discharge frequency of 5 to 7 Hz, while no HR changes were seen with slower ictal activity (Figure A and B) .

The baseline HR showed two types of patterns: a) preserved beat-to-beat variability, and b) markedly diminished or absent HR variability (stable baseline HR). For this purpose, we defined "stable HR" as a coefficient of variation (standard deviation divided by mean times 100%) of less than 2% in all or all but one of the baseline epochs. There was no significant difference between the number of patients with a stable or varying baseline HR that showed ictal HR changes (5/9 vs 3/5, $p = 0.66$, Fisher's exact test). Regarding outcome, there was no significant difference in mortality between patients with preserved and absent baseline HR variability (2/5 vs 7/9, $p = 0.2$, Fisher's exact test), nor between patients that did and did not show ictal HR changes (4/8 vs 5/6, $p = 0.2$, Fisher's exact test).

DISCUSSION

Our study clearly shows that ictal HR changes can occur in neonates, providing evidence for the existence of neonatal cerebral hemispheric connections with brainstem autonomic regulatory centers at birth. However, HR monitoring appears to be a very insensitive method for detecting seizures after birth asphyxia. Ictal HR changes were seen in only 12.4% of the seizures, which is much less frequent than reported (73-98%) in older children and adults (2,4,5). This low occurrence may be due to immaturity of the neonatal brain. Alternatively, it may be secondary to hypoxic brain damage, hypoxia-induced abnormal autonomic cardiovascular control, or the use of sedative medications. Antiepileptic drugs and sedative medications are known to suppress autonomic cardiac responses, and they have probably influenced our results significantly. These medications differed between patients and could not be controlled for, other than by our use of a baseline epoch (6).

In our patients as a group, there was no significant effect of seizure lateralization or localization on the occurrence and nature of ictal HR changes. However, one patient who had temporal region seizures consistently showed ictal tachycardia when the ictal discharges had a frequency of 5-7 Hz. This combination of findings might be explained by spread of the temporal seizure discharges to mesio-limbic structures or insula, resulting in a higher frequency of ictal discharges and tachycardia (7,8).

Diminished HR variability is considered a poor prognostic sign in encephalopathic neonates (9,10). However, we found no significant increase in mortality in the stable baseline HR group, probably due to the small numbers of patients in our study. Our finding of ictal HR changes occurring in similar number of patients with preserved and absent baseline HR variability suggests that the central nervous substrates responsible for ictal HR changes are relatively insensitive to hypoxia induced damage.

Part of this work was presented as a poster at the 33rd annual meeting of the Child Neurology Society held at Ottawa, Canada in October 2004.

ACKNOWLEDGEMENTS

We thank the parents of the babies included in the study and the neonatal ICU staff for their co-operation, and the neurotechnology technicians, especially Els Bröker and Jolanda Geerlings, for consistently performing high quality long-term EEG registrations.

TABLE 2 | Correlation of ictal heart rate (HR) changes with seizure location and laterality

Temporal region involvement		a) Stable baseline			b) Variable baseline			Total a)+b)		
		HR change			HR change			HR change		
		↑	↓	No	↑	↓	No	↑	↓	No
Yes	Right	2	0	15	2	0	15	4	0	30
	Left	7	1	31	2	1	21	9	2	52
No	Right	1	0	28	0	1	2	1	1	30
	Left	1	1	28	0	2	8	1	3	36

↑: Ictal HR increase and ↓: decrease, No: No HR changes

FIG A

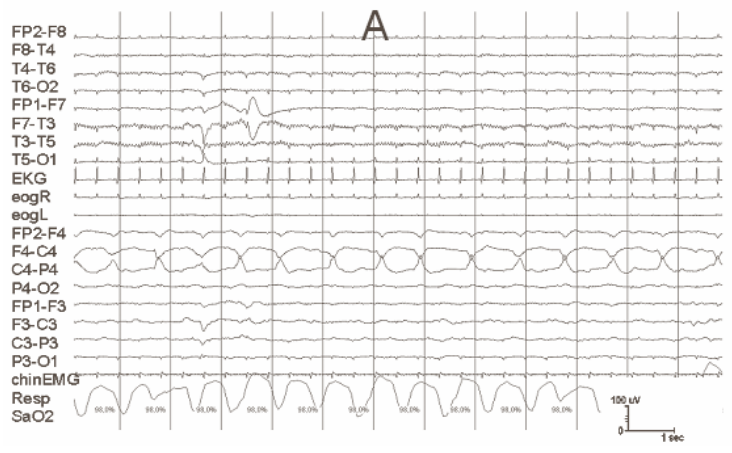

Electrographic seizure of 1 Hz frequency, involving the right central region in patient no.5, not associated with ictal HR changes

FIG B

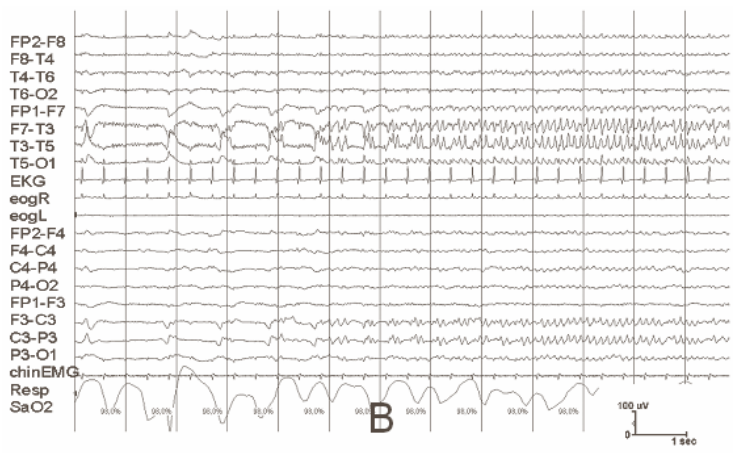

Electrographic seizure starting at a frequency of 1 Hz and evolving to reach 6-7 Hz, involving the left temporal region in the same patient This type of seizure was consistently associated with HR increase

REFERENCES

1. McBride M, Laroia N, Guillet R. Electrographic seizures in neonates correlate with poor neurodevelopmental outcome. Neurology 2000;55:506-13.
2. Leutmezer F, Schernthaner C, Lurger S, et al. Electrocardiographic changes at the onset of epileptic seizures. Epilepsia 2003;44:348-54.
3. Lombroso CT. Neonatal EEG polygraphy in normal and abnormal newborns. In: Niedermeyer E, Lopes da Silva F, editors. Electroencephalography, basic principles, clinical applications, and related fields. 3rd ed. Baltimore, MD: Williams & Wilkins;1993; p. 803-75.
4. Zijlmans M, Flanagan D, Gotman J. Heart rate changes and ECG abnormalities during epileptic seizures: prevalence and definition of an objective clinical sign. Epilepsia 2002;43:847-54.
5. Mayer H, Benninger F, Urak L, et al. EKG abnormalities in children and adolescents with symptomatic temporal lobe epilepsy. Neurology 2004;63:324-28.
6. Persson H, Ericson M, Tomson T. Carbamazepine affects autonomic cardiac control in patients with newly diagnosed epilepsy. Epilepsy Res 2003;57:69-75.
7. Oppenheimer SM, Gelb A, Girvin JP, Hachinski VC. Cardiovascular effects of human insular cortex stimulation. Neurology 1992;42:1727-32 .
8. Pacia SV, Ebersole JS. Intracranial EEG substrates of scalp ictal patterns from temporal lobe foci. Epilepsia 1997;38:642-54.
9. Griffin MP, O'Shea TM, Bissonette EA, et al. Abnormal heart rate characteristics are associated with neonatal mortality. Pediatr Res 2004;55:782-88.
10. Omokhodion SI, Jaiyesimi F, Losekoot TG. Standard 12 lead and 24 hour Holter electrocardiographic observation in a biracial group of perinatally asphyxiated newborns. West Afr J Med 2003;22:253-58.

Chapter 7 | Ictal nystagmus in a newborn baby after birth asphyxia

P. Joseph Cherian

Renate M.C. Swarte

Joleen H. Blok

P.M.M. Bröker-Schenk

Gerhard H. Visser

Clinical EEG and Neuroscience 2006;37:41-45

ABSTRACT

Ictal nystagmus (IN) is an uncommon phenomenon characterized by rhythmic saccadic eye movements occurring during epileptic seizures. We report a newborn baby with severe birth asphyxia, undergoing long-term video EEG monitoring with electro-oculogram (EOG), who showed irregular IN that crossed the midline from left to right and vice versa, resulting in large amplitude of the nystagmoid movements. The nystagmus was followed 15 to 29 seconds later by ictal discharges in the occipital regions. MRI of the brain showed features suggestive of periventricular leukomalacia. This interesting combination of findings suggests a complex mechanism for IN of cortical or subcortical ictal rhythms, which results in (a) the generation of subcortical electrical discharges in the pons and midbrain, causing nystagmoid eye movements, and (b) subsequent occipital spiking. We conclude that this clinical manifestation supports the existence of functioning cortical-subcortical connections between the brainstem ocular motor centres and the occipital cortex at birth.

INTRODUCTION

Epileptic or ictal nystagmus (IN) consists of rapid, repetitive saccadic eye movements caused by epileptic discharges (1). In the majority of patients with IN described in the literature, there is a preponderance of seizure foci in the parieto-temporo-occipital (PTO) cortex (2-5). The youngest patient in whom IN has been reported is a 10 day-old infant described by Harris et al, who had a focal cortical dysplasia involving the PTO region (4). Long-term EEG registrations in newborn babies with a history of birth asphyxia provide information about the severity of brain injury, help in the management and also aid prognostication. Over the last one year, 39 newborn babies have thus been monitored at our centre. Fifteen of these babies had subclinical /electrographic seizures on their EEGs. We observed ictal nystagmus in one of them. Since IN is rare and clinical correlates of seizures in newborn babies are often absent or subtle, we find this combination in our patient worth reporting (6).

CASE REPORT

A baby girl, born at 39 weeks of gestation by caesarean section, weighing 2600 grams, had Apgar scores of 0, 0, and 1 at birth, 5 and 10 minutes respectively, suggesting severe birth asphyxia. She was resuscitated, and regular cardiac rhythm was established after 10 minutes. Arterial blood gases performed 30 minutes post partum showed a pH of 6.7 and a base excess of -16. Infusions of dopamine and dobutamine were required to maintain the blood pressure. Examination showed a head circumference of 33 cm, normal anterior fontanelle and a cephalhematoma (subperiosteal hematoma) over the left parieto-occipital region. The pupils were equal and normally reacting to light and neurological examination revealed no abnormalities. Five hours after birth, generalized convulsions were seen and a loading dose of phenobarbitone (20mg/kg) was given intravenously. No further convulsions were noted.

Long term video EEG monitoring was started 7 hours after birth, using a Nervus™ monitor (Taugagreining hf, Reykjavik, Iceland) and was continued for 40 hours. Scalp EEG electrodes were placed according to the 10-20 international system of electrode placement and 16-channel EEG was monitored. For recording the EOG, 2 electrodes were placed obliquely above each other, one above the eyebrow and the other below the lower eyelid. Two channels were constructed for recording bipolar EOG from the right and the left sides. Four additional channels were used for respiratory movements, the chin EMG, ECG, and pulse oxymetry.

The interictal EEG showed a background activity of normal voltage, with diffuse delta activity of about 50 µV amplitude, intermixed with intermittent theta activity of about 20 µV, over the central and temporal regions, lasting for 1-3 seconds. Various sleep stages were well differentiated. Sporadic sharp waves of 50-100 µV were seen multifocally, with maximum frequency of occurrence in the central midline region. Ictal discharges, defined as paroxysmal abnormal electrographic discharges, consisting of clearly evolving rhythms of sinusoidal slow waves or rhythmic sharp waves, or mixed patterns, coming at a frequency of 0.5-1 Hz, and lasting for 20 - 203 seconds, were seen in the central, temporo-occipital and occipital regions. These discharges met the criteria of neonatal electrographic seizures. In total, they occurred 20 times during the monitoring. Some of the discharges were arrhythmic and were best appreciated with a time base (paper speed) of 15 mm/s. Three of these ictal discharges, occurring in the occipital regions, approximately at 15, 19 and 21 hours after the start of the recording, showed a stereotyped sequence of horizontal nystagmoid eye movements that crossed the midline from left to right and vice versa, lasting for 21-52 seconds, followed by runs of rhythmic sharp waves with a relatively low amplitude of 30–40 µV over one or both occipital regions, lasting for 29-203 seconds (Figures 1a,b and 2).

The nystagmus beat frequency was variable, ranging from 1 to 4 Hz. The temporal relationship of the nystagmus to each of the ictal discharges is shown in Table 1. There was no sustained tonic eye deviation or vertical eye movement associated with the discharges.

The other 17 electrographic seizure discharges had no clinical correlates. They were seen 10 times over the central regions. These central discharges consisted of sinusoidal waves of 150 - 250µV amplitude. The remaining 7 temporo-occipital electrographic seizure discharges had a mixed morphology of sinusoidal patterns with superimposed rhythmic sharp waves of 90-100 µV. These two types of ictal discharges were never associated with nystagmus. There were also two occasions in which the nystagmoid eye movements occurred for shorter periods of time (5 to 8 seconds) without accompanying EEG changes. We carefully reviewed the EOG during the entire EEG registration to look for similar eye movements.

An MRI scan of the brain, performed 12 days after birth, showed bilateral multiple punctate hyperintensities in the periventricular white matter, predominantly in the parieto-occipital region on T1 and T2-weighted as well as fluid attenuated inversion recovery (FLAIR) and 3D spoiled gradient echo (SPGR) images, consistent with small haemorrhages. These findings were suggestive of hypoxic ischaemic brain injury. The cerebral cortex, thalami, basal ganglia and brain stem were normal in appearance.

FIG 1a | EEG showing evolution of a seizure with ictal nystagmus seen best in the electro-oculogram channels (EOG left and right), starting at a frequency of 1 Hz and increasing to 3 Hz. The beginning of ictal rhythmic sharp wave discharges (arrows) are seen over the occipital regions (right › left), starting about 21 seconds after the onset of the nystagmus

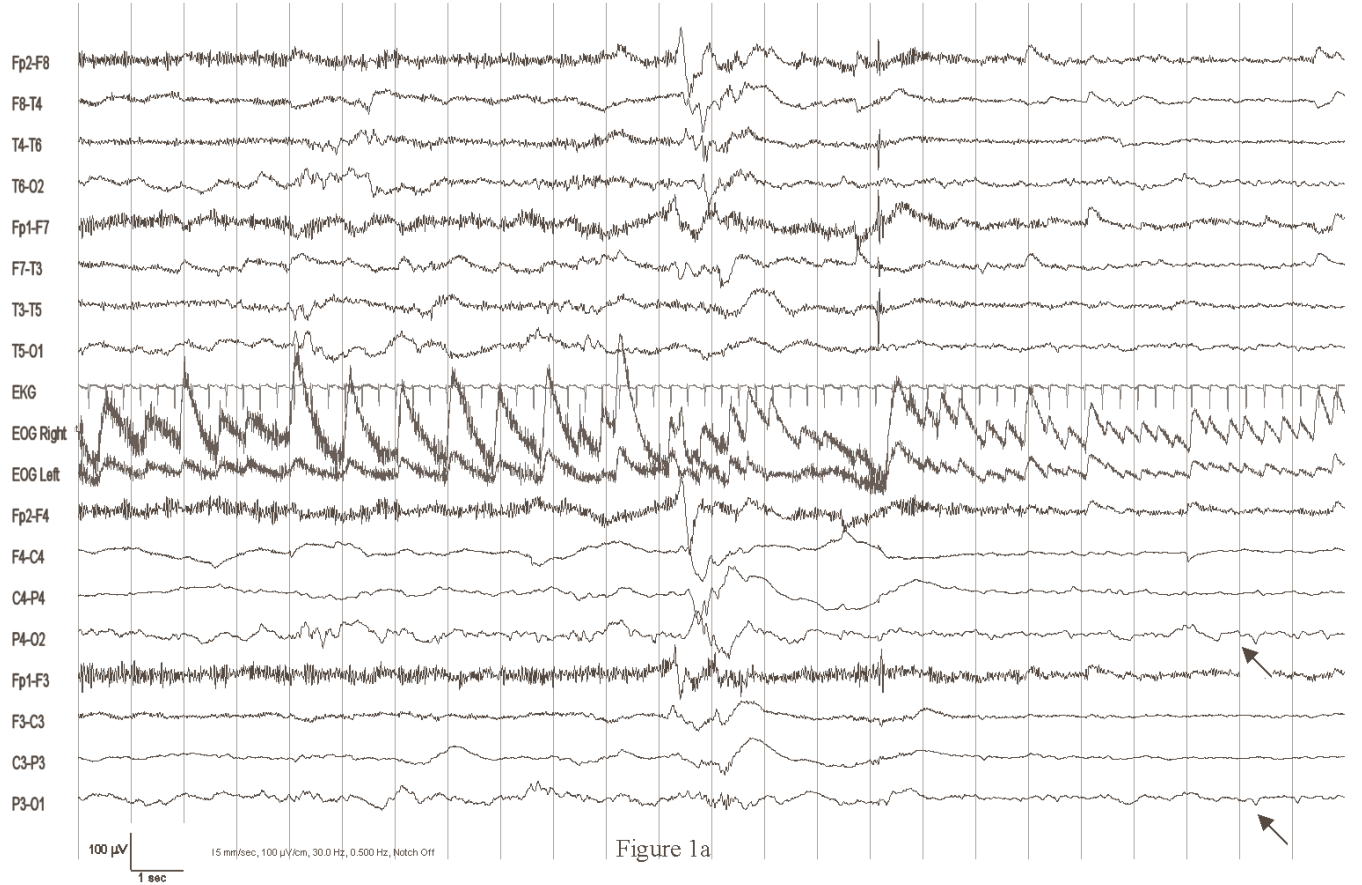

Figure 1a

FIG 1b | Continuation of the seizure in 1a, 74 seconds later. The nystagmus has stopped but the occipital ictal discharges (arrows) continue. Sensitivity 100 µV/cm, DHF 30 Hz, LFF 0.5 Hz, Paper speed 15mm/s

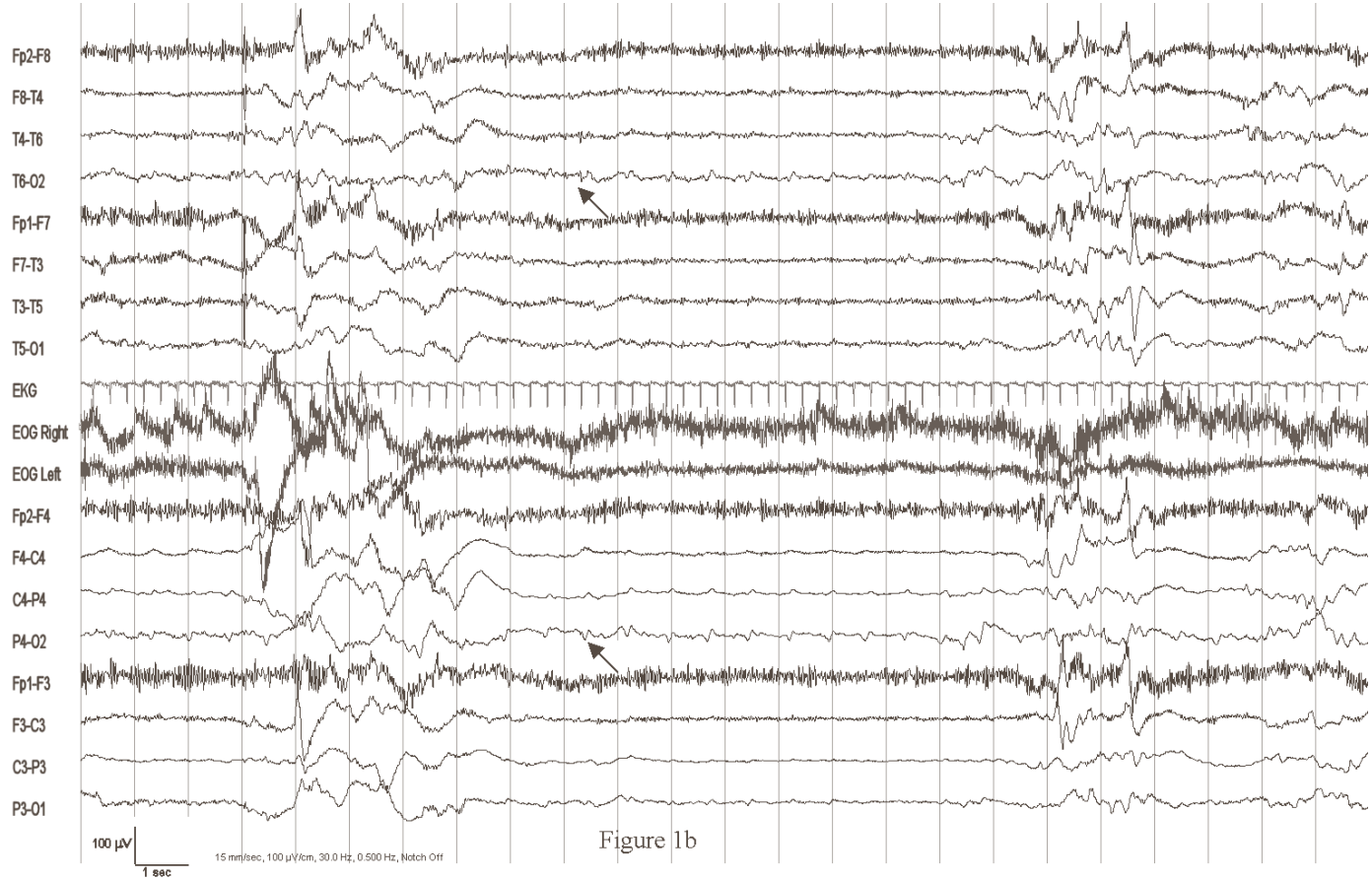

Figure 1b

FIG 2 | Another seizure showing irregular nystagmus recorded by the EOG and anterior temporal channels, followed 11 seconds later by the ictal discharges (arrows) over the right occipital region consisting of rhythmic blunt sharp waves. Sensitivity 100 μV/cm, DHF 30 Hz, LFF 0.5 Hz, Paper speed 15mm/s

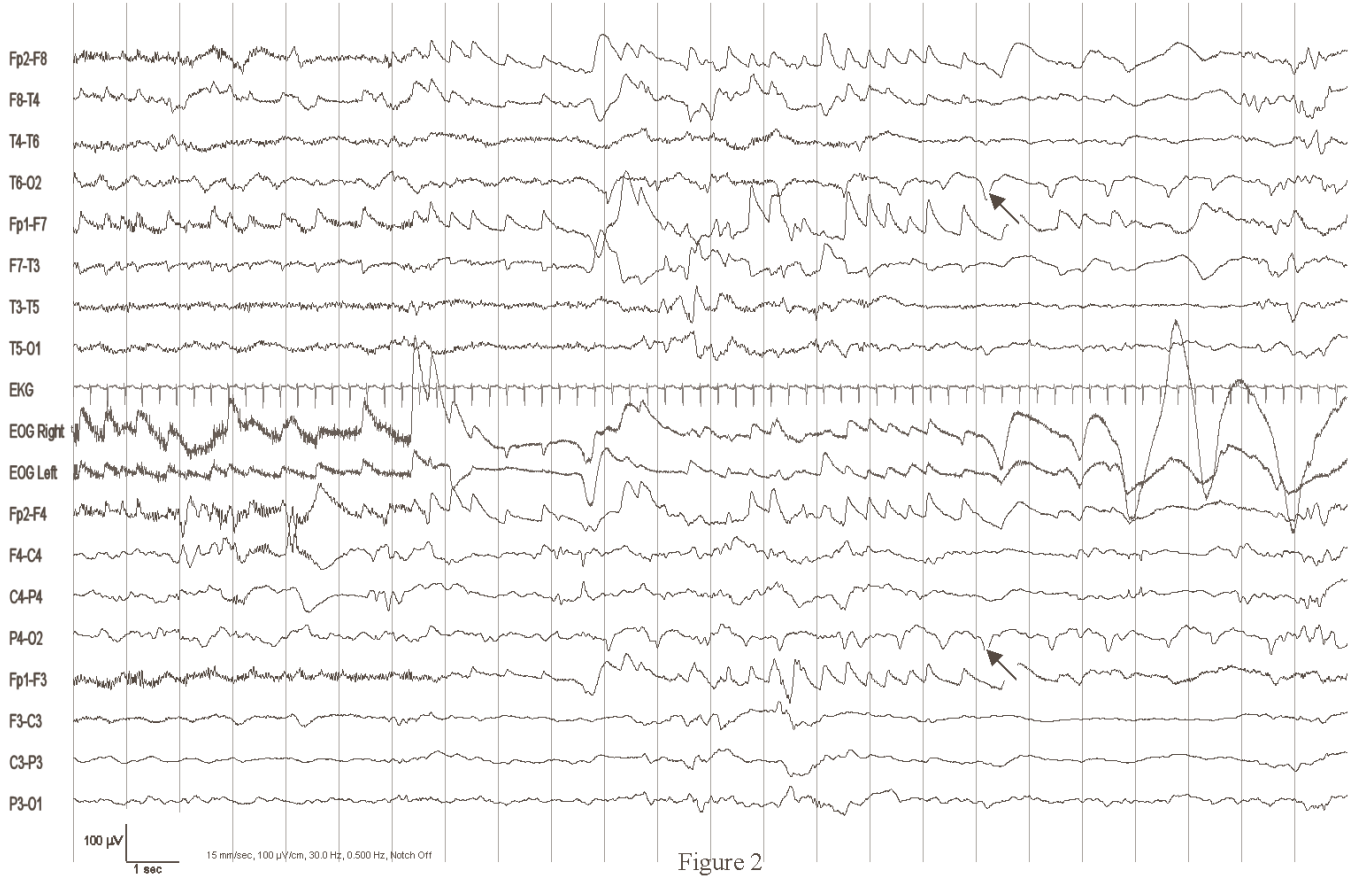

Figure 2

TABLE 1 | Temporal characteristics of the occipital seizures showing ictal nystagmus

Seizure No.	Duration of nystagmus	Delay in onset of ictal rhythms	Duration of ictal rhythms	Discharges outlast nystagmus by
1	28	29	73	74
2	52	21	203	172
3	21	15	29	23

(Time in seconds)

The baby developed necrotising enterocolitis at the end of the first week, requiring resection of a part of small intestine, and subsequently developed renal failure. Despite haemodialysis and other supportive measures, she died on the 17th day.

DISCUSSION

The occurrence of nystagmus and occipital discharges together in our patient raises two possibilities. One is that these two events are unrelated and occurred together purely by chance. The occurrence of nystagmus on 2 occasions without accompanying electrographic discharges might suggest this. The other is that the nystagmus and the simultaneously occurring occipital electrographic discharges are related, and part of a sequence of events. We feel that the latter is the case in this patient because of the consistent, one on one association of the longer trains of nystagmus with the longer runs of occipital discharges. The 2 episodes of nystagmus that occurred without EEG correlate were short, lasting 5-8 rather than 21-52 seconds. Also, the occipital epileptiform abnormalities that occurred at other times during the monitoring without clinical correlate were short, lasting for 1-3 instead of 29-203 seconds. Furthermore, this occasional dissociation of nystagmus and epileptiform discharges would not necessarily undermine our view, since it is known that electrical-clinical dissociation occurs frequently in neonatal seizures, especially after treatment with antiepileptic drugs (7).

One of the two mechanisms commonly believed to be causing IN is epileptic activation of the cortical centre for saccadic movements, with a rapid phase of nystagmus contralateral to the focus, and a slow ipsilateral phase in association with a defect in the gaze-fixing system (so-called 'leaky neural integrator') (2,8). The decelerating ipsiversive slow phases do not cross the midline. The second mechanism of IN is believed to be excitation of cortical smooth pursuit or optokinetic centres, resulting in a large amplitude of the eye movements, with the slow phases crossing the midline (1,9). In our opinion, neither of these mechanisms can adequately explain the unusual combination of characteristics we observed in our patient: irregular saccades which crossed the midline, a morphology and

amplitude of the occipital discharges that were strikingly different from the more common ictal discharge patterns that we recorded in the central and temporo-occipital regions, onset of ictal discharges 15-29 seconds after the onset of nystagmus, and the discharges outlasting the nystagmus by 23-172 seconds.

In adults, a delay between IN and the onset of ictal discharges has sometimes been ascribed to a delayed expression of the ictal EEG over the scalp (10). However, the thinner skull and scalp of a newborn baby may be expected to result in less low pass filtering, leading to a higher amplitude and better expression of EEG patterns on scalp recordings.

The presence of open and prominent anterior and posterior fontanelles in our patient would be expected to have a further enhancing effect on the scalp expression of the EEG. For these reasons, the relatively long delay between the IN and occipital spiking suggests that these ictal discharges probably arise from deeper located brain substrates.

A sequence of events similar to that seen in our patient has been reported by Hughes and Fino in a 6 year-old child (11). They postulated that the ictal discharges that arose from the medial temporal region in their patient spread subcortically to the brainstem, resulting in the generation of waves similar to the ponto-geniculo-occipital (PGO) spikes described in animals during rapid eye movement (REM) sleep (11). Although human REM sleep recordings do not readily show PGO-like spikes, a recent study using positron emission tomography has shown supportive evidence for the existence of processes similar to PGO waves in humans (12).

Horizontal nystagmus has also been registered along with typical absence seizures (13). Subcortical-cortical interactions are prominent in this epileptic syndrome and some published data even suggest involvement of the brainstem in the triggering of absence seizures (14,15).

For our patient, this raises the possibility of a mechanism of ictal nystagmus that is consistent with our observations. The initial cortical or subcortical ictal discharges, which could not be detected in the scalp recording, may have travelled down to the ocular motor nuclei in the brainstem (possibly via the paramedian pontine reticular formation), causing the irregular nystagmoid eye movements that crossed the midline. From the brainstem, the discharges subsequently could have spread to the lateral dorsal tegmental nucleus, the lateral geniculate bodies and, finally, the occipital regions bilaterally. Although the latter pathway remains speculative, the occurrence of ictal nystagmus demonstrates that functioning pathways exist at birth between the occipital cortex and the brainstem gaze centres.

ACKNOWLEDGEMENT

We thank Ms. Monique Strijder for secretarial assistance.

REFERENCES

1 Furman, JMR, Crumrine, PK., Reinmuth, OM., 1990. Epileptic Nystagmus. Ann Neurol 1990;27:686 -8.

2 Kaplan PW, Tusa RJ. Neurophysiologic and clinical correlations of epileptic nystagmus. Neurology 1993;43:2508-14.

3 Beun AM, Beintema DJ, Binnie CD, Debets RM, Overweg J, Van Heycop ten Ham MW. Epileptic nystagmus. Epilepsia 1984;25:609-14.

4 Harris CM, Boyd S, Chong K, Harkness W, Neville BG. Epileptic nystagmus in infancy. J Neurol Sci 1997;151:111-4.

5 Galimberti CA, Versino M, Sartori I, Manni R, Martelli A, Tartara A. Epileptic skew deviation. Neurology 1998;50:1469-72.

6 Mizrahi EM, Kellaway P. Characterization and classification of neonatal seizures. Neurology 1987;37:1837-44.

7 Scher MS, Alvin J, Gaus L, Minnigh B, Painter MJ. Uncoupling of EEG-clinical neonatal seizures after antiepileptic drug use. Pediatr Neurol 2003;28:277-280.

8 Thurston, SE, Leigh, RJ, Osorio, I. Epileptic gaze deviation and nystagmus. Neurology 1985;35:1518- 21.

9 Tusa RJ, Kaplan PW, Hain TC, Naidu S. Ipsiversive eye deviation and epileptic nystagmus. Neurology 1990;40:662-5.

10 Kaplan PW. Neurophysiological localization of epileptic nystagmus. Am J END Technol 1999;39:77-83.

11 Hughes JR, Fino JJ. Epileptic nystagmus and its possible relationship with PGO spikes. Clin Electroencephalogr 2003;34:32-8.

12 Peigneux P, Laureys S, Fuchs S, et al. Generation of rapid eye movements during paradoxical sleep in humans. Neuroimage 2001;14: 701-8.

13 Watanabe K, Negoro T, Matsumoto A, Inokuma K, Takaesu E, Machara M. Epileptic nystagmus associated with typical absence seizures. Epilepsia 1984;25: 22-4.

14 Blumenfeld H. From molecules to networks: cortical/subcortical interactions in the pathophysiology of idiopathic generalized epilepsy. Epilepsia. 2003;44 (Suppl 2):7-15.

15 Kohsaka S, Mizukami S, Uetake K, Sakai T, Kohsaka M. Brainstem triggers absence seizures in human generalized epilepsy. Brain Res 1999;837:277-88.

Chapter 8 | Automated neonatal seizure detection mimicking a human observer reading EEG

W. Deburchgraeve

P.J. Cherian

M. de Vos

R.M. Swarte

J.H. Blok

G.H. Visser

P. Govaert

S. van Huffel

Clinical Neurophysiology 2008;119:2447-2454

ABSTRACT

Objective: The description and evaluation of novel patient independent seizure detection for the EEG of the newborn term infant.

Methods: We identified the characteristics of the neonatal seizure by which a human observer is able to detect them. Neonatal seizures were divided into 2 types. For each type, a fully automated detection algorithm was developed based on the identified human observer characteristics. The first algorithm analyzes the correlation between high-energetic segments of the EEG. The second detects increases in low frequency activity (‹ 8Hz) with high autocorrelation.

Results: The complete algorithm was tested on multi-channel EEG recordings of 21 patients with and 5 patients without electrographic seizures, totaling 217h of EEG. Sensitivity of the combined algorithms was found to be 88%, Positive Predictive Value (PPV) 75% and the false positive rate 0.66 per hour.

Conclusions: Our approach to separate neonatal seizures into two types yields a high sensitivity combined with a good PPV and much lower false positive rate than previously published algorithms.

Significance: The proposed algorithm significantly improves neonatal seizure detection and monitoring.

INTRODUCTION

Seizures occur in 1 to 3.5/1000 births and are a common sign of neurological disorder in neonates (1). The causes of seizures are various, with 90% of all cases being attributed to biochemical imbalances within the CNS, hypoxic ischemic encephalopathy, intracranial hemorrhages and infarcts, intracranial infection, and developmental (structural) anomalies. The newborn brain is very susceptible to seizures as term infants have well-developed excitatory mechanisms and poorly developed inhibitory mechanisms (2). This explains the greater incidence of seizures in the neonatal period than at any other time in life (3). There is controversy about whether or not seizures cause brain damage. However, an increasing number of studies have shown that neonatal seizures cause lasting changes in the CNS, is related to poor outcome and late behavioral effects (2,4-7). In a strategy of neuroprotection of the newborn, effective detection of these seizures is needed in order to assess their potential additional damage and establish timely treatment. The detection of seizures is usually based on clinical signs in conjunction with visual assessment of the EEG. In neonates, the clinical seizures are often subtle and may be missed without constant supervision (8). Furthermore, many seizures tend to be subclinical, implying that they can be detected only by EEG monitoring. Combined with the fact that EEG analysis requires particular skills which are not always present around the clock in the Neonatal Intensive Care Unit (NICU) this means that many seizures are missed (2). Therefore, an automated system that reliably detects neonatal seizures would be of significant value in the NICU.

In the literature, many seizure detection algorithms have been described. The best known methods are based on computing a running autocorrelation function rhythmic discharges detection, modeling and complexity analysis, and wave-sequence analysis (9-12). Others are based on the extraction of features using entropy, wavelets, frequency content, etc., and then training a classifier on these features to correctly categorize the EEG (13-15). We believe that the classifier approach is not suitable for patient-independent seizure detection. Neonatal seizures have an extremely variable morphology, frequency, and topography, even within the same patient (16,17). Due to this large variability, training a classifier with fixed properties on a set of features is a too rigid strategy.

Our approach to the detection of neonatal seizures is to develop an algorithm which mimics a human observer reading EEG, as it is essentially the human observer we are trying to replace. We identified two major characteristics of neonatal seizures which lead to their detection by a human observer. The first characteristic is that all seizures represent a clear change relative to the background EEG. The second and most important characteristic is the repetitiveness of the signal, because nearly all seizures display some kind of recurrent pattern. We aimed to develop an algorithm based on these two characteristics using time domain signal processing, as this is the most straightforward way to mimic the human observer. The implementation is based on several concepts already introduced in the literature, but we combined and improved these and added some of our own concepts.

METHODS

EEG DATASET

All data were recorded at the Sophia Children's Hospital (part of the University Medical Center Rotterdam, the Netherlands). The dataset consisted of long-term video-EEG recordings of 26 full-term neonates with perinatal asphyxia of which 21 contained electrographic seizures and 5 were seizure-free. Fourteen had the full 10-20 set of electrodes (17 electrodes: Fp1,2, F3,4, C3,4, Cz, P3,4, F7,8, T3,4, T5,6, O1,2), while 12 had a restricted 10-20 set of electrodes (13 electrodes: the above set without F3,4 and P3,4). Each measurement started within 24 hours of birth. Monitoring was done for 24 to 48 hours. Segments of EEG containing seizures and at least eight hours long were selected for each patient. Sampling frequency was 256 Hz. Inter-rater agreement between two experienced clinical neurophysiologists in scoring the number of seizures in one-hour segments of EEGs from 10 patients was 73%. Subsequently, the data was reviewed jointly by both and the scored seizures were agreed upon by consensus. The 8-hours segments of EEGs were then scored for seizure activity by one of the raters. Seizures were scored when they showed clear variation from the background EEG activity lasting for at least 10 s and showed evolution in time and or change in amplitude and frequency. The dataset consisted of EEGs with a wide variety of background activity, ranging from low voltage, to burst suppression and normal background activity. No selection has been made regarding artefacts present in the EEG. Before analysis, the data was filtered between 0.3 and 30Hz.

DETECTION METHOD

When analyzing the neonatal seizures, we identified two major seizure types. The first type is what we call the spike train seizure type (Figure 1A); the second is what we call the oscillatory seizure type (Figure 1B). Nearly all neonatal seizures can be classified uniquely into one of these types or as a combination of the two types (Figure 1C). In our dataset, roughly 50% of all seizures consisted of a combination of the two types, 35% were purely consisting of spikes and the remaining 15% were pure oscillatory seizures.

The major difference between the two types is that the oscillatory type is a fluent, continuous seizure, whereas the spike train type consists of isolated spikes appearing on a background of lower voltage EEG. This means that the oscillatory type has a continuous kind of repetitiveness while the spike train type has a discontinuous kind. Another difference is that the oscillatory activity generally has lower frequency content than the high frequency spikes.

We need to stress that this categorization into two seizure types is not based on any physiological interpretation, but was adopted purely from a signal processing point of view. A detection algorithm was developed for each seizure type separately. During analysis, both algorithms run in parallel and detection occurs if one or both of the algorithms detects a seizure. The two algorithms are calculated on each EEG-channel separately. When detection occurs in one channel, the complete EEG at that time instance is regarded as seizure activity, independent of the detection result on the other channels. Although the two algorithms differ completely in their implementation, they are closely related and matched to each other. Figure 2 gives an overview of the complete detection strategy and implementation. The scheme serves as a guide through the paper and each block will be explained in the following sections. We will first explain the spike train type detection and then the oscillatory type detection.

DETECTION ALGORITHM FOR THE SPIKE TRAIN TYPE

Our human observer approach indicated that the spike train algorithm must detect a repetitive train of isolated spike like segments of EEG. Accordingly, the algorithm consists of two steps. The first step isolates the spike-like segments and the second will analyze the similarity between these isolated segments.

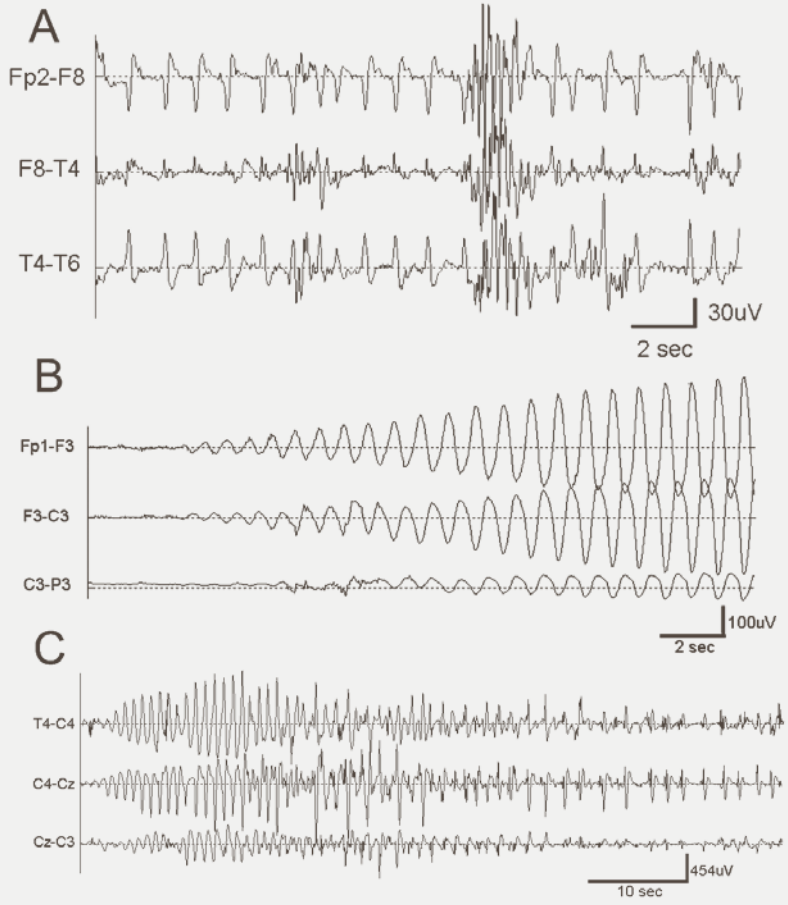

FIG 1a | (A) Example of a spike train type seizure

FIG 1b | Example of an oscillatory type seizure

FIG 1c | Example of a seizure consisting of both morphologies. The seizure starts with oscillatory activity and ends with a spike train

FIG 2 | Schematic overview of the complete seizure detection algorithm. The upper track shows all steps of the spike train type detection, the lower track these of the oscillatory type detection. The complete seizure detection algorithm then consists of the sum of the two detection algorithms

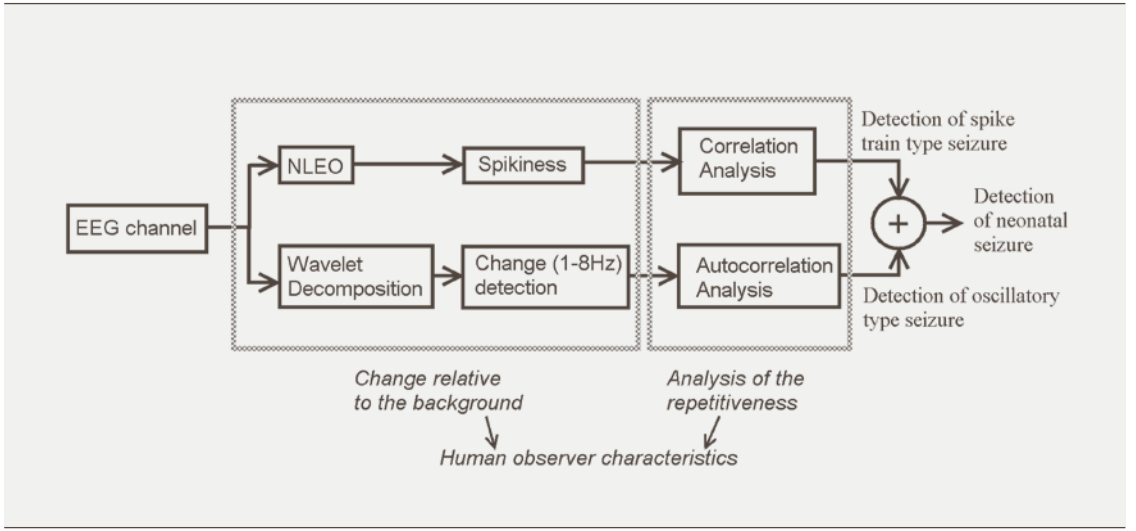

Isolation of the spike like segments.

To detect the local presence of high frequency activity, we use a non-linear energy operator (NLEO) as proposed by Kaiser (1990). The NLEO represents the energy of a discrete time signal, based on the physical energy of the signal producing system. In its discrete form, it is given by:

$$\psi_{kaiser}[x_{(n)}] = x_{(n)}^2 - x_{(n-1)}.x_{(n+1)} \quad (1)$$

With $x_{(n)}$ denoting the current sample of signal x, $x_{(n-1)}$ the first sample before sample n, etc. The key property of this operator can be derived by taking the following signals (Li et al, 2007):

$$x(n) = A.\cos(\omega_0 n + \vartheta)] \quad (2)$$

With A the amplitude, ω_0 the angular frequency and θ the phase,

$$\begin{aligned} x(n+1) &= A.\cos[\omega_0(n+1) + \vartheta)] \\ x(n-1) &= A.\cos[\omega_0(n-1) + \vartheta)] \end{aligned} \quad (3)$$

Using the following trigonometric identities:

$$\begin{aligned} &\cos(\alpha+\beta)\cos(\alpha-\beta) = \frac{1}{2}[\cos(2\alpha) + \cos(2\beta)], \\ &\cos(2\alpha) = 2\cos^2(\alpha) - 1 = 1 - 2\sin^2(\alpha) \end{aligned} \quad (4)$$

We become:

$$\psi_{kaiser}[x_{(n)}] \approx A^2 \sin^2(\omega_0 n) \quad (5)$$

This formula indicates that the output of the NLEO is proportional to the square of both the amplitude and the frequency ($\sin(\omega 0) \approx \omega 0$ for small $\omega 0$). In this regard, the NLEO may be considered superior to other energy estimators that simply average the square of the signal and are independent of frequency. Because of these properties, the NLEO amplifies the high-frequency spikes of the spike train relative to the background EEG. A generalized version, which is more robust to noise, is given by Plotkin et al. (1992):

$$\begin{aligned} \psi[x_{(n)}] &= x_{(n-l)}.x_{(n-p)} - x_{(n-q)}.x_{(n-s)}, \\ l + p &= q + s \end{aligned} \quad (6)$$

As parameter settings, we used l=1, p=2, q=0, and s=3 (Agarwal et al, 1998) to calculate the energy as locally as possible. Subsequently, on the output of the NLEO a moving average with a window size of 120 ms and shift of 1 sample was calculated. This value was chosen as a compromise for sensitivity between short spikes (‹120 ms) and long spikes (›120 ms). The resulting signal was the smoothed, frequency-weighted energy of the EEG.

Next, this signal was divided into overlapping epochs of 5 s (overlap of 4 s). To each epoch, an adaptive threshold was applied that was defined as:

$$Threshold = 0,6.std(epoch) + q_3(epoch) \quad (7)$$

with 'std(...)' and 'q3(...)' the standard deviation and 75th percentile of the epoch, respectively. The 75th percentile guarantees that only the highest energy parts of the signal are selected. The standard deviation adapts the threshold to the variability of the signal.

The human observer approach requires the spikes to be 'isolated' from the background activity. We implemented this requirement by calculating the spikiness of each high-energetic segment using:

$$Spikiness = \frac{max(segment)}{mean(background)} \quad (8)$$

The background is defined as the EEG with the length of the considered segment just before and after the spike. Only segments with a minimum length of 60ms and a spikiness higher than 7 were kept.

To summarize the segmentation, first those segments which are high-energetic with respect to the complete epoch are detected and next, the spikiness further reduces the number of segments to those which are high-energetic on a very local scale (isolated by comparatively low-energetic EEG).

ANALYSIS OF THE CORRELATION.

Following our human observer's approach, we now have to deal with the repetitive character of the seizures. In time domain processing, repetitiveness (or in this case: similarity between segments) can be estimated using correlation analysis (18). To detect the occurrence of a repetitive pattern of segments, we developed a correlation scheme that will grow a set of highly correlated segments (Figure 3). Such a set starts with just one segment and every detected segment of the segmentation step will be used as a starting point for the correlation scheme. In the first step, the cross-correlation of the first segment with the previous segment is calculated. If the maximum value of that cross-correlation is ⋯›0.8, that previous segment is added to the set. Next, the preceding segment is selected and the cross-correlation with the two segments of the set is calculated (step 2). If the mean of those two maximum cross-correlations is ⋯›0.8, that new segment is also added to set. In case of a repetitive signal, repetition of this process (step 3 etc.) leads to a set of segments which are highly correlated with each other. A detection of a seizure occurs when the number of correlated segments in the set is higher than 6.

An important parameter is when to stop the process as it is not efficient to search back for correlated segments indefinitely. This maximum time lag is dependent on the length of the first segment the process started with. Only segments which occur with a time lag less than 40 times the length of the first segment are checked.

By restricting the time lag based on the length of the first segment, the search is adapted to the length of the correlated segments the algorithm is searching for and thus adapted to the patient's EEG. In case the first segment is longer than 0.5 s, the maximum search back length is limited to 20 s. Due to this flexibility, the sensitivity of finding correlated spikes is the same for short as for longer segments (up to 0.5 s).

As this search for correlated segments is calculated for every segment detected in the segmentation step, several (possibly overlapping) sets of correlated spikes will be found in case of a spike-train type seizure. When the spikes of these sets are less than 20 s apart, they are grouped into a single detection. The above process allows for some variation in the morphology of the spikes. The initial correlation must exceed 0.8, which implies a strong similarity. However, when a set starts growing, the similarity may occasionally become less, as only the mean of the correlation with all segments of the set is used.

Figure 4 shows the results of this algorithm. The grey shaded spikes are those that are detected as being part of a spike train type seizure. The segments with a rectangle around them are also detected by the segmentation step, but removed by the spikiness and correlation analysis and thus are not detected as being part of a spike train type seizure.

DETECTION ALGORITHM FOR THE OSCILLATORY TYPE

A human observer seems to detect oscillatory type seizures as continuous repetitive activity that represents an increase of low

FIG 3 | Analysis of the correlation between the segments. In case of a repetitive pattern, a set of highly correlated segments is grown. A spike train seizure is detected when at least 6 correlated segments are found

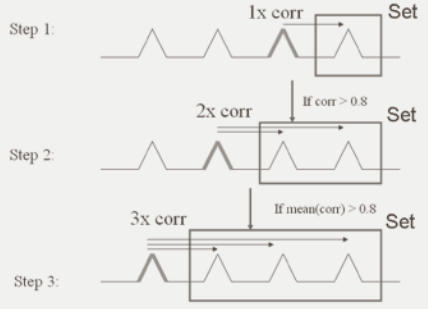

FIG 4 | Example of spike train detection. All marked segments (grey shaded + marked by rectangle) are those detected by the segmentation step. After the spikiness operator and correlation analysis only the shaded segments remain. As a result, only those segments with a high correlation with previous segments (shaded) are kept and are detected as being part of a spike train type seizure

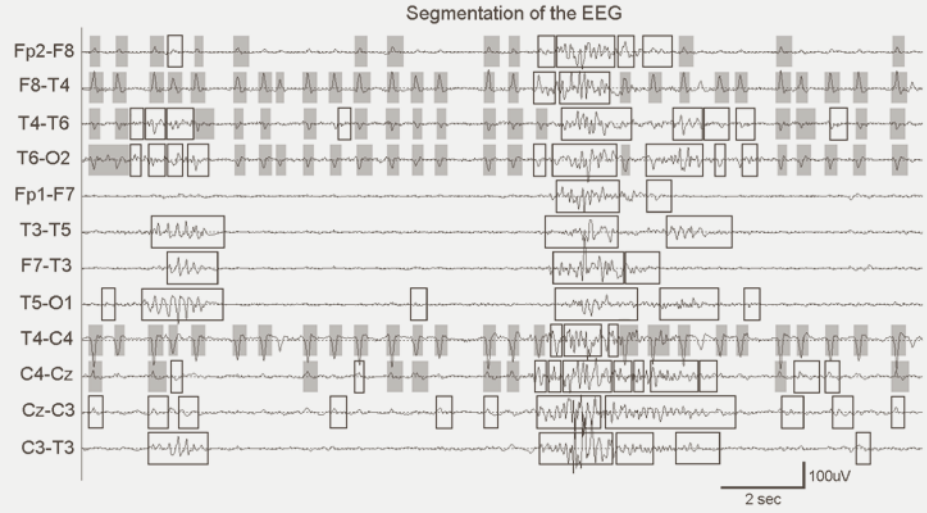

FIG 5 | Difference between the autocorrelation functions (A' and B') of a non-repetitive (A) and repetitive signal (B). The intervals between the zero crossings of the autocorrelation of a repetitive signal (B') are regular. The arrows indicate which intervals are compared (each interval is used twice)

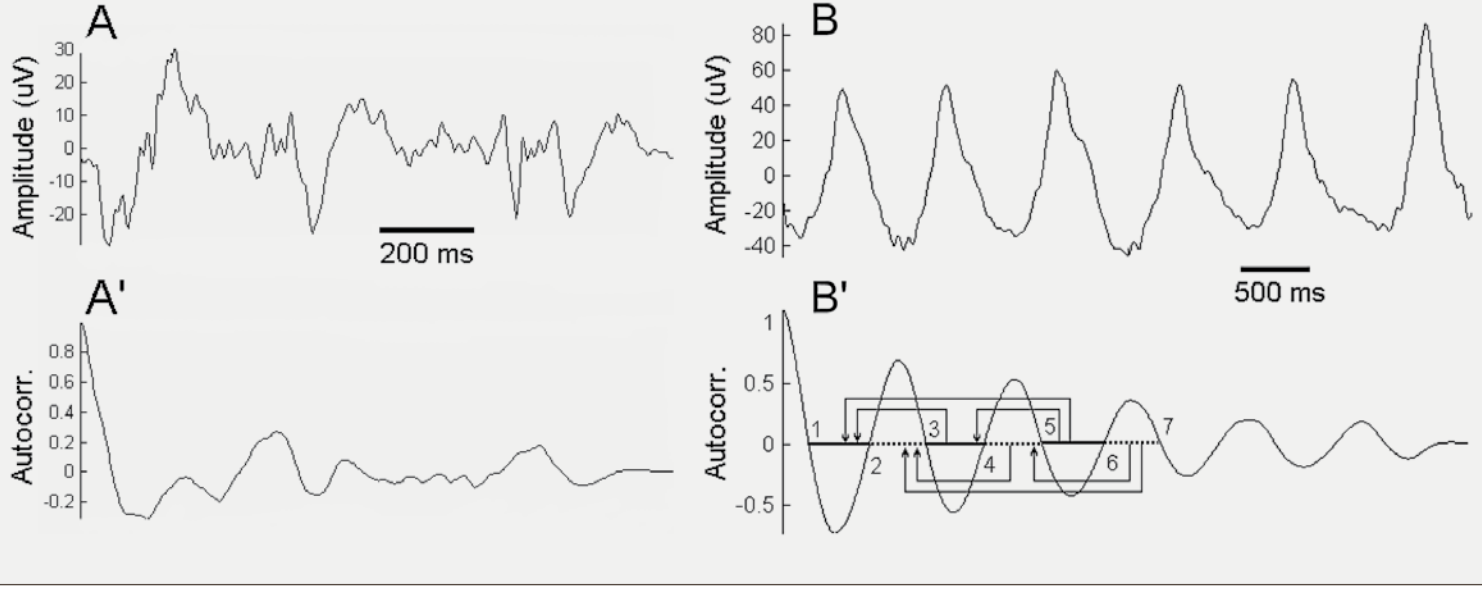

frequency activity relative to the background. In time domain processing, the autocorrelation function is useful for finding a repeating pattern in a signal and, thus, for handling the repetitiveness of oscillator-type seizures. The autocorrelation is the cross-correlation of a signal with a delayed version of itself. Liu et al. suggested a method based on the autocorrelation function to detect rhythmic discharges in the neonatal EEG (9). Navakatikyan et al. have shown that Liu's method displays a high sensitivity but also a high number of false positives (12). We therefore aimed to develop an autocorrelation-based analysis with a very low false positive rate. This algorithm consists of 2 steps. The first step detects an increase of low-frequency activity and the second analyzes the autocorrelation function of these increases.

DETECTION OF AN INCREASE IN LOW FREQUENCY CONTENT.

Every EEG channel is decomposed using the discrete wavelet transform (DWT). The signal is passed through two complementary filters and emerges as two signals. One is the low-frequency component, which is called the approximation, and the other is the high-frequency component or the detail. This process is repeated several times by successive filtering of the approximation. As a result, at each iteration (also called scale), a lower frequency component is extracted. As mother wavelet, we used a biorthogonal wavelet with decomposition order 3, as this wavelet matches the shape of the oscillatory activity we are looking for (19). The oscillatory activity is most prominent in the δ (0.5-4 Hz) and θ (4-8 Hz) range of frequencies. Therefore, only those wavelet coefficients which correspond to scales of 1-2 Hz, 2-4 Hz and 4-8 Hz are used for further analysis.

Next, the derivative of each selected scale is calculated, and, the result is squared to make it positive and to enlarge differences. To detect significant changes in the resulting signal, a window with a length of 3 s is moved along the signal. Detection occurs if the third quartile of the signal in the window is higher than 2.5 times the third quartile of the previous 30 s of EEG. If a window is detected for a particular scale, the signal in that window represents a significant increase of activity in that specific wavelet sub-band, compared to the background. This activity is considered potential oscillatory seizure activity.

AUTOCORRELATION ANALYSIS.

At this point, we have detected significant changes of activity in specific wavelet sub-bands of 1-8 Hz. What remains is the analysis of the repetitive aspect of the signal. As described above, our goal is to detect repetitive signals by means of the autocorrelation function. The detected windows in step 1 are divided into 5 s epochs (4 s overlap between epochs) and the autocorrelation function of the epochs is calculated. Figure 5 shows two examples of epochs with their autocorrelation functions.

For our purpose, two features of the autocorrelation function are particularly useful. First, the autocorrelation of an oscillating signal is very symmetric around zero, whereas that of a random signal is not (Figure 5). To exploit this difference, we calculate the skewness of the autocorrelation. Because of the symmetry, the skewness of the autocorrelation of an oscillating signal will be lower than that of a random signal. The second discriminatory feature compares the percentage difference of intervals between the zero-crossings of the autocorrelation (Figure 5B').

For the high-activity, low-frequency windows detected in step 1 to be classified as oscillatory seizure, their skewness must be lower than 0.4, and the mean of the interval differences between the zero crossings must be less than 6%.

COMBINATION OF THE TWO DETECTION ALGORITHMS

Roughly 50% of the seizures consist of a combination of spike train activity and oscillatory activity. In these cases, both detection algorithms are needed for a complete detection of the seizure. Figure 6 shows a seizure that starts with oscillatory activity and ends with spike train activity. The oscillation-detection algorithm detects the beginning of the seizure but not the end (grey shaded areas). Conversely, the spike train detection algorithm detects the spike train at the end of the seizure,

but not the beginning (areas with rectangle). There is a certain overlap between what is detected by both algorithms (channel Fp1-F3). When the seizure changes from oscillatory to spike train activity, the oscillation becomes spikier but the seizure is still continuous, resulting in detection by both algorithms. When the results of both algorithms are combined, almost the entire seizure is detected.

A neurologist reading the EEG usually classifies rhythmic EEG activity as a seizure if it is present for at least 10 s (20). To mimic the human observer and to be able to detect these short seizures, we have set the minimum duration in our algorithm to 8 s.

EVALUATION OF THE ALGORITHM

Presenting the performance of a seizure detection algorithm is not straightforward. Different ways to measure the performance of an algorithm have been reported in the literature, leading to varying results, which cannot easily be compared. In addition, all these algorithms were tested on different datasets, which makes a comparison even more difficult.

We defined the sensitivity per patient (*SensPP*) as the percentage of the number of seizures marked by the neurologist that are detected.

$$SensPP = (SZ\det PP / SZtotPP).100 \quad (9)$$

with *SZtotPP* the number of seizures marked by the neurologist for a patient, and *SZdetPP* the number detected by the algorithm for that patient. A seizure was considered as detected when there was a temporal overlap between the marked seizure and the detection.

The total sensitivity for all patients is calculated using 2 methods. The first method simply averages all sensitivities per patient (*SensT_PP*). The second method (*SensT*) measures the percentage of seizures detected of all seizures present in the complete dataset. So, *SensT_PP* measures the expected sensitivity at the patient level and *SensT* at the seizure level. The importance of the difference is that in *SensT_PP*, a patient with only a few seizures is considered to be equally important as a patient with many seizures. *SensT*, on the other hand, regards all seizures as equally important regardless of the patient they occurred in.

The Positive Predictive Value (*PPV*) is defined as the percentage of detected events that match seizures.

$$PPV = (EVsz / EVtot).100 \quad (10)$$

with EVtot the total number of detected events and EVsz the total number of detected seizures. Occasionally, a single seizure was detected several times by the algorithm. All such events were combined into a single EVsz detection. The PPV is dependent of the a priori likelihood of seizures in the dataset, which makes it difficult to compare the PPV of different datasets. But nevertheless it is an interesting measure for the performance of the detector.

Another useful measure of performance is the number of false positive detections per hour (fp/h). This measure represents an important indicator of the practical usability of the algorithm, because each FP implies that somebody in the NICU will have to check the patient and the raw EEG recording unnecessarily.

RESULTS

The results are given in Table 1.

The *SensT_PP* was 85%, *SensT* was 88%, as the algorithms detected 482 out of 550 seizures present in the dataset. The mean *PPV* was 75%. There were 143 false positive detections, or 0.66 fp/h. Of all false positives, 45% occurred in 2 of the 26 patients (patient 7 and 23). Closer analysis of these 2 patients revealed that both had low voltage EEG background activity (‹15uV) and thus were very susceptible to artifacts. When these 2 patients were excluded from the analysis, the false positive rate dropped to 0.39 fp/h.

DISCUSSION

In this paper, we introduce a new approach to detecting neonatal seizures. Our approach is based on two major characteristics of seizures (repetitiveness and a change relative to the background) that a human observer seems to employ. Although all seizures share these properties, their appearance can be very different (continuous versus discontinuous, low versus high frequency). Close observation, however, led to the identification of two types and, consequently, the development of two detection algorithms.

For this purpose, we use several concepts that were previously introduced in the literature (autocorrelation, NLEO, and wavelets), but we improve and combine them, while adding some of our own concepts. For example, just like Liu et al., we make use of the autocorrelation – but we only use it to detect seizures with a continuous type of repetitiveness (9). Furthermore, instead of analyzing the autocorrelation of the complete EEG, we limit the analysis to those parts of the signal that represent an important increase of low-frequency activity relative to the background. The combination of these improvements results in a lower false positive rate compared to previously published algorithms without altering the sensitivity.

A novel property of the spike train detection algorithm is its ability to detect repetitive segments of EEG even when two neighboring seizure segments are interrupted by other EEG activity (Figure 4). This adaptive, segmentation-based detection is much more flexible than analyzing a fixed epoch of EEG (like classifier-based approaches do). It is known that neonatal seizures are extremely variable in morphology and frequency, which makes it very difficult to develop a patient-independent algorithm (16,17). To deal with this variability, it is important to develop a data-driven algorithm that either derives its thresholds from the data or uses parameters that are independent of the variability. For instance, in our approach, the thresholds for the segmentation of the EEG in the spike train detection are derived from the data ('q3' and 'std' of the amplitude). Similarly, in the oscillation detection, the algorithm references to the background EEG. The remaining fixed thresholds are the correlation between the segments and the features derived from the autocorrelation. However, these parameters are independent of the variability of the seizures, because they only exploit the repetitiveness of the seizures and are independent of the actual seizure shape.

The sensitivity of the combined algorithms was good ($SensT\_PP$ 85%, $SensT$ 88%) at a practically acceptable false positive rate of 0.66 fp/h and mean PPV of 75%. For comparison, the algorithm by Navakatikyan et al. reported sensitivities of 83-95%. PPV of 48-77% and 2 fp/h (12). The algorithms of Gotman and Liu were also evaluated by Navakatikyan et al. (10). In their evaluation, the sensitivity of the Gotman algorithm ranged between 39.3 and 87.9%, and for the Liu algorithm between 97.9 and 99.2%. However, the false positive rate for the Gotman algorithm ranged from 7.4 to 10.4 fp/h, and an even higher 15.7 fp/h for the Liu algorithm. Faul et al. have also evaluated the performance of the Liu and Gotman algorithms (21). They reported a sensitivity of 62.5% for the Gotman algorithm and 42.9% for the Liu algorithm. Unfortunately, no fp/h measure was given.

In general, for both algorithms, long, high-amplitude seizures are rarely missed. The algorithms' sensitivity is lowest for subtle, short seizures which lack repetitiveness (arrhythmic) (Figure 7). Finally, Figure 8 provides a few examples of false positive detections of extra-cerebral activity of biological origin; Figure 9 shows some false positives caused by non-biological external sources. The ECG artefact was very dominant and present throughout the recording in a few patients. To deal with this artefact we developed an ECG reduction algorithm based on Independent Component Analysis (ICA) and applied it to the EEG before the seizure detection algorithm was run (a detailed description of this algorithm is beyond the scope of this paper). This greatly improved the false positive rate, but in spite of this step, the ECG artefact remained responsible for some false positives.

FIG 6 | Result of the combination of both detection algorithms. The oscillation detection detects the beginning of the seizure (shaded areas) but not the last part (on channels Fp1-F3, F3-C3 and C3-P3). The spike train detection algorithm detects the last part of the seizure (marked by rectangle), which was not detected by the oscillation detection algorithm. The combination of both algorithms yields a complete detection. There is an overlap between the detection of both algorithms on channel Fp1-F3

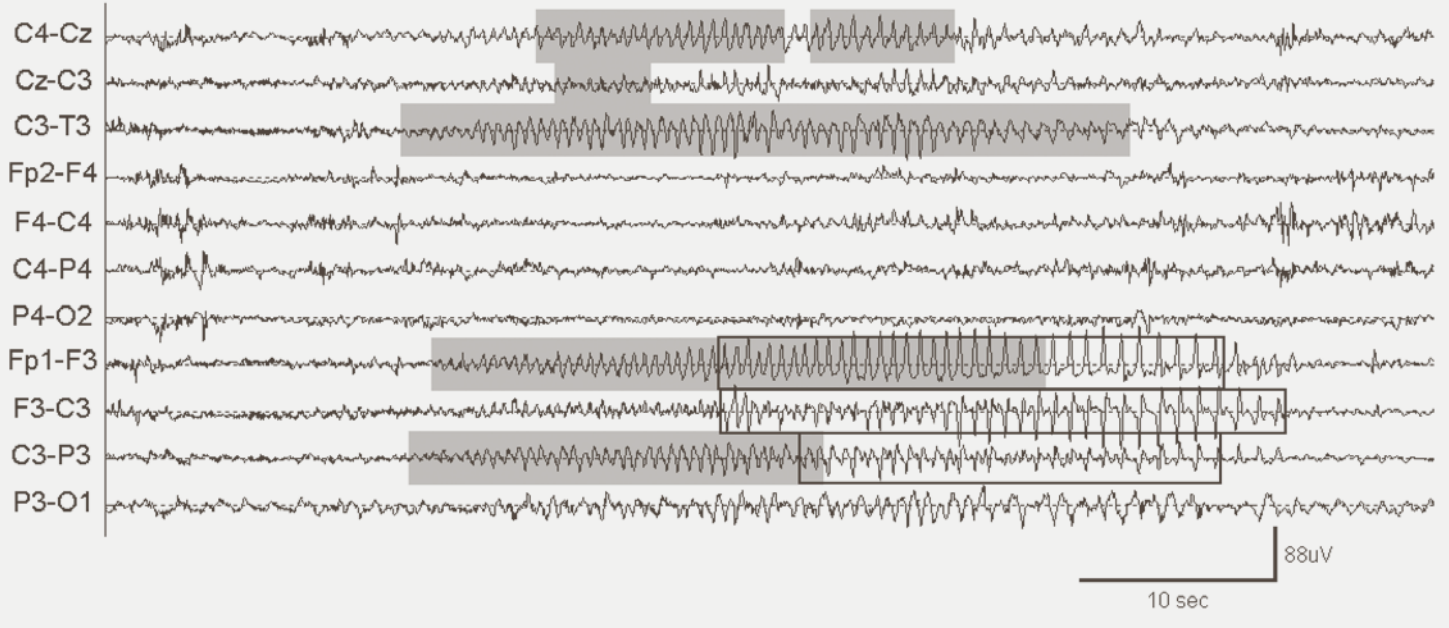

TABLE 1 | Results of the combined algorithms. Patient 22 to 26 were seizure-free and thus no SensPP and PPV is given. (rec. len. is the recording length)

id number	SensPP (%)	PPV (%)	fp/h	rec. len. (h)
1	92	94	0,51	7,9
2	100	32	1,65	7,9
3	92	65	1,52	7,9
4	90	72	1,27	7,9
5	100	80	0,13	7,9
6	90	100	0,00	7,9
7	89	60	4,05	7,9
8	82	64	0,63	7,9
9	100	100	0,00	7,9
10	100	90	0,13	7,9
11	100	33	0,51	7,9
12	100	90	0,25	7,9
13	96	85	0,51	7,9
14	96	83	0,63	7,9
15	45	71	0,25	7,9
16	50	50	0,13	7,9
17	38	89	0,13	7,9
18	86	86	0,13	7,9
19	60	75	0,13	7,9
20	100	61	1,39	7,9
21	82	100	0,00	7,9
22	x	x	0,00	20
23	x	x	4,05	7,9
24	x	x	0,13	7,9
25	x	x	0,00	7,9
26	x	x	0,00	7,9

SensT_PP: **85%**
SensT: **88%**
PPV: **75%**
fp/h: **0,66**

During validation of our methodology, we regularly encountered rhythmic activity in the EEG, detected by the algorithm. The origin of that EEG activity was not always clear, even for the neurologist, by only using the information from the scalp electrodes. In those cases, additional information from the simultaneously recorded polygraphic channels of ECG, respiration, movement sensor or even video were needed to establish that the activity present in the EEG was cerebral in nature or caused by an extra-cerebral source. To decrease the false positive rate of our algorithm further, these signals will have to be included in the analysis, as it is impossible to correctly classify them based on EEG analysis alone. At this point, we have only included the simultaneously recorded ECG in our analysis, by performing an ECG reduction on the data before the seizure detection algorithm was run.

The present parameter settings are for offline analysis and to obtain maximum sensitivity at an acceptable false positive rate. These values are based on expert estimation and trial and error. It is nearly impossible to estimate the parameters in a more systematic approach (e.g. using ROC-curves). Because there are many parameters, which are dependent of each other, we would need an almost infinite amount of ROC-curves to define the optimum parameter values. This optimum would also only be optimal for this particular dataset. We think our approach proves the robustness of the algorithm as it is able to perform without extreme optimization of the parameters. In a monitoring environment it might be desirable to obtain a lower false positive rate at the cost of a lower sensitivity. For the spike train type detection algorithm this can be achieved by increasing the threshold on the correlation between the detected segments. For the oscillatory type detection, the threshold on the skewness and the allowed percentage difference between the zero crossings may be decreased. By tuning these parameters we believe the algorithm to be suitable for online monitoring with sufficient sensitivity and practical false positive rate. The dataset on which the algorithm was tested consisted only of full-term neonates with perinatal asphyxia. In the future we would like to test it on preterm neonates. Nevertheless, the fact that our algorithm demonstrates a high sensitivity in the presence of all possible types of background activity suggests that it may also perform well on other kinds of EEG, including preterm EEG. The dataset used in this study comes from one center only. To further corroborate these results we need to test it on multi-center datasets. This is what we are planning to do in the near future.

FIG 7 | Examples of missed seizures; (A) high-amplitude, arrhythmic oscillatory seizure, (B) short, low-amplitude spike train (complete seizure is shown), (C)short, focal, high-amplitude seizure (complete seizure is shown)

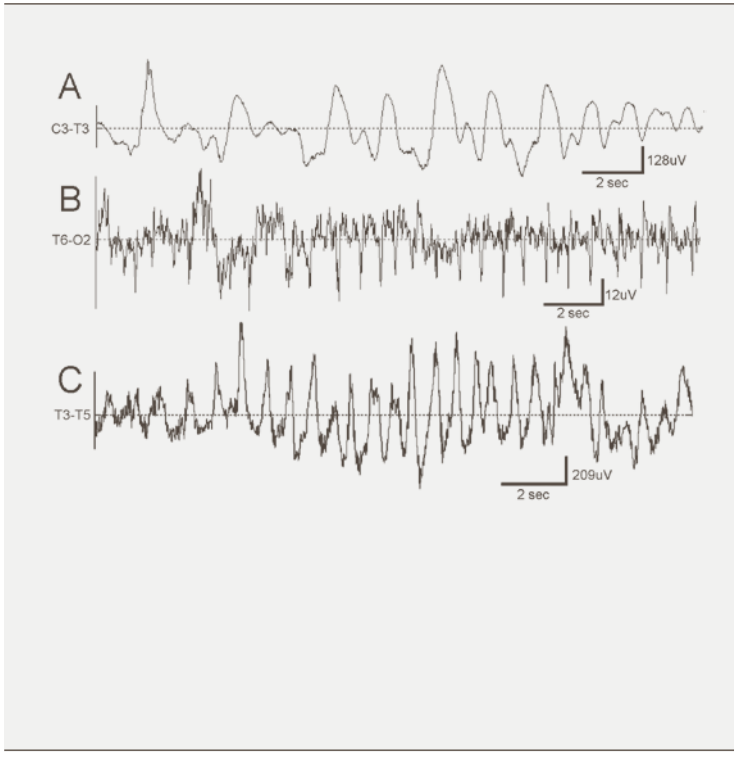

FIG 8 | Examples of false detections of biological origin; (A) ECG artefact, (B) tremor artefact, (C) pathological fast eye movements (nystagmus)

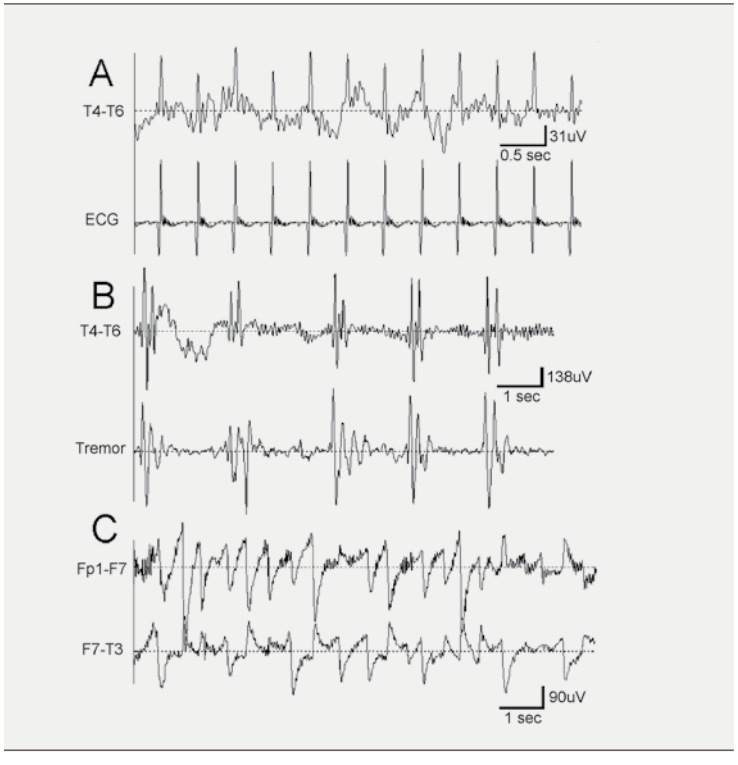

FIG 9 | Examples of false positive detections of non-biological origin; (A) high-frequency artifact, due to the heating of the bed, (B) ventilation artifact, as shown by the high correlation with a sensor on the abdomen

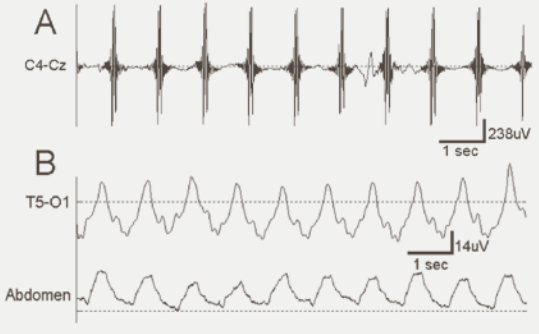

REFERENCES

1. Volpe J. Neurology of the newborn. 4the ed. Philadelphia: WB Saunders, 2001.
2. McBride MC, Laroia N, Guillet R. Electrographic seizures in neonates correlate with poor neurodevelopmental outcome. Neurology 2000;55:506-14.
3. Patrizi S, Holmes GL, Orzalesi M, Allemand F. Neonatal seizures: characteristics of EEG ictal activity in preterm and fullterm infants. Brain Dev 2003;25:427-37.
4. Liu Z, Yang Y, Silveira DC, Sarkisian MR, Tandon P, Huang LT, Stafstrom CE, Holmes GL. Consequences of recurrent seizures during early brain development. Neuroscience 1999;92:1443-54.
5. Schmid R, Tandon P, Stafstrom CE, Holmes GL. Effects of neonatal seizures on subsequent seizure-induced brain injury. Neurology 1999;53:1754-61.
6. Holmes GL, Gairsa JL, Chevassus-Au-Louis N, Ben-Ari Y. Consequences of neonatal seizures in the rat: Morphological and behavioral effects. Ann Neurol 1998;44:845-57.
7. Koh S, Storey TW, Santos TC, Mian AY, Cole AJ. Early-life seizures in rats increase susceptibility to seizure-induced brain injury in adulthood. Neurology 1999;53:915-21.
8. Clancy RR, Legido A, Lewis D. Occult neonatal seizures. Epilepsia 1988;29:256-61.
9. Liu A, Hahn JS, Heldt GP, Coen RW. Detection of neonatal seizures through computerized EEG analysis. Electroencephalogr Clin Neurophysiol 1992;82:363-69.
10. Gotman J, Flanagan D, Zhang J, Rosenblatt B. Automatic seizure detection in the newborn: methods and initial evaluation. Electroencephalogr Clin Neurophysiol 1997;103:356-62.
11. Celka P, Colditz P. A computer-aided detection of EEG seizures in infants: a singular spectrum approach and performance comparison. IEEE Trans Biomed Eng, 2002;49:455-62.
12. Navakatikyan MA, Colditz PB, Burke CJ, Inder TE, Richmond J and Williams CE. Seizuredetection algorithm for neonates based on wave-sequence analysis. Clin Neurophysiol 2006;117:1190-203.
13. Greene BR, Boylan GB, Reilly RB, de Chazal P, Connolly S. Combination of EEG and ECG for improved automatic neonatal seizure detection. Clin Neurophysiol 2007;118:1348-59.
14. Zarjam P, Mesbah M, Boashash B. An optimal feature set for seizure detection systems for newborn EEG signal. Proceedings of the International Symposium on Circuits and Systems, ISCAS (5), 2003;33-36.
15. Aarabi A, Wallois F, Grebe R. Automated neonatal seizure detection: A multistage classification system through feature selection based on relevance and redundancy analysis. Clin Neurophysiol 2006;117:328-40.
16. Lombroso CT. Neonatal seizures: a clinician's overview. Brain Dev 1996;18:1-28.
17. Shewmon DA. What is a neonatal seizure? Problems in definition and quantification for investigative and clinical purposes. J Clin Neurophysiol 1990;7:315-68.
18. van Putten M.J.A.M, van Putten M.H.P.M. Discovery of recurrent multiple brain states in non-convulsive status epilepticus. Clin Neurophysiol 2007;118:2798:804.
19. Daubechies I. Ten lectures on wavelets. SIAM, 1992
20. Shellhaas RA, Clancy RR. Characterization of neonatal seizures by conventional EEG And single-channel EEG. Clin Neurophysiol 2007;118:2156-61.
21. Faul S, Boylan G, Connolly S, Marnane L, Lightbody G. An evaluation of automated neonatal seizure detection methods. Clin Neurophysiol 2005;116:1533-41.

Chapter 9 | Summary, general discussion and future perspectives

Hypoxic-ischaemic encephalopathy still affects many term newborns. Some die and many of the survivors may develop cognitive and motor dysfunction. The neurodevelopmental outcome is often difficult to ascertain early in life. Yet, prognostication is very important particularly in medical ethical discussions. A variety of techniques such as neuroradiological (cerebral ultrasound (US)/MRI), neurophysiological [(amplitude integrated EEG (a-EEG), full-channel electroencephalogram (EEG) and Evoked Potentials (EPs)] and neurobehavioural tests have been used for assessment and prognostication in the first few days after birth. Although each of these techniques in itself has a reasonably good prognostic value, they are often combined for prognostication. However, it still remains difficult to fortell outcome in certain cases. The aEEG and full EEG (done for a short duration) have been widely studied in this respect. Fewer reports are published about 24-hours full EEG monitoring and the relation between EEG and MRI.

The main purpose of this thesis was to describe EEG background abnormalities in relation to MRI patterns in term asphyxiated newborns, aimed at gaining further insight into the pathophysiological mechanisms involved in perinatal asphyxia. With this in mind, new scoring systems for cerebral ultrasound (US)/MRI and 24-hours EEG monitoring were introduced (chapter 2 and 5). The results in this thesis are restricted to term asphyxiated newborns.

In **chapter 2**, a new imaging scoring system was introduced based on separate grading of injury to deep grey matter (TBG-score) and to (sub)cortical white matter (CWM-score) using US and MRI. Six patterns of brain injury were found in our cohort. Deep grey matter injury with either limited (pattern 1) or extensive cortical involvement (pattern 2), damage to deep grey matter with watershed injury (pattern 3), isolated watershed injury (pattern 4), isolated white matter injury (leukomalacia; pattern 5) and islolated extensive cortical injury (isolated cortical necrosis; pattern 6). Leukomalacia, and isolated cortical necrosis (patterns 5 and 6) were added to the brain injury patterns described in literature. In leukomalacia, we found that US plays an important role in the confirmation of this pattern, that is, in addition to MRI. A few combinations of lesions were not seen: deep grey matter lesions (TBG-scores 3 to 6) with periventricular white matter haemorrhage (CWM-score 1) and leukomalacia (CWM-score 5) with deep grey matter injury (TBG-scores 3 to 6). Still, there are lesions outside this score.

Chapter 3 compared our scoring system (referred to as the Sophia score), described in chapter 2, to the existing MRI scoring systems. To this aim, we limited scoring to MRI and left out US findings. The Sophia MRI sum score (lumping TBG- and CWM-scores) correlated with both the Hammersmith and the Barkovich scores. Judging from ROC curves, the Hammersmith score seems to be the best score to predict outcome. The Hammersmith score and Sophia TBG-score had equally high correlation with poor outcome. However, lumping of the Sophia TBG- and CWM-scores lowered the correlation coefficients, because outcomes after (sub)cortical and white matter injury are heterogeneous. It seems, therefore, that the Hammersmith score is quite useful in clinical practice. On the other hand, the two armed Sophia score reveals additional brain injury patterns like leukomalacia and isolated extensive cortical injury.

In **chapter 4**, we investigated the additional value of somatosensory evoked potentials (SEPs) in brain injury patterns in term asphyxiated infants. We found a significant relation between 24-hours EEG, deep grey matter injury and SEPs separately to outcome. Furthermore, SEPs provided additional value when added to EEG and MRI results. Normal/unilaterally abnormal SEPs showed high predictive values for good outcome, while bilaterally abnormal SEPs in the first week of life were highly predictive of poor outcome. For neonates with deep grey matter injury (MRI patterns 1, 2 and 3) the SEPs had no additional value in predicting outcome. However, in isolated watershed injury (pattern 4), leukomalacia (pattern 5) and isolated extensive cortical injury (pattern 6) outcome prediction was improved by using SEP results. In these patterns, symmetrical and asymmetrical brain lesions were seen. In asymmetrical isolated watershed injury, SEPs agreed with the MRI findings; posterior

frontal and parietal cortex affected on one side correlated with unilaterally abnormal SEP and with subsequent development of hemiparesis. In symmetrical isolated watershed injury and leukomalacia, the SEPs were symmetrical (bilaterally normal or abnormal) and predictive of the motor outcome, whereas such predictions were sometimes difficult based on MRI alone. In general, SEPs seemed to be more prognostic of motor than cognitive outcome.

Chapter 5 introduced an eight grade EEG scoring system, based on evolution of discontinuity over 24 hours as well as presence of sleep wake cycling, and correlated with brain injury patterns seen on MRI. A high correlation between 24-hours EEG scores and brain injury patterns was found. Interestingly the EEG subgroup with the most severe abnormalities (scores 5-8) showed two major injury patterns: deep grey matter injury (patterns 1, 2 and 3) and isolated extensive cortical injury (pattern 6). It is well known from MRI studies that persistence of severe EEG discontinuity is associated with severe basal ganglia/thalamus injury combined with cortical injury. We added isolated extensive cortical injury (pattern 6) to this group. With the pattern of primary white matter injury (leukomalacia, pattern 5) EEGs ranged from normal to moderately abnormal (scores 0-2). This is a unique pattern of injury, rarely described in the literature in term neonates. Previous studies describing white matter injury reported more severe EEG abnormalities presumably because they included patients with white matter injury combined with cortical lesions.

Normal to moderately abnormal EEGs (scores 0-4) predicted good outcome, which could be improved when MRI findings were added, in contrast to severely abnormal EEGs (scores 5-8) where MRI had no added value. Further subdividing the first group into normal/mildly abnormal (scores 0-2) and moderately abnormal EEGs (scores 2-4) the MRI results were found to improve outcome predictions only in the latter subgroup. However, even then, outcome cannot be accurately predicted in a small number of patients. We suggest that a 24-hours EEG scoring system comprizing 5 instead of 8 grades is sufficient enough for grading evolution of discontinuity (combining grades 5 to 8 into a single grade). Furthermore, we feel that prolongation of the EEG monitoring in moderately abnormal EEGs (scores 2-4) for another 24 hours for recovery of background activity and return of SWC may improve prognostication.

Clinical observations such as increase in heart rate in relation to seizure occurrence and ictal nystagmus are described in **chapters 6** and **7**. No fewer than 169 seizures in 14 neonates with severe birth asphyxia were studied and described in **chapter 6**. Heart range changes were found in 12.4% of the seizures in 8 patients. Both an increase and a decrease of heart frequency or a combination of these two were seen, which makes heart rate monitoring insensitive for detecting seizures in this group of patients. **Chapter 7** described a neonate with ictal nystagmus followed by occipital ictal discharges. This sequence suggests the existence of connections between the ocular motor centers in the brainstem and the occipital cortex.

Seizures occurring in the context of perinatal asphyxia in term infants usually reflect serious underlying brain injury. The occurrence of seizures and their relation to EEG background and outcome is the subject of another thesis. It is well known that after initial treatment of clinical seizures, subclinical seizures may continue (called electro-clinical dissociation). One study in the literature mentions that treatment of subclinical neonatal seizures detected by aEEG results in a reduction of the incidence of epilepsy in later childhood. Detection of seizures in the sick neonate has thus important therapeutic and prognostic consequences. The detection rate of seizures on aEEG and full EEG varies in literature. To address this problem, we developed an automatic seizure detection algorithm for the neonatal EEG, which is described in **chapter 8**. Because neonatal seizures are extremely variable in morphology and frequency, it was difficult for previous researchers to develop a patient independent algorithm. Hence we chose to develop a system that closely mimics the human interpreter. Neonatal seizures were divided into two morphological types: spike train seizure and oscillatory seizure. Nearly all neonatal seizures could be classified into these two patterns or a combination of

these two. For each type an automated detection algorithm was developed which both run in parallel. High predictive values, sensitivity and a low false positive rate of 0.66 per hour compared to other algorithms were found. Presently the algorithm works off line. Online analysis is being tested at the bed side.

From the findings of this thesis we designed a flow chart of parameters important for prognostication in term asphyxiated neonates (Figure 1). Even then, it remains difficult to reach an accurate prognosis in a small number of patients.

FUTURE PERSPECTIVES

Cerebral monitoring is very important in the asphyxiated neonate. Both aEEG and full EEG are well suited for estimating abnormalities of background activity whereas aEEG performs suboptimally in detecting seizures. Expertise is needed for interpretation of both. Also, artefacts (physiological as well as non-physiological) can influence both EEG and aEEG and are a challenge for both visual and automatic interpretation of EEG. We are improving artefact reduction in our seizure detection algorithm. We are also working on automatic quantification of the EEG background with the future of goal of developing a user friendly and accurate bedside brain monitor.

In the group of patients with moderately abnormal EEGs (scores 2-4) prolonged monitoring (for 36-48 hours) may improve the prognostication. Further studies have to be done to correlate the time of improvement of EEG background activity with outcome.

Furthermore, we are setting up a database to relate particular EEG abnormalities and brain lesions in each patient. We hope to find a relation between these two that would improve our understanding of the pathophysiological mechanisms involved in post asphyxial brain injury.

Finally, therapeutic hypothermia as an early treatment for term asphyxiated babies with encephalopathy has recently been introduced in our center. Future studies are needed to assess the value of investigations like EEG, MRI and SEPs in the context of this treatment.

FIG 1 | Algorithm to predict poor outcome in term asphyxiated newborns

Appendix

NEDERLANDSE SAMENVATTING

HET VOORSPELLEN VAN DE ONTWIKKELING VAN EEN KIND MET ASFYXIE

Zuurstofgebrek bij de geboorte, ofwel asfyxie, komt nog steeds veelvuldig voor. De structuren in de hersenen die bij asfyxie beschadigd kunnen worden liggen in de witte stof, hersenschors, diepe grijze stof of een combinatie hiervan. Een deel van de kinderen met asfyxie overlijdt en veel van de overlevenden ontwikkelen een geestelijke en/of motorische handicap. Het is belangrijk de verdere ontwikkeling van een kind met asfyxie in de eerste week te voorspellen, met name voor medisch-ethische beslissingen zoals bijvoorbeeld het beperken of stoppen van de behandeling. Dit promotieonderzoek beperkt zich tot kinderen die op tijd zijn geboren. Te vroeg geboren kinderen moeten apart worden onderzocht omdat zij mogelijk minder schade en een ander patroon oplopen dan op tijd geborenen.

Er zijn veel klinische onderzoeken mogelijk om een beeld te krijgen van de latere ontwikkeling van een kind met asfyxie. Dit zijn onder andere een twee- of meer-kanaals EEG (hersenfilmpje), echo of MRI van de hersenen en het meten van de tijd (in seconden) die een prikkel, gegeven aan de zenuw in de pols, erover doet om de hersenschors te bereiken (SEP). Al deze klinische onderzoeken zijn op zichzelf prognostisch voor de latere ontwikkeling van het kind. In de praktijk wordt die voorspelling gebaseerd op een combinatie van deze onderzoeken.

DOEL VAN HET ONDERZOEK

Het EEG wordt meestal direct na de geboorte aangesloten. MRI en SEP worden vaak 72 uur na de geboorte verricht. De echo kan dagelijks gedaan worden. Het doel waarmee ik aan dit proefschrift ben begonnen was om een verband te vinden tussen afwijkingen op het EEG en afwijkingen op de MRI. Omdat we bij de al bestaande classificaties voor de afwijkingen op MRI en EEG de resultaten van de kinderen in dit onderzoek niet altijd konden classificeren, hebben we een andere manier van classificeren voor beide gemaakt.

MRI

Wat betreft classificatie van MRI gebruiken we zowel de echo als MRI-beelden. We passen een aparte gradering toe voor de diepe grijze stof afwijkingen en één voor de witte stof/hersenschors afwijkingen. De afwijkingen in deze twee categorieën kunnen op zichzelf voorkomen of in combinatie met elkaar. Dit in tegenstelling tot de oude classificaties waarbij enkele vormen van schade niet zijn in te delen. Wij vonden twee op zichzelf staande schadepatronen die nog niet eerder in detail zijn beschreven; geïsoleerde witte stof schade (patroon 5) en geïsoleerde hersenschorsschade (patroon 6). De vier overige patronen van schade die we hebben gevonden zijn: diepe grijze stof schade geïsoleerd (patroon 1) of met hersenschorsschade (patroon 2) of met schade in de waterscheidingsgebieden van de grote hersenvaten (patroon 3) of schade in waterscheidingsgebieden geïsoleerd (patroon 4). Het blijkt dat de echo een belangrijke rol speelt in het bevestigen van geïsoleerde witte stof schade (patroon 4).

De bovenstaande gradering (uitgesplitst voor alleen MRI, de echo weglatend) hebben we vergeleken met de bestaande scoresystemen voor afwijkingen op MRI. Er is een sterk verband tussen de twee beschreven scoresystemen en ons systeem; hoe ernstiger de score, hoe ernstiger de afwijkingen op MRI. Eveneens hebben ze allemaal een goede voorspellende waarde naar de ontwikkeling van een kind.

EEG

Ook de classificatie van het EEG hebben we aangepast. In ons onderzoek hebben we gebruik gemaakt van een meer-kanaals EEG. Daarbij hebben we het EEG gedurende langere tijd (24 uur) geregistreerd. Beide in afwijking van vele eerdere onderzoeken die gedaan zijn.

In onze patiëntengroep konden we een indeling maken in acht graden van ernst. Dit hebben we teruggebracht naar twee groepen; normaal tot matig ernstig (graad 1-4) en zeer ernstig afwijkend EEG (graad 5-8). Het blijkt dat deze classificatie in twee groepen goed voorspellend is voor de te verwachten ontwikkeling van het kind.

Verdeel je de normaal tot ernstig afwijkende EEG nog verder op in normaal tot mild afwijkend (graad 0-1) en matig ernstig afwijkend EEG (graad 2-4), dan blijkt in de laatste groep de voorspelling ten aanzien van de ontwikkeling van het kind op basis van alleen het EEG moeilijk. Hier heeft de uitslag van de MRI een belangrijke aanvullende waarde.

Wanneer op de MRI de witte stof/hersenschors beschadigd is - dat wil zeggen in geïsoleerde witte stof schade (patroon 5), geïsoleerde hersenschorsschade (patroon 6) en geïsoleerde schade in de waterscheidingsgebieden (patroon 4) - kan de SEP nog van toevoegende waarde zijn. In de andere patronen (1, 2 en 3) van schade op de MRI heeft de SEP geen meerwaarde.

Mogelijk dat nog langere monitoring, dus meer dan 24 uur, zinvol is in de groep kinderen met een matig ernstig afwijkend EEG (graad 2-4) om tot een beter prognose alleen met EEG te komen.

ALGORITME

Het onderzoek heeft geleid tot een algoritme dat gebruikt kan worden bij kinderen met asfyxie en dat aangeeft wanneer behalve een 24-uurs EEG, een MRI dan wel SEP meerwaarde geeft bij de voorspelling van de ontwikkeling. Als er echter alleen op basis van het 24-uurs EEG al een zeer slechte prognose is ten aanzien van de ontwikkeling, zodanig dat er overwogen wordt om de behandeling te beperken of te stoppen, zullen altijd meerdere klinische onderzoeken worden verricht. Echter, in een kleine groep patiënten blijft het moeilijk om een goede prognose naar ontwikkeling te doen.

BEVINDINGEN

Dit proefschrift toont aan dat er inderdaad een sterke correlatie is tussen afwijkingen op het EEG en afwijkingen op de MRI. Een zeer ernstig afwijkend EEG (graad 5-8) gaat in alle gevallen samen met geïsoleerde hersenschorsschade (patroon 6) of diepe grijze stof schade (wel patroon 2) of niet (patroon 1) gecombineerd met hersenschorsschade dan wel schade in de waterscheidingsgebieden (patroon 3). Dus niet als de witte stof alleen is aangedaan (patroon 5) of als alleen de waterscheidingsgebieden zijn aangedaan (patroon 4). Alle kinderen in het onderzoek met een zeer ernstig afwijkend EEG zijn overleden. Geïsoleerde witte stof schade (patroon 5) laat geen zeer ernstige afwijkingen zien op het EEG (gaat samen met graad 0-2).

Bij kinderen met asfyxie kunnen trekkingen optreden, ook wel convulsies genoemd. Het is belangrijk om deze convulsies te behandelen, omdat mogelijk een verhoogde kans op epilepsie bestaat op latere leeftijd. Afhankelijk van de locatie van de convulsies kunnen ze een effect hebben op de hartfunctie. De monitoring van hartfrequentie is mogelijk een methode om deze convulsies te detecteren. We vonden echter dat de verandering, zowel het omhoog als omlaag gaan, van hartfrequentie bij een kind niet gerelateerd is aan het optreden van convulsies. De veranderingen in hartfrequentie kunnen dus niet als klinische parameter gebruikt worden voor het detecteren van convulsies.

We hebben wel een algoritme ontwikkeld dat convulsies automatisch detecteert op het EEG. Het is betrouwbaarder dan de bestaande algoritmen. Echter het werkt nu alleen nog maar offline. In de toekomst moet dit online gaan werken als het EEG wordt geregistreerd bij een patiënt. Men kan dan direct tot behandeling overgaan.

DANKWOORD

In mijn loopbaan ben ik veel mensen in het vakgebied tegengekomen die een rol hebben gespeeld in de keuzes die ik heb gemaakt. Het zijn er teveel om allemaal op te noemen maar enkele wil ik eruit lichten. In Alkmaar maakte ik kennis met de neonatologie. Wilfried Hack, met jou heb ik mijn eerste case reports geschreven. Frank van Bel, in Leiden heb ik mijn kennis van de neonatologie uitgebreid. In die periode besteedde je al veel tijd aan onderzoek en ik vind het dan ook een hele eer dat jij aanwezig bent op mijn verdediging en plaats neemt in de kleine en grote commissie. Joke Kok, jij hebt gezorgd dat ik mijn wens, een stage in het buitenland, heb kunnen verwezenlijken waar ik op vele manieren rijker door geworden ben.

Ruim 10 jaar geleden vertrok ik uit Amsterdam om in Rotterdam als fellow op de afdeling neonatologie te beginnen. Samen met Monique Williams en Daan Roofthooft deed ik veel patiëntenzorg. Ik heb veel geleerd, maar er was weinig tijd voor onderzoek. Aan het eind van mijn fellowship, mede door de komst van Paul Govaert waardoor de neurologie binnen de neonatologie meer aandacht kreeg, was het duidelijk dat het onderwerp van mijn thesis de neuroneonatologie zou zijn.

Gezien de ziektebeelden die we bij de patiënten op de afdeling tegenkwamen vonden we het wenselijk om de à terme kinderen met asfyxie beter in kaart te brengen. Samen met de afdeling kinderradiologie en de kinderneurofysiologie hebben we een onderzoeksplan gemaakt dat uiteindelijk tot de huidige thesis heeft geleid.

John van den Anker en Luc Zimmerman, ik wil jullie bedanken voor de mogelijkheid die jullie me hebben geboden om aan dit onderzoek te beginnen. Jullie hebben me in Rotterdam enthousiast ontvangen. Luc, jij hebt veel tijd moeten steken in de afspraken die moesten worden gemaakt met verschillende afdelingen wat heeft geresulteerd in de goede samenwerking.

Hans van Goudoever, mijn promotor, je doorzettingsvermogen en optimisme zijn aanstekelijk. De laatste twee jaren heb jij een belangrijke rol gespeeld in de sturing en timing van het afronden van het proefschrift. Als we ergens tegenaan liepen wist jij altijd wel een oplossing te bedenken en ook jouw logisch redeneren was voor mij zeer verhelderend. Jammer dat je ons als hoofd van de neonatologie gaat verlaten, maar je gaat een mooie nieuwe uitdaging aan.

Paul Govaert, mijn co-promotor, door deze thesis zijn we samen op een trein gestapt. In het begin wisten we nog niet waar we precies zouden uitkomen. Jij hebt mij het belang laten zien van het doen van klinisch onderzoek direct gerelateerd aan de dagelijkse patiëntenzorg. Door goed naar een specifieke patiëntengroep te kijken zijn er nog veel dingen te ontdekken die de klinische zorg en behandeling ten goede komen. Jouw enorme kennis van de neuroneonatologie is inspirerend en je hebt mij veel geleerd. Jouw deur staat altijd open en ik kan altijd bij je terecht om even te brainstormen. Ik hoop dat we na het maken van deze thesis weer samen op een trein zullen stappen die nu zijn eindpunt nog niet kent.

Gerhard Visser, mijn co-promotor, de neurofysiologie en de neonatologie zijn door dit onderzoek dichter naar elkaar toegegroeid. Het maken van deze thesis heeft de samenwerking en de patiëntenzorg goed gedaan. Er zijn weinig tot geen ziekenhuizen waar zo vaak een meerkanaals EEG wordt aangelegd als op onze afdeling. Jouw inbreng bij de artikelen kwam de structuur en helderheid van het manuscript ten goede.

Maarten Lequin, mijn co-promotor, nog voordat het onderzoek begonnen was, was je al betrokken bij deze groep patiënten. Als er bij een kind een MRI gemaakt moest worden wist jij altijd precies wanneer er nog een plekje vrij was. Ook bij het maken van echo's kon ik een beroep op je doen en was je altijd bereid om even mee te kijken. Naast het maken van echo's en MRI's ben je altijd zeer geïnteresseerd in de patiënt en denk je graag over alles mee.

Opponenten: dank dat jullie plaats willen nemen in de promotiecommissie.

Joseph Perumpillichira, met jouw verhalen over de patiëntenzorg in India benadruk je de grote verschillen in de wereld. Samen promoveren we op het monitoren van à terme pasgeborenen met asfyxie. Jij met de focus op de neurofysiologie en ik op de klinische kant. Met jou heb ik uren alle EEG's zitten scoren. Als ik een vraag heb is er altijd een antwoord en hoe druk je het ook hebt, je vindt altijd tijd voor iedereen. We hebben dan wel geen dubbelpromotie, maar ik zal je graag als paranimf terzijde staan op je promotie in september.

Collega's, op de afdeling neonatologie delen we veel met elkaar. Het vakgebied maakt dat het zeer intens is om hier te werken. Zeker in de afgelopen periode een zware taak. Ondanks dit hebben jullie altijd interesse getoond in het verloop van mijn thesis. Door jullie medewerking kon ik enkele maanden achter elkaar schrijven waardoor het nu is afgerond. Ik hoop dat jullie in de gelegenheid zijn om mijn verdediging bij te wonen en daarna het glas te heffen.

Verpleging van de afdeling neonatologie en laboranten van de afdeling neurofysiologie, zonder jullie had ik dit onderzoek niet kunnen verrichten. Laboranten, jullie hebben alle EEG's aangelegd. Els en Jolande hebben hierbij een belangrijke rol gespeeld. Verpleegkundigen, jullie hebben de klinische gegevens bij het lopend EEG ingevuld die ik weer konden gebruiken bij mijn analyse.

Daan van de Laar en Arianne Jacobs, tijdens de administratieve fase hebben jullie me erg geholpen met alles, dank!

Karin, bijna vanaf het begin dat ik in Rotterdam woon, kennen we elkaar. We woonden allebei op de Kop van Zuid. Een periode waarin we elkaar regelmatig zagen en een tennisclub hebben opgezet die helaas maar kort heeft bestaan. Door mijn verhuizing naar Kralingen en met het vorderen van mijn proefschrift zien we elkaar minder. Het feit dat jij mijn paranimf bent maakt het enigszins goed, maar als we nu samen afspreken moeten er ook vaak dingen geregeld worden. Na mijn promotie hoop ik dat we de oude draad weer kunnen oppakken. PR en communicatie is jouw vakgebied. Ik vind het erg fijn dat je mijn paranimf wilt zijn en dat je ondanks je volle agenda altijd nog tijd vindt mij met raad en daad bij te staan bij het afronden van mijn proefschrift.

Yvonne en Marcel, ook behorend bij de 'Club op Zuid'. Yvonne, jij staat altijd klaar voor iedereen. Dank zij jouw flexibele agenda vinden we nog af en toe tijd voor elkaar. Echter, ik mis wel onze gezellige stamppotavondjes en fietstochtjes. Marcel, als er bijzondere gelegenheden zijn ben jij meestal degene met een fotocamera om alles vast te leggen. Ik waardeer het dan ook zeer dat jij rond mijn promotie één van de fotografen wilt zijn, zodat we later alles nog eens rustig kunnen bekijken.

Eveline, onze wegen kruisten elkaar in Nijmegen. Sindsdien hebben we als goede vriendinnen nog steeds regelmatig contact. Ondanks het feit dat we ieder een andere weg zijn gegaan blijf jij altijd belangstelling tonen voor mijn leven en het vorderen van mijn proefschrift, wat ik zeer waardeer.

Frea, zoals het goede vriendinnen betaamt, zijn er niet veel woorden nodig om elkaar te begrijpen. Met jouw enthousiasme voor werk en leven ben je altijd een inspiratiebron voor me geweest.

Vic, als zussen zijn we samen opgegroeid. Ik herinner me nog het slapen onder de sterrenhemel in Heidelberg met Quinty aan onze voeten. Jij ging in Groningen studeren waarop de logeerpartijtjes volgden en het studeren in de bibliotheek waarbij een reep chocolade niet mocht ontbreken. In Leiden en Amsterdam kwamen onze wegen weer samen. Daarna bracht jouw baan je naar de omgeving van Apeldoorn. Na mijn promotie

heb ik weer wat meer tijd; voor een partijtje golf misschien?
“Als je op een zonnige dag over de fairway slentert loop je eigenlijk door een stukje hemel op aarde” (Frank Coffey)

Maar eerst staan we op 22 april samen. Ik vind het fijn dat je mijn paranimf bent op deze belangrijke dag.

Tom, ik waardeer het zeer dat jij samen met Marcel een belangrijke taak op je wilt nemen: het maken van de foto’s.

Pap en mam, voor een deel van wat ik heb bereikt zijn jullie de grondleggers geweest. We hebben door de jaren heen samen veel leuke dingen gedaan en jullie hebben mij een aantal wijze levenslessen meegegeven. Twee daarvan wil ik nu even aanstippen. Een leuke zelfstandige baan is een belangrijk onderdeel van je levensgeluk. Ik ben dan ook blij dat ik de verdediging van mijn thesis met jullie kan delen. Ook leerden jullie me doorzetten, en dat is iets wat je bij promoveren zeker nodig hebt.

Emile, we leerden elkaar kennen terwijl we ‘chaka’ de berg af skieden. Afgelopen periode hebben we allebei keihard gewerkt, jij in je nieuwe functie als kwartiermaker en ik bij het afronden van mijn promotie. Gelukkig is het ‘chaka’ gevoel gebleven. Ondanks je drukke baan blijf je jouw humor behouden, heb je altijd een luisterend oor en ben je er voor mij. Daarnaast ben ik erg blij dat jij sommige dingen wat meer als een uitdaging ziet dan ik, zodat ik in een kritieke fase van mijn proefschrift een beroep op jou kon doen. Dit jaar gaan we niet ‘chaka’ de berg af. Wat het ons wel zal brengen is nog een verrassing, maar het zal zeker de moeite waard zijn.

Allen die ik niet genoemd heb, maar die mij op een of andere manier tot steun of voorbeeld zijn geweest, die me hebben geholpen, soms alleen al door er te zijn, aan jullie alsnog mijn dank!

CURRICULUM VITAE

Renate Swarte werd geboren op 22 mei 1964 te Goor. Na het behalen van het Gymnasium diploma aan de Grundel in Hengelo startte zij de studie geneeskunde aan de Katholieke Universiteit te Nijmegen die ze in 1990 afrondde. In deze periode is ze 3 maanden in het Children's Hospital in Philadelphia (Prof.dr. R. Polin) geweest om wat meer inzicht te krijgen in de kindergeneeskunde en in het onderzoek op het laboratorium. De kliniek trok meer dan het laboratorium en zij begon aan de opleiding tot kinderarts (opleider Prof.dr. H.S.A. Heymans) in het Emma Kinderziekenhuis van het Academisch Medisch Centrum te Amsterdam die in 1999 werd afgerond. In die periode deed ze een buitenlandse stage van 3 maanden op de kinderafdeling van het Bristol Children's Hospital te Bristol (Dr. R. Martin) in Engeland. Na de voltooiing van de opleiding startte zij als fellow neonatologie in het Erasmus MC-Sophia (opleider Prof.dr. J. van den Anker) te Rotterdam. Tijdens de afronding hiervan in 2001 werd een aanvang gemaakt met het opzetten van het promotietraject dat in 2003 daadwerkelijk van start kon gaan en resulteerde in dit proefschrift (promotor Prof.dr. J.B. van Goudoever en co-promotoren Dr. P. Govaert, Dr. M.H. Lequin en Dr. G.H. Visser). Vanaf 2001 is zij werkzaam als neonatoloog in het Erasmus MC-Sophia. Daarnaast is zij vanaf 2008 coördinator van de poli neonatologie.

LIST OF PUBLICATIONS

Technical standards for recording and interpretation of neonatal electroencephalogram in clinical practice
Cherian PJ, Swarte RM, Visser GH. Ann Indian Acad Neurol. 2009 Jan;12(1):58-70.

Imaging patterns of brain injury in term-birth asphyxia
Swarte R, Lequin M, Cherian P, Zecic A, van Goudoever J, Govaert P. Acta Paediatr. 2009 Mar;98(3):586-92.

Neonatal seizure localization using PARAFAC decomposition
Deburchgraeve W, Cherian PJ, De Vos M, Swarte RM, Blok JH, Visser GH, Govaert P, Van Huffel S. Clin Neurophysiol. 2009 Oct;120(10):1787-96.

Network injury to pulvinar with neonatal arterial ischemic stroke
Govaert P, Zingman A, Jung YH, Dudink J, Swarte R, Zecic A, Meersschaut V, van Engelen S, Lequin M.Neuroimage. 2008 Feb 15;39(4):1850-7.

Automated neonatal seizure detection mimicking a human observer reading EEG
Deburchgraeve W, Cherian PJ, De Vos M, Swarte RM, Blok JH, Visser GH, Govaert P, Van Huffel S. Clin Neurophysiol. 2008 Nov;119(11):2447-54.

Ictal nystagmus in a newborn baby after birth asphyxia
Cherian PJ, Swarte RM, Blok JH, Bröker-Schenk PM, Visser GH. Clin EEG Neurosci. 2006 Jan;37(1):41-5.

Postnatal onset cortical dysplasia associated with infarction of white matter
Govaert P, Lequin M, Korsten A, Swarte R, Kroon A, Barkovich AJ. Brain Res. 2006 Nov 22;1121(1):250-5.

Heart rate changes are insensitive for detecting postasphyxial seizures in neonates
Cherian PJ, Blok JH, Swarte RM, Govaert P, Visser GH. Neurology. 2006 Dec 26;67(12):2221-3.

Bacillus cereus meningoencephalitis in preterm infants: neuroimaging characteristics
Lequin MH, Vermeulen JR, van Elburg RM, Barkhof F, Kornelisse RF, Swarte R, Govaert PP. AJNR Am J Neuroradiol. 2005 Sep;26(8):2137-43.

Sonographic appearance of the normal and abnormal insula of Reil
Govaert P, Swarte R, De Vos A, Lequin M. Dev Med Child Neurol. 2004 Sep;46(9):610-6.

Factor II gene(prothrombin G20210A)mutation and neonatal cerebrovenous thrombosis
Swarte R, Appel I, Lequin M, van Mol C, Govaert P. Thromb Haemost. 2004 Oct;92(4):719-21.

Changes in globus pallidus with (pre)term kernicterus
Govaert P, Lequin M, Swarte R, Robben S, De Coo R, Weisglas-Kuperus N, De Rijke Y, Sinaasappel M, Barkovich J. Pediatrics. 2003 Dec;112(6 Pt 1):1256-63.

Neonatal infarction within basal cerebral vein territory
Govaert P, Swarte R, Oostra A, Zecic A, Vanzieleghem B, Van Langenhove P. Dev Med Child Neurol. 2001 Aug;43(8):559-62.

PhD Portfolio Summary

Name PhD student: R.M.C. Swarte Erasmus MC Department: Neonatologie	PhD period: 2003-2010 Promotor: J.B. van Goudoever Supervisor: P. Govaert, M. Lequin, G.H. Visser

1. PhD training

	Year	Workload (Hours)
General academic skills	**2005**	**128**
- Cambridge English Writing and Communication (Volksuniversiteit)		
Research skills	2004	144
- Statistics (NIHES)		
Presentations		
- Presentation "Nederlandse Vereniging Neuroneonatologie"	2004	25
- Presentation "Nederlandse Vereniging Neuroneonatologie"	2006	25
- Presentation "Nederlandse Vereniging Neuroneonatologie"	2007	25
- Presentation "Nederlandse Vereniging Neuroneonatologie"	2008	25
- Presentation "Sectie vergadering Kindergeneeskunde"	2005	25
- Presentation "Vlaams-Nederlandse werkgroep EEG"	2005	25
- Presentation "Vlaams-Nederlandse werkgroep EEG"	2007	25
- Presentation "Vlaams-Nederlandse werkgroep EEG"	2008	25
- Presentation "NVK"	2009	25
International conferences		
- Poster Boston	2003	25
- Posterwalk ESPR Sienna	2005	25
- Oral presentation ESPR Barcelona	2006	25
- Poster SRP Honolulu	2008	25
Seminars and workshops		
- Presentation "Schedelechografie I"	2006	25
- Presentation "Schedelechografie II"	2007	25

2. Teaching activities		
- Workshop CFM: “Neonatologie aan de Maas”	2006	35
- CFM and one channel EEG (for nurses of the NICU)	2007	25
- Presentation “PAOK: Hoofdzaken”	2008	25
- Presentation “PAOK: Op de kleintjes letten”	2009	25
- Presentation “Kinderartsen regio”	2009	25
- Presentation “Kinderartsenweek: Acute geneeskunde”	2010	25
- Presentation “Kinderartsen regio”	2010	25
Total		**832 H=30 ECTS**

The publication of this thesis and the symposium, organized preceeding the PhD defence, were financially supported by Abbott, Acertys/Natus, The Surgical Company, Nutricia, Friso Kindervoeding and Esaote - Pie Medical Benelux B.V.

“Ik werk graag met kinderen. Soms zijn ze verlegen en hebben ze tijd nodig om los te komen. Maar altijd zijn ze ontwapenend, ongecompliceerd en eerlijk. Het is hun veerkracht waarmee er na een tegenslag al snel weer een lach op het gezicht verschijnt. En dat is eigenlijk het mooiste resultaat.”

Renate Swarte